SPSD II

VALIDATION OF ALTERNATIVE MARINE CALCAREOUS SKELETONS AS RECORDERS OF GLOBAL CLIMATE CHANGES (CALMARS)

PH. WILLENZ, L. ANDRE, R. BLUST, F. DEHAIRS, PH. DUBOIS

PART 2

GLOBAL CHANGE, ECOSYSTEMS AND BIODIVERSITY

- ATMOSPHERE AND CLIMATE
- MARINE ECOSYSTEMS AND BIODIVERSITY
- TERRESTRIAL ECOSYSTEMS AND BIODIVERSITY
- NORTH SEA
- ANTARCTICA
- BIODIVERSITY

.be

SCIENTIFIC SUPPORT PLAN FOR A SUSTAINABLE DEVELOPMENT POLICY
(SPSD II)

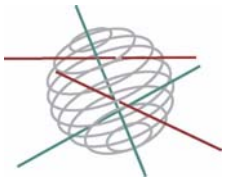

Part 2:
Global change, Ecosystems and Biodiversity

FINAL REPORT

VALIDATION OF ALTERNATIVE MARINE CALCAREOUS SKELETONS AS RECORDERS OF GLOBAL CLIMATE CHANGES

(CALMARS)

EV/04

Philippe Willenz & & Lorraine Berry - IRSNB/Department of Invertebrates
Frank Dehairs, Willy Baeyens, David P. Gillikin – VUB/Department of Analytical and Environmental Chemistry (ANCH)
Eddy Keppens – VUB/ Department of Geology
Fjo De Ridder – VUB/ Department of Electricity and Instrumentation
Luc André, Sophie Verheyden, Anne Lorrain – MRAC/Section of Petrography-Mineralogy-Geochemistry
Philippe Dubois, Herwig Ranner – ULB/Laboratory of Marine Biology
Ronny Blust, Valentine Mubiana Kayawe - UA/Department of Biology

Juin 2006

D/2006/1191/22
Published in 2006 by the Belgian Science Policy
Rue de la Science 8
Wetenschapsstraat 8
B-1000 Brussels
Belgium
Tel: +32 (0)2 238 34 11 – Fax: +32 (0)2 230 59 12
http://www.belspo.be

Contact person:
Mrs Martine Vanderstraeten
Secretariat: +32 (0)2 238 36 13

TABLE OF CONTENTS

ABSTRACT

Understanding environmental proxies stored in biogenic carbonates has become a major task and a multidisciplinary endeavour. The CALMARs project (CALcareous MARine Skeletons as recorders of global climate changes) involved reading these records stored in biogenic carbonates and aimed at validating the skeletons of sclerosponges, bivalves and echinoderms as environmental proxies.

The first aim was to determine the growth rates of two hyper calcified sponges: *Ceratoporella nicholsoni* and *Petrobiona massiliana*. Accumulative data for all specimens of *C. nicholsoni* collected and measured showed the mean average growth rate to be 198.25µm/yr (9 specimens: n=557, σ=15.23 µm/yr). The mean growth rate of *Petrobiona massiliana* was 242.76 µm/yr (13 specimens, n=189, σ=161.42 µm/yr). However, the growth rate of this species shows much variation between and within specimens, but falls within the range observed in other hyper calcified sponges. Secondly, we investigated the uptake route of elements into the tissues of *Petrobiona massiliana*. Transmission Electron Microscopy (TEM) observations showed uptake and accumulation of particles inside endocytic vesicles of specific cell types. Bacteria marked with strontium were also accumulated within phagosomes of the same cells and retained their strontium after incorporation. Incubations with the dissolved elements (up to 10 mM) did not allow the location of elements to be determined within the sponge tissue. However, supersaturated incubations (providing particulate ions) allowed element hotspots to be discovered using Scanning Electron Microscopy (SEM) + Energy Dispersive X-ray analysis (EDX). Focused Ion Beam-cut sections from the element hotspots enabled positive analysis using the Scanning TEM + EDX, but the exact cellular locations are still to be determined at the ultrastructural level. Thirdly, lead profiles from several sclerosponge skeletons were investigated. Nine lead profiles covering more than 130 years from eight sclerosponges of two different species, Ceratoporella nicholsoni and Stromatospongia vermicola, collected off Jamaica, Acklins Island and Turks and Caicos Island are compared. All the profiles display i) the rise in lead around 1950 linked with the atmospheric pollution due to the increasing use of leaded gasoline, and ii) the decrease in lead content during the eighties following the introduction of unleaded gasoline. It is demonstrated that lead curves from sclerosponges are reproducible within single specimens as well as between different specimens from similar locations. In addition, the study reveals information on the physiological functioning of sclerosponges and suggests non-linearity of the lead partitioning coefficient.

Bivalve shells offer a great potential as environmental proxies, since they have a wide geographical range and are well represented in the fossil record since the Cretaceous. Nevertheless, they are much less studied than corals and foraminifera and are largely limited to isotopic studies. The general aim of this project was to increase our knowledge of $\delta^{18}O$, $\delta^{13}C$, Sr/Ca, Mg/Ca, U/Ca, Ba/Ca, and Pb/Ca in bivalve aragonite and calcite.

The most well studied proxy of sea surface temperature (SST) in bivalve carbonate is $\delta^{18}O$, and it is well known that in addition to SST, the $\delta^{18}O$ of the water dictates the $\delta^{18}O$ value of the shell. This study clearly demonstrates that unknown $\delta^{18}O$ of the water can cause severe errors when calculating SST from estuarine bivalve shells; with the example presented here providing calculated SSTs 1.7 to 6.4 □C warmer than measured. Therefore, a salinity independent or salinity proxy would greatly benefit SST reconstructions. In estuaries, shell $\delta^{13}C$ has long been regarded as a potential salinity indicator. However, this study highlights the problems associated with the incorporation of light metabolic CO_2 in the shell. Therefore, interpreting $\delta^{13}C$ values in bivalve carbonate should be done with caution. In addition to $\delta^{13}C$, Ba/Ca ratios were investigated as a salinity proxy as well. In the calcite shells of M. edulis a strong linear relationship between shell 'background' Ba/Ca and water Ba/Ca was found in both the laboratory and field. Although each estuary will have different relationships between salinity and water Ba/Ca, shell Ba/Ca can be used as an indicator of salinity within one estuary. Similar patterns of relatively stable background levels interrupted with sharp episodic peaks were also found in the aragonite shells of S. giganteus, and appear nearly ubiquitous to all bivalves. However, there was an ontogenic decrease in S. giganteus background Ba/Ca ratios, illustrating that these proxies can be species specific. The ratios of Sr/Ca, Mg/Ca and U/Ca were investigated as salinity independent SST proxies, but none were correlated to SST in the two aragonitic and one calcitic bivalve studied. Finally, the use of bivalve shells as recorders of pollution was also assessed. There was both large inter- and intra-specimen variability in Pb/Ca ratios of M. mercenaria shells, but when enough shells were averaged, the typical anthropogenic Pb profile from 1949 to 2003 was evident.

Biomineralization is obviously a biological process, and therefore, understanding the pathway of elemental incorporation is vital to understanding proxy incorporation under different temperature and salinity regimes. Results for the mussel, Mytilus edulis, showed uptake of Ca, Cd, Co, Cu and Hg displayed saturation kinetics. Because steady-state was observed at all the different metal exposure levels, it was unlikely that either internal metal binding sites or membrane transporters were saturated under those conditions. Our results indicate that uptake of trace elements

and further processing in mussels involves different combinations of the general pathways including those intended for homeostasis of major ions such as Ca and Mg. There was no clear distinction between uptakes of essential and non- essential metals. Through uptake of trace elements is dependent mainly on free ion activity in the exposure water, our results have shown that there are cases when other chemical species may also be important predominantly taken up via the dietary route. Also the effect of temperature and salinity clearly shows deviations from the free ion activity model indicative for physiological regulation.

Echinoderms are abundant in a wide geographical range from equatorial to Polar Regions and several species are rather long-lived (60 to 100y). In the present study, we investigated the effects of temperature on the incorporation of minor and trace elements and on the $\delta^{18}O$ and $\delta^{13}C$ in the skeleton of the wide-ranged temperate starfish Asterias rubens and in closely related sea urchin species collected from boreal to tropical latitudes. A highly significant temperature effect on the Mg incorporation in the skeleton in both experimental and field conditions was evidenced and matches the relation obtained in benthic foraminifera. This effect was independent of growth rate, contrary to previous statements. The slope of relative $\delta^{18}O$ versus temperature in skeletons of starfish is also highly significant and neatly matches slopes measured in corals or molluscs. The Mg/Ca ratios of museum specimens are below those of present day specimens indicating a general warming trend.

Keywords: paleoclimate, carbon cycle, climate change, sea surface temperature

1. INTRODUCTION

All of what we know about the history of the Earth's climate and environments is obtained from records stored in substrates formed during the period of interest. Reading these records has become a major task and a multidisciplinary endeavour. As Lea (2003) wrote: "Temperature is the most primary representation of the state of the climate system, and the temperature of the oceans is critical because the oceans are the most important single component of the Earth's climate system." Considering the concept that the 'past is equal to the present,' and that the thermometer was only invented at the turn of the 17th century (Middleton, 1966), it is clear why records of paleotemperature are important. In order to obtain this information, proxies are used, which are geochemical or physical signals recorded in different biological or geological deposits that reflect an environmental signal. However, many records are restricted in their distribution, and the importance of regional climate is becoming increasingly clear (IPCC, 2001). For example, trees provide only terrestrial records and there are many problems reading the records stored in tropical trees (Jacoby, 1989; Verheyden, 2004). Moreover, many proxies used to extract information from these substrates are not fully understood. Each type of archive provides a valuable record, with unique strengths and weaknesses. For example, sediments often provide low resolution profiles and bioturbation may be a problem, scleractinian corals are mostly restricted to the tropics, and foraminifera are small organisms making detailed ontogenic studies difficult (although this has recently been achieved; Eggins *et al*., 2004).

The chemical or isotopic composition of calcareous skeletons has long been recognized as records of past and present environmental conditions and thus allows reconstruction of past environmental conditions. Because the composition of biogenic carbonates is also clearly influenced by biological factors, the correct interpretation of these chemical archives requires a precise multidisciplinary understanding of the processes controlling the incorporation of proxies. Furthermore, to make the reconstruction of past environmental conditions as reliable as possible at a global scale implies that recorders from the widest taxonomic, geographical, and ecological ranges are used, which cover both short (annual to decadal) and long-term periods (millennia).

Marine invertebrates with skeletons formed by sequentially deposited calcium carbonate layers allow access to time resolved (from less than a day to centuries) environmental conditions. The reconstruction of time series from these carbonate skeletons is generally based on a seasonal or yearly periodicity of the proxy signal (Mg/Ca; Sr/Ca; $\delta^{18}O$; etc.); however, reconstructing a 'time base' from this growth

axis is not straightforward. Hermatypic coral skeletons, for instance, are among the highest resolution and most used marine paleoclimate recorders and provide multidecadal information on SST, salinity, nutrients, the precipitation evaporation balance, near surface ocean circulation, past mixing rates and distribution of fossil fuel CO_2 in the upper ocean (Weber & Woodhead, 1970; Weber, 1973; Lea *et al*., 1989; Swart *et al*., 1996; Gagan *et al*., 2000; Ren *et al*., 2003; Reuer *et al*., 2003). However, they have a distribution restricted to shallow tropical seawaters due to their compulsory symbiosis with photosynthetic algae. This means that most climatic reconstructions based on corals are derived from a restricted latitudinal, bathymetrical, and ecological range. The solution proposed by several authors is to expand the multi-proxy approach and explore other potential paleoclimate archives with different time and geographical scales in order to synthesize compatible data sets (Shen *et al.* 1996; Gagan *et al*., 2000).

The aim of the CALMARS I research project was to extend the environmental records of oceanic origin by validating the archive function of skeletons from selected marine invertebrates, belonging to three different phyla and living in varied geographical, bathymetrical, and ecological areas. The selected taxa are sclerosponges, molluscs, and echinoderms for which earlier work has emphasized the environmental archive potential (Swart *et al*., 1998; Andreasson and Schmitz, 1998). More specifically, this project focused on the following: (1) determining the correlations between proxies in the skeleton and environmental conditions in the field such as SST, salinity or bio-availability, for sclerosponges, bivalves and echinoderms; (2) measure and model the impact of variable proxies concentrations and environmental conditions (SST, salinity, nutrients, etc.) on the element composition in tissue and skeleton in controlled experimental setups; (3) investigate physiological conditions that modulate proxy concentrations in the skeleton (importance of element routing and compartmentalization); (4) based on the former results, develop transfer functions (corrected for physiological effects) relating the proxy to the environmental variable(s); (5) reconstruct at high resolution (day to seasonal depending on taxa), climatic and environmental conditions from a comparison between specimens of the same species from contrasted geographical regions and from different periods (historical time scale, from museum collections); (6) compare our results with those obtained from other calcareous skeletons such as corals.

2. MATERIALS AND METHODS

Study sites were located both in the topics (Jamaica; Acklins Island; Turks and Caicos Islands) and temperate regions (The Mediterranean Sea; The Netherlands; Belgium; North Carolina and Puget Sound, Washington, USA) (Fig. 1). Echinoderms were collected from around the world (see Annex 1). This project focused on three taxa: sclerosponges, bivalves and echinoderms.

Figure 1. World map showing main sampling stations (see also Annex 1).

2.1 Sclerosponges

2.1.1 Species

Three species of sclerosponges were studied: *Ceratoporella nicholsoni*, *Stromatospongia vermicola* and *Petrobiona massiliana*. Samples were collected from the Caribbean and Mediterranean.

Ceratopora nicholsoni Hickson, 1911 is a calcified demosponge belonging to the family Astroscleridae (Vacelet, 2002), (Order Agelasida Hartman, 1980) (Fig. 2). It is monotypic and endemic to the Caribbean, found in localised submarine caves and epibathyal cliffs, between depths of 8 and 184 m. Young specimens are pendunculate or cone shaped, with orange living tissue growing over a basal skeleton. Older specimens are mound shaped, growing up to 100 cm in diameter and 50 cm in thickness. The massive calcite basal skeleton forms the main mass of the specimen and is made up of sclerodermites with a clinogonal microstructure, consisting of closely packed crystalline units that diverge at a low angle, superficially organised into polygonal calicular units of 1-1.2 mm depth and 0.2-0.4 mm across. The living tissue forms a thin veneer over the surface, extending down into each calicle; total thickness of the tissue is 1.5mm. Each calicular unit corresponds to a single inhalant and exhalant canal. Canals bearing special valvules. Choanocyte chambers small, 20.7µm in mean diameter. Exhalant collecting system leaving

stellate depressions (astrorhizae) on the surface of the skeleton. Intercellular symbiotic bacteria abundant and highly diverse in shape. Growth rate of the skeleton 0.21–0.23 mm/y in Jamaican caves (Willenz & Hartman, 1999). Siliceous spicules occur free in the living tissue and entrapped into the calicle walls. Entrapped spicules progressively dissolve within the basal calcareous skeleton.

Figure 2. *Ceratoporella nicholsoni:* Specimens *in situ*
(Photo Ph. Willenz)

Stromatospongia vermicola Hartman, 1969 belongs to the same family (Vacelet, 2002). It is encrusting to massive, with an aragonitic basal skeleton associated with the calcareous tubes of serpulid worms. Siliceous spicules are verticillately spined styles more or less completely entrapped in the basal skeleton. Surface of the basal skeleton is ornamented with processes 0.8 to 2 mm high. Living tissue forms a thin veneer in the spaces between the processes of the basal skeleton. It is encrusting to massive, always growing in association with tangled masses of serpulid worms. Colour is apricot to light salmon pink in life. Size up to 40 cm in diameter and 10 cm in height. Basal skeleton is intimately mixed with serpulid worm tubes, superficially marked by numerous upright, multibranched processes, 1.5–2 mm high, with the living tissue extending down into irregular spaces left between the processes. Sclerodermites with aragonite crystals radiating in all directions from centres of calcification usually located around spicule heads. Siliceous are verticillately spined styles, with whorls of spines on the shaft, more or less completely overgrown by the aragonite. Living tissue forms a thin veneer between the processes of the surface of the basal skeleton. The association with serpulids appears obligatory. Depth range: 10–95 m under overhangs of deep fore-reefs. The association with serpulids, which appears to be a good distinctive character for the Caribbean species, is less characterized for the Pacific representative (Hartman & Goreau, 1976), and the genus is possibly synonym with *Ceratoporella* (Hartman & Goreau, 1972; Willenz & Hartman, 1989). Its superficial skeleton, however, is devoid of the regular calicles

highly characteristic of *Ceratoporella*. The distribution is Mostly Caribbean. One species described from the Central Pacific (Hartman & Goreau, 1976).

Petrobiona massiliana is the only species in the Family Petrobionidae Borojevic, 1979, one of the two families in the Order Lithonida Vacelet, 1981 (Fig. 3). *P. massiliana*, is a survivor of fossil 'pharetronids', presently restricted to littoral submarine caves and to bathyal rocky environments between depths of 0.5 and 25m (Vacelet, 2002). This Calcarea has a calcitic massive basal skeleton of high Mg content and is easily accessible in shallow submarine caves. Its growth form alters according to the conditions, subspherical or multilobate with a dead stalk in calm environments and encrusting in high-energy environments. Maximum size is 1.0-1.2 cm and 6cm in diameter for the stalked and encrusting growth forms respectively. The basal skeleton is calcite, with crests and depressions on the surface, in which the white tissue is located, projecting downwards into the caniculi of the basal skeleton. Spicules are randomly arranged in the tissue, and entrapped in the skeleton with no signs of dissolution.

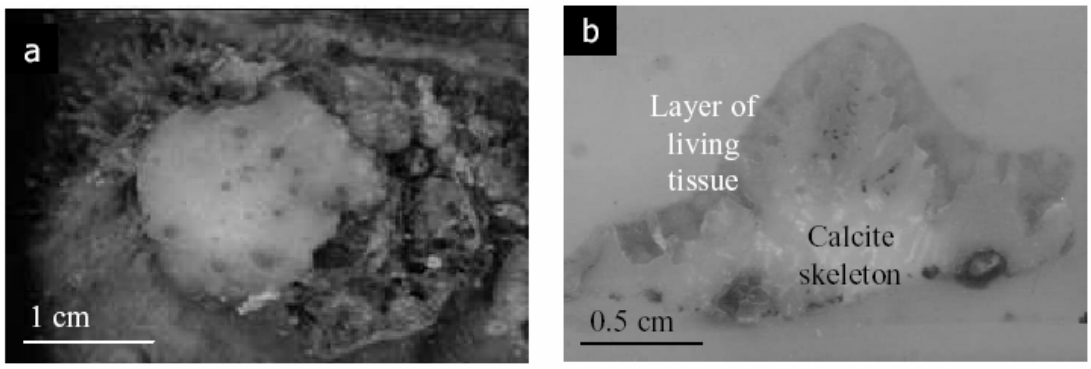

Figure 3. *Petrobiona massiliana*: Specimen *in situ* (a); Cross section through an embedded specimen (b).

2.1.2 Calcein labelling (C. nicholsoni)

Suitable specimens of *C. nicholsoni* were selected in a submarine cave at Pear Tree Bottom, east of Discovery Bay Marine Lab (Jamaica) for the *in situ* calcein incubations. A two litre plastic bag was filled with seawater and placed over the specimen and then sealed around the base of the specimen where it was attached to the cave wall. Calcein was injected into the bag (final concentration 100 mg/L) and left for 24 hours, after which the bag was removed. The specimens were later collected for growth measurements (Fig. 4).

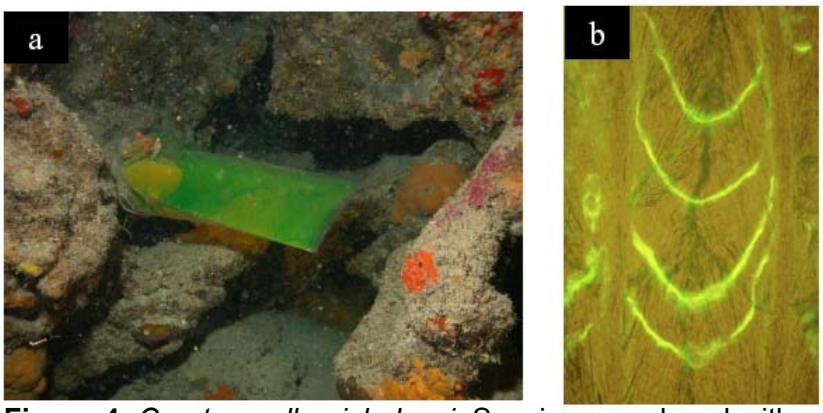

Figure 4. *Ceratoporella nicholsoni:* Specimen enclosed with a plastic bag to perform *in situ* calcein incubation (a); Optical image of skeleton section: Epifluorescence reveals successive calcein marks allowing determination of growth rate (b). (Photo Ph. Willenz).

2.1.3 Collection of *P. massiliana* for laboratory experiments and preparation of plates

Laboratory and uptake experiments were performed on the Mediterranean calcifying sponge *P. massiliana* as these specimens were easily and economically accessible (compared to the Caribbean sponge *C. nicholsoni*). Specimens were collected by SCUBA diving from an underwater cave (Sous la Villa; 3 to 5m depth) just east of the Centre Océanologique de Marseille, South of France. Specimens of less than 0.5 cm in diameter were carefully removed from the substrate and transported to the laboratory in individual containers immediately after collection. The sponges were maintained in aquaria containing seawater at 13°C. A number of sponges were placed into smaller aquaria set up for incubation experiments with particles or bacteria. The remaining sponges were cemented to Plexiglas plates (8 specimens / 12x 12cm plate) with epoxy underwater patching compound (Pettit Paint Co no. 7050 & 7055). Once the cement was dry, the plated sponges were then returned to the cave. The plates had a central hole to allow the plate to be attached with a screw to a pre-prepared cemented screw-plug in the cave wall. This allowed the plate of sponges to be reattached and later collected without direct handling (Fig. 5a).

2.1.4 Calcein labelling (*P. massiliana*)

Three sets of calcein incubations were performed on *P. massiliana.*

The first set of specimens was collected by SCUBA diving in the marine cave 'Grotte du Figuier', Endoume, Marseille (July 1997). The specimens were brought to the laboratory immediately after collection and cemented to Plexiglas plates. Once the cement was dry, the plated sponges were then incubated with calcein (Fluka 21030) dissolved in seawater to give a final concentration of 100 mg/L. After a 24-hour

calcein incubation, the plates holding the sponges were rinsed in seawater and returned to a different sea cave, 'Grotte Sous la Villa' where they were secured *in situ* at 3-5m depth by suspending the plates from ropes in the cave. Two of the surviving plates were collected after 13.5 months for calcein measurement.

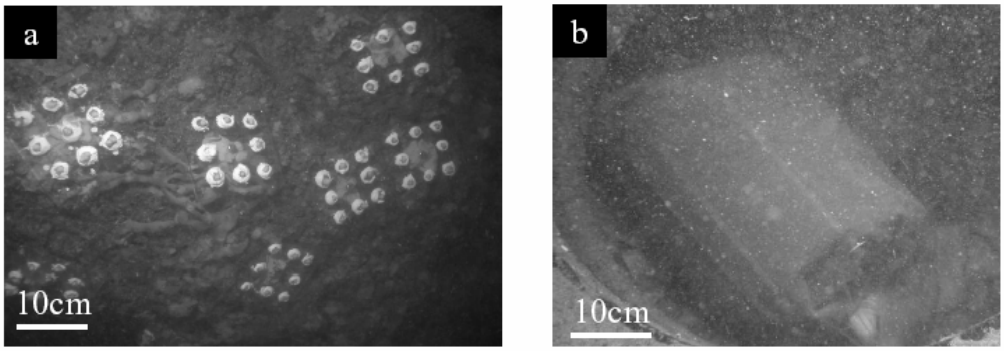

Figure 5. *Petrobiona massiliana*: Specimens glued onto plates and secured with a screw to the original cave wall (a); Incubation with calcein (b). (Photo Ph. Willenz).

Calcein incubations were refined and repeated on a second set of specimens in May 2000. A further 100 specimens were collected from Grotte du Figuier, removed from the substrate and immediately cemented to 20 Plexiglas plates (5 specimens per plate). This time, the sponges were allowed to recover for a few days before *in situ* calcein incubations were performed. For staining *in situ*, the plates were held in a rack, which was enclosed in a plastic bag. Calcein, dissolved in seawater, was injected into the bag to reach a final concentration of 100 mg/L (Fig. 5b). The bag was removed after 24 hours, and the plates secured in the cave with rope. Five plates were collected after 6 months, and the remaining plates collected at 13 months (June 2001).

The remaining 3 plates of specimens still maintained in the cave from the first set were relabelled with calcein a second time (this time *in situ*) in August 2000 (37 months after initial plating). The plates were collected 18 months later (February 2002), forming set 3.

2.1.5 Growth rate measurements

Specimens were dehydrated in a graded alcohol series and embedded in Spurr's medium (Spurr, 1969). Sections parallel to the growth axis were cut with a low speed diamond saw (Bennet Labcut 1010) and mechanically ground using diamond grinding disks (Beuhler ULTRAPREP^{TM}) on a semi-automatic grinder (Buehler Minimet 1000) to a thickness of 5-10µm. Cleaned sections were observed using epifluorescence and differential interference contrast (DIC) (Nikon Optiphot-2 microscope, excitation filter 340-380 nm, barrier filter 420 nm) microscopy.

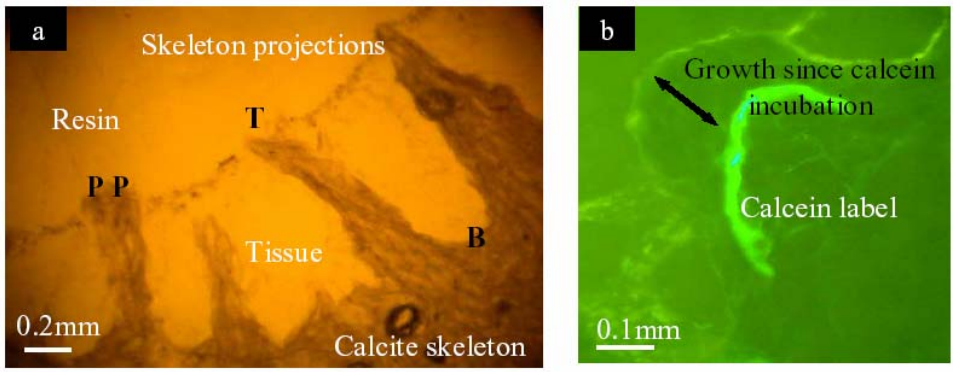

Figure 6. *Petrobiona massiliana*: Optical image showing skeletal cross section (a). Points of measurement (black labels) are indicated as T (tip of the skeletal projections), P (parallel to the top surface along wide skeletal projections), and B (base between projections); Example of tip measurement (b): Epifluorescence reveals calcein mark near the tip of a skeletal projection.

Growth was measured as the linear extension along the growth axis between the calcein label and the new surface of the skeleton, or between calcein labels where calcein incubations had been performed on the same specimen over consecutive years, using the techniques outlined in Willenz & Hartman (1985, 1999) (Figs. 4b and 6) for *C. nicholsoni* and *P. massiliana* respectively).

2.1.6 Analysis of growth measurements

The data did not fit the normal distribution (Kolmogorov-Smirnov test), hence non parametric tests were used. The mean annual growth rates measured over 13 months immediately after plating and over 18 months (37 months after initial plating), as well as the differences between specimens, were compared using the Kruskal-Wallis non-parametric 1-way ANOVA . Significant differences were concluded at the $p < 0.005$ level.

2.1.7 Incubation experiments with strontium and barium

The plates prepared with sponges and returned to the cave were left for eight months, allowing the sponges plenty of time for recovery, after which *in situ* incubation experiments were performed with strontium and barium. The plates were placed in a plastic bag filled with ambient seawater and sealed, and the metal solution (either $SrCl_2$ or $BaCl_2$) was injected into the bag (Fig. 7). A second bag was placed around the first incubation bag chamber and a lead weight placed inside before sealing, to ensure that the bag would remain in place, with the plate holding the sponges in position during the incubation. The incubation was performed *in situ* over 24 hours, and a final dive performed to collect the plated sponges. The sponges were returned to the laboratory and either chemically fixed (Eisenman & Alfert, 1982;

Willenz & Hartman, 1989, Van der Wal *et al*., 1985) or cryoplunged into isopentane and freeze substituted (Ryan *et al*., 1987).

Figure 7. *Petrobiona massiliana*: Pre-plated specimens prepared for *in situ* incubations with trace metals. (Photo Ph. Willenz).

2.1.8 Fixation techniques

2.1.8.1 Chemical fixation 1

Sponges were fixed in two solution: Solution A (4% glutaraldehyde in 0.2M sodium cacodylate buffer; pH 7.4, supplemented with 0.35M sucrose and 0.1M NaCl to obtain a final osmotic pressure of 1700, OsM) and solution B (1% osmium tetroxide in 0.2M sodium cacodylate supplemented with 0.3M NaCl to obtain a final osmotic pressure of 1040 mOsM) (Eisenman & Alfert, 1982; Willenz & Hartman, 1989). Sponges were fixed overnight in Solution A at ambient temperatures, washed six times in the same buffer and postfixed for 3 h in Solution B prior to dehydration in a graded EtOH series.

2.1.8.2 Chemical fixation 2

Samples were fixed using a series of solutions containing glutaraldehyde and K-pyroantimonate for the precipitation of divalent ions (Van der Wal *et al*., 1985): (1) 3% glutaraldehyde, 9 mM potassium oxalate, 0.4 M sucrose for 2-4 h at 4°C; (2) 90 mM potassium oxalate, 0.4 M sucrose for 1.5 hr at 4°C; (3) 90 mM potassium oxalate 0.2 M sucrose overnight at 4°C; (4) 1% osmium, 2% pyroantimonate for 2h at 4°C; (5) 2% pyroantimonate for 45 min at 4°C, repeated twice, initially at pH 7.4, then pH 10. All solutions (unless specified) at pH 7.4, adjusted with KOH. Samples were put through an ethanol dehydration series prior to embedding in Spurs resin.

2.1.8.3 Cryo-plunging and freeze-substitution

Sponge samples of 1mm^2 fragments were plunged into liquid isopentane (-170°C to -196°C) cooled in liquid N_2 (Ryan *et al*., 1987). The specimen remained in the liquid iso-pentane for 30 s and was then transferred to a cryotube containing liquid N_2. All cryoplunged specimens were stored in a dry carrier containing liquid nitrogen and transferred to the laboratory in Belgium for processing until freeze-substituted and embedded in resin. For freeze-substitution, frozen samples were placed in a precooled cryotube containing acetone at –85°C. Fixative (2% osmium tetroxide) was added after 3 days so that cell components would be stabilised (fixed) immediately on removal from liquid nitrogen (McDonald, 1999). After 18 h with the Osmium tetroxide, the temperature was raised 2°C/h from –85°C to –30°C, the solution changed to pure acetone, and the temperature increased again by 2°C/hr until 4°C was reached. Samples were maintained at 4°C for 8 h prior to further temperature increases (2°C/h) until room temperature (22°C). Samples were put through an ethanol dehydration series prior to embedding in Spurs resin.

2.1.9 Embedding and sectioning

Samples were embedded in Spurrs resin for sectioning. Both the freeze-substituted and chemically-fixed specimens underwent stepwise embedding in EtOH/Spurrs (30, 70, and 100%). The infiltration times were 6h at each resin concentration followed two changes of 100% spurrs. Polymerisation was completed at 60°C (333K) for 12 hours. Resin-embedded specimens were either sliced for direct viewing and analyses in the SEM, or sectioned on a Reichert Ultracut microtome for viewing and analyses in the STEM. In addition, the blockface of the specimens sectioned for STEM were also prepared for viewing and analyses in the SEM.

2.1.10 Elemental analysis of samples

2.1.10.1 STEM / EDX

Semi-thin sections (0.25 – 0.3 µm) were mounted onto carbon grids for STEM / EDX analyses, performed using a Philips CM30-T scanning transmission electron microscope (STEM) with a thin-window EDX detector (Link). Sections were viewed in the scanning transmission mode at 200 keV at various magnifications.
Analyses were carried out using the analytical programme Link Isis. The point-to-point resolution of the microscope was 0.23 nm and the information limit was 0.14 nm.

2.1.10.2 SEM / EDX / FIB

For analysis of sliced sample blocks and the sample block faces (after sectioning on the microtome), specimens were fixed to SEM stubs using carbon-paint, ensuring that the carbon paint connected the surface of the specimen with the stub. The surface was then carbon coated to reduce specimen excitation. Specimens were analysed in an SEM, equipped with an Energy Dispersive X-ray (EDX) system. Analyses were performed at 5 kV and a 52° tilt angle was used for EDX collection. Focused ion beam (FIB) - milled sections were taken from metal hotspots located using SEM/EDX for further TEM investigations.

2.1.11 SEM of the skeleton

The organic matter was removed using Perhydrol 15% H_2O_2. The bare skeleton was sputter-coated with gold and observed with a Philips XL30 ESEM TMP scanning electron microscope at 15 and 25 kV.

2.1.12 Collection and analysis of lead in *Ceratoporella nicholsoni* and *Stromatospongia vermicola* skeletons

Five *C. nicholsoni* (from Jamaica and Acklins Island) and one *S. vermicola* (from Turks and Caicos) specimens were compared for their lead profiles. The Jamaican samples (RB1, RB2 and RB3) were collected in September 1999 from depths of -25 m under overhangs along the fore reef wall near the mouth of the Rio Bueno, Jamaica (18.5°N, 77.5°W) (fig. 8). The Acklins Island specimens, AC1 and AC2 were sampled from approximately -25 m, in respectively in August 1985 and in June 1988 at the southern tip of Acklins Island (22.1°N, 74.3°W), Bahamas. The AC1 sample was used in the study of Lazareth *et al*. (2000). The *S. vermicola* sample from Turks and Caicos (TC1) was collected by manned submersible off the deep fore reef of Turks and Caicos Islands (21.4°N, 71.2°W) at a depth of 130 meters in November 1994. None of the samples, viewed under microscope, presented diagenetic features along the sampled profiles.

Slabs were prepared by sectioning the sclerosponge perpendicular to its surface. For solution ICP analyses, the slabs were drilled approximately every millimetre with a 0.6-mm-drill along the growth axis of the sclerosponge, corresponding to a measurement every 4.5 years. The upper five to nine samples were taken in duplicate, at each side of the 5 mm slab, in order to test the reproducibility of the signal. Powders (~12mg each) were dissolved in 10% bi-distilled HNO_3 and analysed with a Fisons -VG PlasmaQuad II+ ICP-MS. Calibration was done using international

standards DWA-1 and CCH-1 (values from Govindaraju, 1994), two natural rock standards. The analytical uncertainty was <10% (1σ).

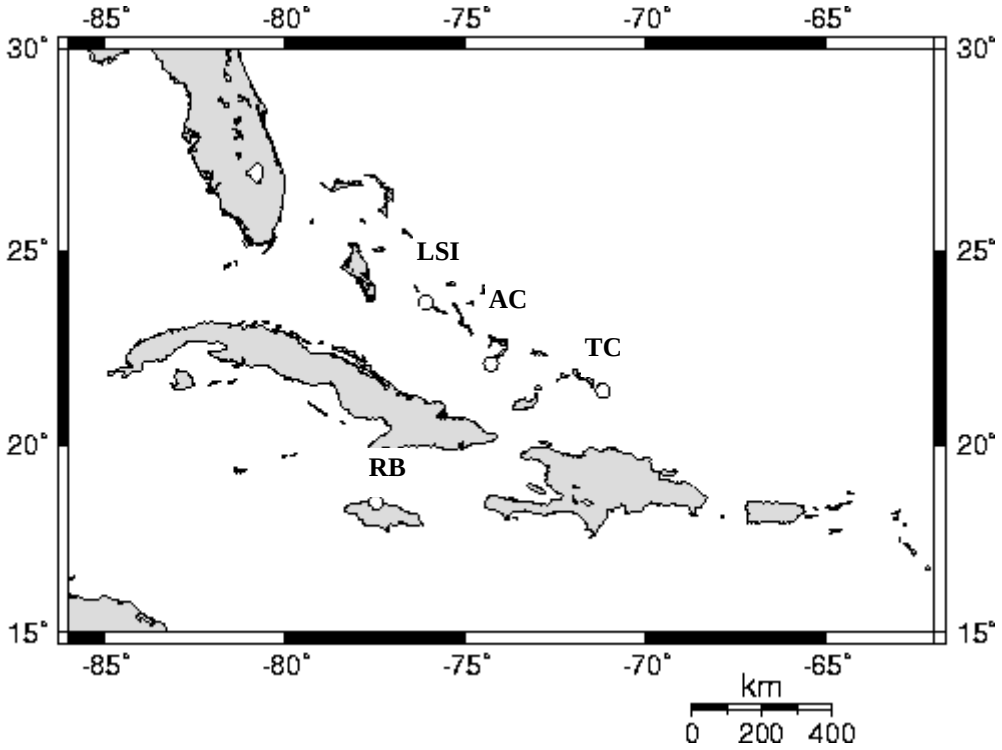

Figure 8. Location of the different sampling sites. RB: Rio Bueno (Jamaica), LSI: Lee Stocking Island (Bahamas), AC: Acklins Island (Bahamas), TC: Turks and Caicos Island (Bahamas).

The skeletons of sclerosponges, unlike corals, do not deposit clear annual increments of calcium carbonate analogous to density banding in zooxanthellate corals. This poses a challenge with regards to increased difficulty of high resolution dating of sclerosponges. Nonetheless, geochemical data can be used to provide additional growth rate information due to the presence of intra-annual cycles observable in high-resolution data, such as that from LA-ICP-MS (Swart *et al*., 2002, Haase-Schramm *et al*., 2003). In absence of this type of high-resolution data for the current project, we assumed that the surface layers of the actively growing sclerosponges were deposited at the date of sampling. We constructed time-series by assuming a growth rate of 233 (±33) µm/yr, which is the mean growth rate of *C. nicholsoni* (Willenz & Hartman, 1999). These hypotheses match the growth rate deduced by Lazareth *et al.* (2000) from the sclerosponges $\delta^{13}C$ profile.

Regressions between the replicate samples (intra-specimen) were calculated using bivariate least squares (BLS) statistics. Unlike ordinary least square regressions, the BLS considers errors on both the dependent and independent variables and is more appropriate for comparison between data having the same error (see Riu and Rius, 1996; Verheyden *et al*., 2005). Inter-specimen reproducibility was tested by separating the Pb profiles into different sections. For sections with significant slopes

(Pb vs year), slopes were compared and when the slope was not significant, the raw data were compared using Student's T-test. Significance tests for the slope and intercept of the regressions and correlation coefficients are based on the joint confidence interval. Errors of the regression coefficients are given as 95% confidence intervals (CI).

2.2 Bivalves

2.2.1 Collection and sample preparation

Four species of bivalves were studied, including three families: Mytilidae (the common blue mussel *Mytilus edulis* (L.)), Veneroidea (both the hard clam *Mercenaria mercenaria* (L.), and the butter clam *Saxidomus giganteus* (DeShayes, 1839)) and Pectinidae (the great scallop, *Pecten maximus* (L.)). *Mytilus edulis* were studied both along the estuarine gradient of the Schelde (The Netherlands and Belgium) and in laboratory settings. The clams *Mercenaria mercenaria* and *Saxidomus giganteus* were collected alive by hand from intertidal sediments in North Carolina (USA) and Puget Sound, Washington (USA), respectively. The great scallop, *Pecten maximus*, were collected either by SCUBA or dredging from the Bay of Brest (France).

Samples were taken from the cross sections of shells (Fig. 9); except for Pecten, where the surface of the left valve was sampled. Typically, the middle or outer layer was sampled, depending on the application and species (e.g., outer for *Saxidomus* and *Mytilus* and middle for *Mercenaria*). Carbonate powders were drilled using a Mercantek MicroMill. Either lines or spots were used, again depending on application and species, typically, a 300 µm bit was used. After drilling, samples were collected using scalpels and were placed in glass inserts and stored at 50 ºC to be later analyzed using a ThermoFinnigan Kiel III (automated carbonate preparation device) coupled to a ThermoFinnigan Delta^{plus}XL dual inlet IRMS. Samples for elemental analysis were transferred to acid washed 2 ml vials and capped.

Tissues were dissected from the shells using a sterile scalpel and were stored at -20 ºC in Eppendorf tubes for elemental analyses or were immediately freeze dried for isotopic analyses. Hemolymph and extrapallial fluid (EPF) were sampled using a sterile needle and syringe and were stored similar to tissues. Hemolymph was extracted from the adductor muscle.

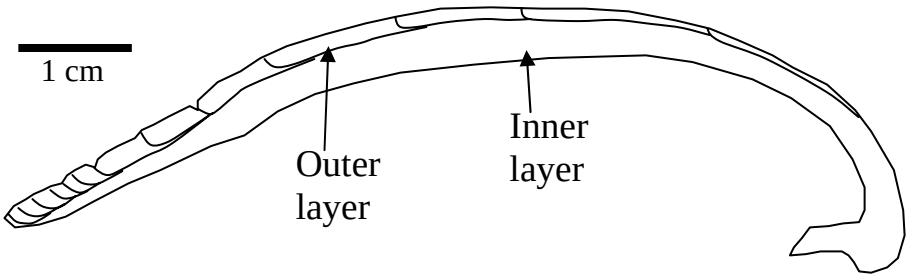

Figure 9. Cross section of *Saxidomus giganteus* shell showing the successive growth increments in the outer layer of the shell.

2.2.2 Field experiments on bivalves

All *Mercenaria mercenaria* (North Carolina, USA) and *Pecten maximus* (Bay of Brest, France) were sampled from their natural habitat. *Mytilus edulis* specimens (~ 3 cm) were collected from the Oosterschelde (The Netherlands; Fig. 10). The Oosterschelde estuary was dammed in the late eighties and now has more or less marine salinities (S > 30; Gerringa *et al*., 1998). Mussels were transported back to the laboratory where epibionts were removed. They were then stained with calcein as in the previously described experiments. Within the next week (on 24 Oct. 2001), 50 mussels were placed into four stainless steel cages and these were deployed along an estuarine salinity gradient in the Westerschelde estuary (Fig. 10; see Baeyens *et al*., 1998 for a general description of the Westerschelde). Cages were attached at the same tidal level as the highest density of 'local' mussels at Ossenisse (OS; the most upstream occurrence of wild *Mytilus* populations), Griete (GR), Hooftplaat (HF), and Knokke (KN; Fig. 1). Water temperature was monitored at each site hourly using a TidBit data logger. Water was sampled monthly for one year (Nov. 2001- Nov. 2002) and every two weeks between March and May for salinity, dissolved Ba/Ca, particulate Ba and chlorophyll a (hereafter, Chl a). $[Ba/Ca]_{water}$ was sampled by filtering 250 to 500 ml of seawater through 0.4 µm polycarbonate filters (Osmonics poretics). The filtrate was acidified with trace metal grade HNO_3 to ~ pH 3. Blanks were prepared by filtering MilliQ water (>18MΩ cm^{-1}) through the same system and blank filter.

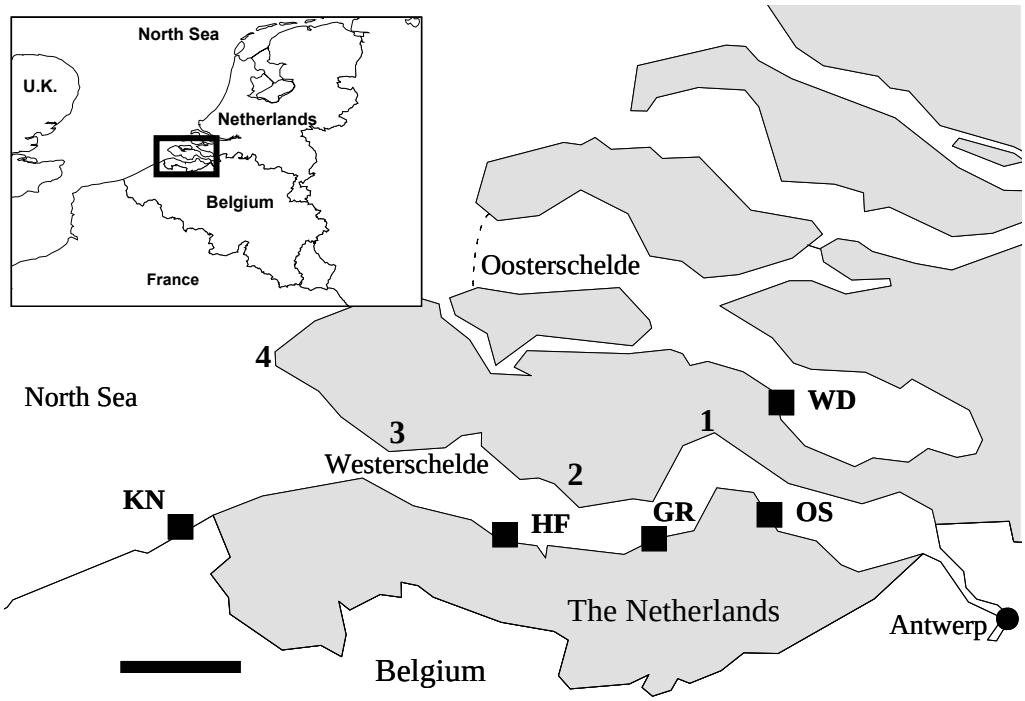

Figure 10. Map of the Westerschelde and Oosterschelde estuaries. The mussel collection site at Wemmeldinge (WD) and the four study sites (barium study) are indicated Knokke (KN), Hooftplaat (HF), Griete (GR) and Ossenisse (OS). Scale bar = 10 km. The numbers refer to sampling stations for the heavy metal study

Mussels were collected on four different dates (29 Sept. 02, 9 Dec. 02, 20 Feb. 03 and 21 Apr. 03). Mussels transplanted to OS did not survive (undoubtedly due to the salinity shock) and therefore local mussels from this site were used. Similarly, the wave action at KN repeatedly destroyed cages and all mussels were lost; so again at this site, mussels from the local population were used.

2.2.3 Laboratory experiments on bivalves

2.2.3.1 Barium incorporation in Mytilus edulis *shells*

Mytilus edulis were collected from the Oosterschelde estuary near Wemmeldinge, the Netherlands (salinity ~ 35; temperature ~ 8 ºC) in March 2004 (Fig. 10). Epibionts were gently removed and the mussels were acclimated to laboratory conditions at 9.2 ± 0.3 ºC (mean ± standard deviation) for 7 days, then another 14 days at 14.7 ± 0.2 ºC (*i.e.*, 21 days acclimation; temperature monitored hourly with a TidBit data logger). During acclimation, mussels were fed three times per week with 12 mg of dried yeast per animal per week (Artemic Systems, LANSY PZ). After the acclimation period, 40 mussels (2.8 ± 0.3 cm length) were selected for the 'dissolved Ba' experiment and were stained with calcein (200 mg l^{-1}; $C_{30}H_{26}N_2O_{13}$; Sigmal Chemical) for 20 hours to mark the beginning of the experiment in the shell (see Rowley and Mackinnon, 1995). Afterwards, 10 mussels were placed in each of four aquaria containing 10 l of filtered

(10 µm) North Sea water spiked with approximately 0, 110, 220 and 440 nmol l^{-1} of Ba (as $BaCl_2$) (Table 1). Water was continuously circulated through acid washed plastic filters (except during feeding periods, see further) and was aerated. Mussels were fed the same quantities of yeast as during the acclimation period. Feeding took place for three hours, three times per week. Mussels were fed in their separate aquaria during which the filtration pumps were turned off. This experiment ran for 36 days, during which the water in all tanks was changed weekly (similar to Lorens & Bender, 1980) and was maintained at 16.4 ± 0.6 ºC with a pH of 7.9 ± 0.1 and salinity of 36.4 ± 0.9 (on occasion salinity was adjusted with MilliQ water (>18MΩ cm^{-1}) to compensate for evaporation; pH and salinity were measured with a WTW multiline P4 multimeter). Water samples were taken two times per week for $[Ba/Ca]_{water}$ using syringe filters (Macherey-Nagel; Chromafil A45/25; cellulose mixed esters; 0.45 µm pore size), once just before and after a water change, and were acidified with trace metal grade HCl to ~ pH 3. Procedural blanks were also taken by filtering MilliQ water (>18MΩ cm^{-1}).

Table 1. Summary of average seawater $[Ba/Ca]_{water}$ (µmol/mol; ± SE) for each laboratory $[Ba/Ca]_{water}$ treatment group. N = 8 water samples per treatment, spread over the experiment.

Tank	Treatment *	$[Ba/Ca]_{water}$ (µmol/mol)
1	Ambient	5.08 ± 0.22
2	+110 nmol l^{-1}	19.38 ± 0.71
3	+220 nmol l^{-1}	36.34 ± 0.91
4	+440 nmol l^{-1}	65.05 ± 2.37
5	Feeding*	4.61 ± 0.45

*see text

To assess the effect of Ba being ingested as food, a feeding experiment was conducted. In a fifth aquarium, two plastic mesh baskets, each with 10 mussels were held under the same conditions, except that there was 20 l of water to compensate for the higher density of animals and they were fed differently. These mussels were fed in separate aquaria with different foods. One batch was fed a slurry of living phytoplankton (*Chlamidomonas reinhardii*) grown in a 'normal' Tris-Acetate-Phosphate (TAP) medium (hereafter referred to as phyto +0) with the phytoplankton containing 5.87 ± 0.51 nmol g^{-1} dry weight (DW) Ba (n = 3), whereas the other batch were fed the same phytoplankton species, which were grown in a Ba rich TAP medium (spiked with 730 nmol l^{-1} Ba; hereafter referred to as phyto +100; see Steenmans (2004) for more details regarding phytoplankton culturing) with [Ba] = 14.56 ± 0.95 nmol g^{-1} DW (n = 3). Both batches were fed for 1 hour per day, five days per week, with a total of 18 mg phytoplankton (DW) per animal per week. This provided three levels of Ba in food given to mussels maintained in normal seawater

Ba concentrations (*i.e.*, yeast (with [Ba] = 3.35 ± 0.32 nmol g^{-1} DW (n = 3)), phyto +0 and phyto +100). After feeding, mussels were returned to their aquarium. This experiment was run for 29 days; water maintenance and sampling was similar to the dissolved Ba experiment.

After the experiments were completed, mussels were removed from their aquaria one at a time and were sampled for hemolymph, soft tissues and shells. Hemolymph was sampled by blotting the shell dry, and then gently prying open the valves with a scalpel, draining the mantle cavity and then sampling the hemolymph from the adductor muscle with a sterile 5 ml syringe and needle. Procedural blanks were prepared by drawing MilliQ water into a new syringe and injecting it into a micro-centrifuge tube. Whole tissues were dissected from the valves using a scalpel. Samples (hemolymph and tissues) were transferred to micro-centrifuge tubes and were immediately frozen to -20 ºC until analysis. Shells were rinsed with MilliQ water (>18MΩ cm^{-1}) and were air dried.

A condition index was used to compare mussel health at the end of the experiments ([shell length / shell width] / tissue dry weight) to mussels health at the end of the acclimation period (beginning of experiments), which indicated that all animals were healthy (ANOVA, LSD test, $p > 0.05$ for all).

2.2.3.2 Metal uptake in mussels: Mechanisms and available pathways

Mussels used in these experiments were collected from Westkapelle on the Dutch coast (Fig. 10). Before use in the experiments, animals kept in clean artificial seawater at 15 °C for 21 days during which they were fed a daily ration of 0.5 mg per individual with enriched yeast cells Lansy PZ (INVE Technologies, Belgium).

Experiments were conducted with chemically defined seawater, which was prepared by dissolving analytical grade salts (Merck KGaA, Germany) in deionised water as described in Vercauteren & Blust (1999). In the experiments to study pathways involved in metal uptake, solutions of inhibitors of different pathways and mechanisms were prepared by dissolving the chemicals in clean seawater. The concentrations used were 250µM $LaCl_3$, 250µM diltiazem, 100µM nifedipine, 250µM verapamil, 0.5mM DIDS, 1.0mM ouabain, 1.0mM NaCN, 1.0mM and 2,4-dinitrophenol. The conditions and concentrations used were adapted from literature (George and Coombs, 1977; Carpene and George, 1981; Vercauteren & Blust, 1999; Endo *et al*. 1998).

Isolated gills were individually exposed in at four levels of dissolved metals 0 µM (control), 0.25 µM, 0.5 µM and 1.0 µM, and at time intervals (0, 20, 40, 90, 130 and

180 minutes) seven gills were sampled from each solution and samples were prepared for metal measurements according to a standardized protocol (Mubiana & Blust, *in press*). Metals in the final solutions were measured with ICP-MS (UltraMass 700, Varian, Australia). Metal uptake kinetics in the gills was then modelled using single compartment metal accumulation models for linear uptake (Ag, Pb) and a non-linear model [Eq 2] (Ca, Cd, Co, Cu, Hg).

$$CG_t = CG_0 + k_u C W t \qquad [1]$$

$$CG_t = CG_0 + \frac{k_u}{k_e} C W \left(1 - e^{-k_e t}\right) \qquad [2]$$

where, CG_t is gill metal concentration (nmol/g) at time t (h), CG_0 is initial gill metal concentration (nmol/g) prior to experiment, CW is dissolved metal concentration (µM) in solution, k_u and k_e are the uptake and elimination rate constants (h^{-1}), respectively.

To study pathways involved in metal uptake, gills first incubated in inhibitor solutions for 30 minutes prior to exposure to metals. At the end of metal exposures gills prepared for metal analysis and measured with ICP-MS as described earlier.

In the case of calcium, due to naturally high calcium in seawater, uptake experiments were performed using radioactive ^{45}Ca as a tracer. The exposure water was spiked with 740 kBq/L of radioactive ^{45}Ca and at the end of the exposure calcium uptake rate in the gills (nmol/g/h) was then calculated according to the expression:

$$Ca^{2+} \text{ uptake rate (nmol/g/h)} = A / (60\, E\, W\, t\, S)$$

where A is ^{45}Ca activity (cpm) counted in the gills after exposure, E is counting efficiency of the tracer, W is the gills dry weight (g), t is exposure time (h) and S is specific activity of ^{45}Ca exposure (Bq/nmol).

2.2.3.2 Effects of environmental variables, temperature, salinity and dissolved organic matter on metal uptake in Mytilus edulis

Mussels used in the experiment were collected from Wemeldinge in the clean part of the Scheldt estuary (Eastern Scheldt, Fig. 10). They were acclimation to laboratory conditions for 3 weeks. In the case of salinity and temperature experiments, animals were further acclimated for another 3 weeks to respective experimental temperatures and salinities. Metal exposures were set but sufficient to result in measurable accumulation. Metals were introduced in the tanks 3 days prior to start of the experiments, this allowed concentrations to stabilize and Table 2 shows the

measured concentrations at the start of the experiments. The standard deviations indicate variations among the test tanks.

Table 2. Average dissolved metal concentrations (µg/L) in the exposure water during the different experiments

	Ag	**Cd**	**Co**	**Cu**	**Pb**
Salinity Expt	2.0 (0.1)	8.6 (0.2)	6.6 (0.2)	5.6 (0.1)	3.4 (0.1)
Temperature Expt	1.0 (0.04)	3.2 (0.1)	3.0 (0.1)	4.1 (0.2)	2.2 (0.1)
Humic acid Expt	1.5 (0.05)	4.3 (0.1)	4.0 (0.1)	4.5 (0.2)	3.1 (0.1)

With the exception of the salinity experiment, metal exposures lasted 28 days during which a sub-samples of 7 -10 individuals were sampled at time interval and analyzed for metal content. At the end of 28 days, mussels were transferred in clean water for the elimination phase during 28 days. During that period water was changed twice a week in the first 2 weeks and then weekly for the remaining 2 weeks. 7 -10 individuals were sampled from each tank at time interval and measured for metal content.

Metal measurements in the tissues were according to standard protocols (see Mubiana *et al*., 2005). Soft tissues were dried in the oven, 5 ml nitric acid and 0.25 ml hydrogen peroxide were added and the mixture was heated in a microwave for 20 minutes in four steps of 5 minutes at starting at 80, 120, 200 and 280 watts. Metal concentrations in the final solutions were then measured with ICP-AES and for low concentrations ICP-MS was used.

2.3 Echinoderms

2.3.1. Laboratory Experiments

2.3.1.1 *Juvenile* Asterias rubens

Three aerated, temperature controlled closed circuit aquarium systems each containing 1200 litres of seawater at a salinity of 32 were used. A batch of 200 juvenile *A.rubens* of 15-25 mm arm length was collected at Knokke on October 27th 2003. These were acclimated at 14 °C to for 25 days. At the end of this period 20 individuals were frozen at -20°C. Each aquarium system was fitted with 3 Plexiglas containers (25 l) and 20 juveniles were put into each of the nine aquaria. Size distribution was identical between the aquaria. At the beginning all three systems were set at a temperature of 14 °C. Temperature in two systems was then modified

by 1 °C/day to reach the desired temperatures of 9 °C (system A), 14 °C (system B) and 17 °C (system C). The experiment lasted 4 months from November 21, 2003 to March 22, 2004. Stowaway Tidbit Temp Loggers were used to monitor temperature in the 3 systems at intervals of 8 hours. Actual temperatures (mean ± sd) over the 4 month period were 9.2 ± 0.2 °C (A), 13.6 ± 1.1 (B) and 16.2 ± 0.8 (C). The starfish arm length was measured monthly and food was provided in excess using 3 different batches of mussels of appropriate size (8-25 mm). All starfish grew at the same rate at the three temperatures (Fig. 11). Water quality measurements were carried out twice a week. Salinity and pH were measured using a WTW Multi 340i multi-meter equipped with a conductivity cell and a pH electrode. Nitrites and Nitrates were measured using Tetra ready-to-use tests. Salinity was adjusted to compensate for evaporation in system C (17 °C) by adding tap water and for condensation in systems A (9 °C) and B (14 °C) by adding Instant Ocean sea salts. Arm length of the animals was measured using a slide calliper (precision of 1 mm) from the centre of the mouth to the end of the arm. At halftime (January 20, 2004), the starfish were divided into size classes and half of the individuals of each size class were frozen. The remaining half was sampled at the end of the experiment.

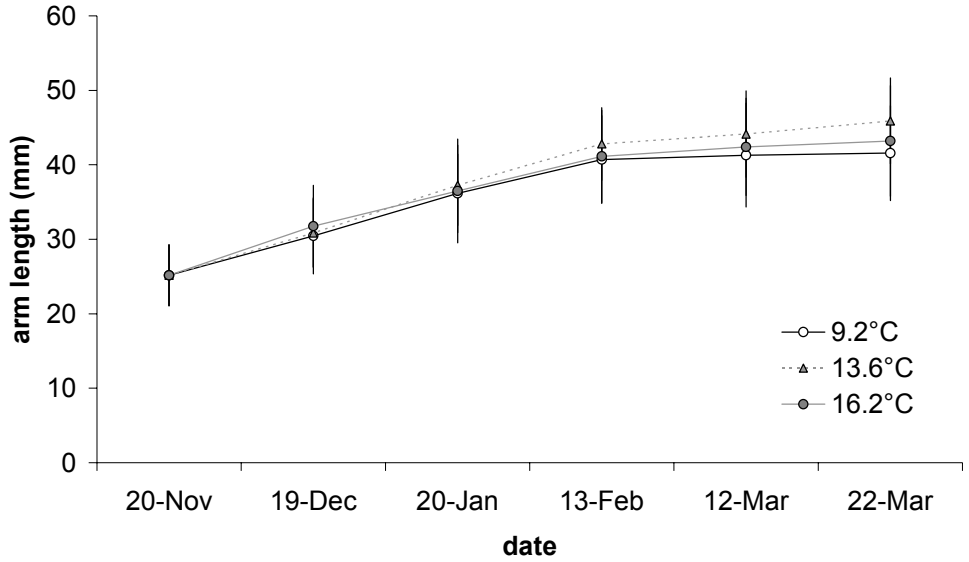

Figure 11. Growth rate of juvenile starfish raised in aquaria a three different temperatures

Every two weeks water samples were taken in threefold replicates from the three different systems using 50 ml acid cleaned NALGENE recipients and then stored at -20 °C; in total 90 water samples were taken. Tissue samples were taken from two of the largest individuals of every mussel batch used and stored in polyethylene containers at -20 °C.

Newly formed parts of juvenile arms were determined using the monthly measurements and fitting normal curves to size frequency distributions (data not shown). 5 mm length of newly formed arm (distal end) was sampled from each starfish collected after 2 and 4 months. Each segment was put into an acid-rinsed Petri dish and immersed in analytical grade 2M NaOH to remove organic tissue. Petri dishes were mildly stirred throughout the cleanup. The NaOH solution was replaced once. The segments stayed immersed till all the ossicles were completely detached from one another and no trace organic matter was visible through a stereomicroscope. This method was checked using scanning emission microscopy (SEM).

Clean ossicles were rinsed 3 times in MilliQ water for 5 minutes. All manipulation of the ossicles was done by using 3 ml polyethylene pipettes. Ossicles were air dried overnight. Dry ossicles were recuperated using a thin brush, weighed and stored in acid-washed Eppendorf tubes.

2.3.1.2 Regeneration of Paracentrotus lividus *spines*

Spines of *P. lividus* were regenerated over a period of 10 weeks (1st batch) and 4 weeks (2nd batch). A Plexiglas container (25 l) with 6 *P. lividus* was put into each of the three aforementioned systems. Regeneration of the spines was induced by cutting half of the spines with stainless steel scissors on an easy to find area of the sea urchin. The regenerated spines were sampled with aid of stainless steel tweezers and a scalpel. Cleanup was carried out as described for juvenile starfish ossicles.

2.3.2 Field and historical samples

Starfish and sea urchins were sampled by SCUBA diving, dredging or collecting at low tide at multiple sites along a large latitudinal and thus temperature gradient (Table 3). Starfish were cut open at the distal ends to remove the coelomic fluid. Sea urchins were opened by cutting around the peristomial membrane to remove the inner organs and the Aristotle's lantern. All samples were air dried onsite or at 45 °C in a drying oven. Dry samples were stored in clean polyethylene bags. Whole starfish were immersed in acid cleaned Teflon beakers containing analytical grade 2MNaOH at 40-50 °C until all organic matter was dissolved. If necessary, the NaOH solution was replaced once and the clean skeleton was rinsed 3 times in MilliQ water. After a drying step at 45 °C overnight the skeleton was ground to a fine homogenous powder on an FRITSCH Pulverisette orbital grinder and stored in acid cleaned polyethylene containers.

Table 3. List of sea urchin samples collected in this study.

Species	Location	Latitude	Longitude
Tripneustes ventricosus	France, Caribbean, Guadeloupe, Pointe d'Antigues	16.44 N	61.54W
Tripneustes ventricosus	Jamaica, Caribbean, Pear Tree Bottom	18.15N	77.30W
Tripneustes gratilla	Reunion, Indian Ocean, Hermitage Reef	21.04S	55.22E
Tripneustes gratilla	Madagascar, Indian Ocean, Toliara	23.20S	43.41E
Sphaerechinus granularis	Greece, Mediterranean, Antiparos	37.04N	25.08E
Sphaerechinus granularis	Portugal, Atlantic, Azores, São Jorge	38.55N	27.77W
Sphaerechinus granularis	France, Mediterranean, Marseille	43.3N	5.4E
Sphaerechinus granularis	France, Atlantic, Brest	48.4N	4.48W
Strongylocentrotus droebachiensis	Norway, North Sea, Sørfjørd	60.41N	6.53E
Strongylocentrotus droebachiensis	Norway, North Sea, Bødø	67.28N	14.38E

Historical samples of starfish and sea urchins were obtained through courtesy of the Belgian and the French Natural History Museums. Only dry preserved specimens were used to avoid possible post-mortem changes in the skeletal composition (Renaud et. al 1995). Cleanup of the skeleton and mineralization was achieved by the same means as for field samples.

2.3.3 Mineralization and Analysis

Upon thawing, water samples were diluted 20 times and immediately analysed. Ossicles of juvenile and adult starfish were mineralised in 1 ml of 1.8% (v/v) H_2O2 and 6.3% HNO_3 in acid rinsed Eppendorf vials. This base solution was diluted between 20 and 100 times and analysed.

Mussel samples were thawed and dried at 60 °C in an oven during two days. 0.25 g of sample was mineralised in a Milestone 1200 mega microwave oven in a closed Teflon beaker containing 3.5 ml of 27.3% HNO_3 and 8.6% H_20_2, filtered over a GF/A Whatman filter with 1.6 µm pore size, and brought to a final volume of 25 ml. This base solution was diluted 25 times for analysis.

Spines were cut into regenerate and stump with the aid of a scalpel and a stereomicroscope and analysed separately. Mineralization was carried out in an acid rinsed NALGENE tube in 1ml of 1.8% H_2O2 and 6.3% HNO_3, brought to a final volume of 5.5 ml by adding MilliQ water and diluted two times for analysis.

For field and historical samples, 0.2 g of powdered skeleton were mineralized in a Milestone 1200 mega microwave oven in 2 ml of 63% HNO_3 and 1.8% H_2O_2, filtered

over a GF/A Whatman filter, brought to a final volume of 20ml with MilliQ water and diluted between 5 and 10 times for analysis.

The major and minor elements Ca, Mg, Sr and S were analysed on an IRIS Advantage (Thermo Jarrel Ash) Induced Coupled Plasma Atomic Emission Spectrometer (ICP-AES). Calibration was achieved using artificial multi-elemental solutions made from certified mono-elemental solutions (ICP standard solution 1000 µg/ml, Alfa Johnson Matthey, Germany) and two international natural standards: DWA-1 and CCH-1. The error of the measurements ranged between 5-10%, depending on the concentration of the analyzed solution.

Trace elements Ba, Cu, Zn, Pb, Co and Cd were analyzed with a VG Plasma Quad and (FISONS) Inductively Coupled Plasma Mass Spectrometer (ICPMS). Indium was used as an internal standard and added to each sample to compensate for machine drift and matrix effects. Calibration was carried out according to the ICP-AES method. The error of the measurements ranged between 2-5%, depending on the concentration of the analyzed solution (see below).

2.4 Analytical procedures

2.4.1 Isotopic analyses

2.4.1.1 Carbonates

The Kiel III is simply an automated carbonate preparation device that works using the method originally outlined by McCrea in 1950. Briefly, carbonates are reacted with 100% phosphoric acid at 70 ºC for six minutes, and are then cryogenically purified using liquid nitrogen. The reaction of phosphoric acid with $CaCO_3$ produces solid calcium hydrogen phosphate, water, and carbon dioxide through the following chemical reaction:

$$CaCO_3 + H_3PO_4 \rightarrow CaHPO_4 + H_2O + CO_2$$

The standard used for correction in our laboratory is MAR1, produced by the University of Gent, Belgium. The NBS-19 standard was run to check for accuracy. Furthermore, NBS-18 is sporadically run, also to check for accuracy. Both NBS-19 and NBS-18 illustrate that these analyses are very precise and accurate (see table 4).

Table 4. Long-term (Nov. 2003 – Oct. 2004) NBS-19 and NBS-18 data corrected using MAR1.

	NBS-19		NBS-18	
	$\delta^{13}C_{VPDB}$ (‰)	$\delta^{18}O_{VPDB}$ (‰)	$\delta^{13}C_{VPDB}$ (‰)	$\delta^{18}O_{VPDB}$ (‰)
Actual	1.95	-2.20	-5.04	-23.05
Measured‡	1.93	-2.19	-5.03	-23.06
SD‡	0.039	0.085	0.068	0.111
N	292	292	22	22

‡ Mean and standard deviation; N = total number of standards run

2.4.1.2 Organics

Dry tissues were homogenized using an agate mortar and pestle and were prepared following Bouillon (2002). Briefly, one mg of homogenized tissue was subsampled and placed in a silver cup (5 x 12 mm). The sample was then decalcified by adding a few drops of dilute HCl in situ, after which the sample was dried for 24 hours at 60 ºC and folded closed.

Samples were analyzed for $\delta^{13}C$ with an Element Analyzer (Flash 1112 Series EA ThermoFinnigan) coupled via a CONFLO III to an IRMS (Delta^{plus}XL, ThermoFinnigan). Sucrose was used as a standard (IAEA-CH-6, $\delta^{13}C$ = -10.4 ± 0.1 ‰). Results are reported using the conventional δ notation relative to the VPDB standard. The analytical precision of the method is on the order of 0.1 ‰. Using this same instrument and method, Verheyden *et al*. (2004) report a long term analytical precision of 0.08 ‰ on 214 analyses of the IAEA-CH-6 standard (1σ).

2.4.1.3 $\delta^{18}O$ of water

Water samples for $\delta^{18}O$ ($\delta^{18}O_W$) analysis were taken by filling 100 ml polyethylene containers and adding 60 µl of supersaturated $HgCl_2$ solution (7 g per 100 ml). Containers were capped tightly and wrapped with Parafilm to avoid evaporation and were stored at room temperature. All water $\delta^{18}O$ was measured using the CO_2 equilibration technique of Epstein and Mayeda (1953). The procedure for measuring $\delta^{18}O_W$ is modified from Prosser *et al*. (1991), where equilibration and gas extraction is done directly in a headspace vial. Ten ml headspace vials were first flushed with He gas and are capped with a rubber septum and aluminum seal. Approximately 500 µl of sample water was injected into the vial, then 200 µl of pure CO_2 from a tank was injected using a gas tight syringe. The samples were then placed in a shaker for 2 hours and left to equilibrate for about 24 hours for freshwater and more than 48 hours for seawater at ambient laboratory temperature (± 23 ºC). In addition to samples, two in-house well-calibrated (against VSMOW, GISP and SLAP) secondary standard

water samples were similarly processed (a seawater (SW1) and tap water (TAP0409) standard; see Gillikin, 2005). After equilibration, 1000 µl of CO_2 from the headspace is drawn into a gas tight syringe and is injected into the carrier gas stream after the combustion columns of a ThermoFinnigan Delta^{plus}XL continuous flow IRMS. Precision was better than 0.15 ‰ (1σ), determined by repeated analysis of the seawater standard and replicate sample analyses.

2.4.1.4 $\delta^{13}C$ of dissolved inorganic carbon

Water samples for determination of $\delta^{13}C$ of dissolved inorganic carbon (DIC) were sampled by gently over-filling headspace vials (25, 20, 10 or 6 ml) with seawater. Sixty µl of supersaturated $HgCl_2$ solution was added and the vials were capped and stored at room temperature until analysis. A method slightly modified from Salata *et al*. (2000) was used for $\delta^{13}C_{DIC}$ analysis. A headspace was created by inserting an empty, fully depressed, syringe and needle through the septum, then inserting a needle attached to a He bottle, until the required volume of water has been replaced. After the He syringe is removed, the pressure is equalized in the other syringe. Once the headspace is created, 99% phosphoric acid was added. Samples were shaken, and placed on their side or turned upside down so that there is no contact between headspace and septum to reduce the possibility of exchange with atmospheric CO_2. Samples were allowed to equilibrate for one day in a sample shaker.

To correct for the partitioning of CO_2 between headspace and the water phase and to calculate the $\delta^{13}C$ of the total DIC, the equation of Miyajima *et al*. (1995) was used:

$$\delta^{13}C_{DIC} = \frac{V_{headspace} * \delta^{13}C_{measured} + \left(V_{bottle} - V_{headspace}\right) * \beta * (\delta^{13}C_{measured} + \varepsilon_g^a)}{V_{headspace} + \left(V_{bottle} - V_{headspace}\right) * \beta}$$

where □ = 0.872 at 23 °C (Ostwald solubility coefficient); ε_g^a is calculated from □ = -373 / T(K) + 0.19 thus □= -1.07 at 23 °C; V_{bottle} and $V_{headspace}$ = internal volume of sampling vial and headspace volume, respectively. These data were further corrected using calibrated CO_2 gas (from a tank), which is injected periodically throughout the analysis period. Typically, the standard deviation of this gas was less than 0.2 ‰ for the day.

2.4.2 Elemental analyses

2.4.2.1 HR-ICP-MS

Carbonate powders for high resolution ICP-MS (HR-ICP-MS; ThermoFinnigan Element2) were dissolved in a 1 ml 5% bi-distilled HNO_3 solution containing 1 $\mu g\ l^{-1}$ of In and Bi, which were used as internal standards. Multi-element calibration standards were prepared from certified single element stock solutions. The isotopes ^{111}Cd, ^{135}Ba, ^{208}Pb were analyzed in low resolution, and ^{11}B, ^{26}Mg, ^{43}Ca, ^{55}Mn, ^{59}Co, ^{65}Cu, ^{86}Sr were analyzed in medium resolution. Four reference materials were run MACS1, CCH1, and two in-house shell standards (S-gig and M-ed). The MACS1 is a pressed powder carbonate standard developed by S. Wilson of the USGS. The natural limestone standard, CCH1 was run to obtain accuracy for Mg/Ca and U/Ca (data from Govindaraju, 1994), for which there are no data for MACS1. The in-house standards, were produced from a *S. giganteus* shell (S-gig; approximately 25 mg of milled carbonate was dissolved in 50 ml of 5% bi-distilled HNO_3, diluting this four times at the time of analysis provided similar concentrations to the samples) and a *M. edulis* shell (M-ed; approximately 12 mg of milled carbonate was dissolved in 25 ml of 5% bi-distilled HNO_3). Elemental concentrations as provided by the Element2 software were directly converted to molar ratios (Me/Ca).

The HR-ICP-MS reproducibility data over the entire sampling period, as determined from the in-house shell standards, is given in Table 5 along with accuracy data from MACS1. The reproducibility for the shell standards are given because they had a similar concentration to the samples, whereas the MACS1 did not. Note that accuracy data for Mg/Ca and U/Ca are from the CCH standard as these elements are not present in MACS1. The minor elemental data, Sr/Ca and Mg/Ca, are both precise (%RSD ≤ 3%) and accurate (within 2% RV). The trace element data are good as well (%RSD < 10%, within ~ 5% RV), aside from U/Ca. The poor results for U/Ca are undoubtedly due to the low concentrations.

Table 5. Detection limit, precision, and accuracy of HR-ICP-MS carbonate standards.

		Sr/Ca	Mg/Ca	Ba/Ca	Pb/Ca	Mn/Ca	U/Ca
DL (3σ)	(ppt)	11.1	63	0.42	0.59	NM	0.007
S-gig	Mean	1.99	1.09	3.76	0.36	4.00	0.02
N = 9	sd	0.05	0.03	0.15	0.04	0.27	0.00
	%RSD	2.6	3.0	3.9	9.8	6.8	13.5
M-ed	Mean	1.30	5.94	1.21	0.25	27.21	BDL
N = 10	sd	0.05	0.24	0.08	0.03	3.12	BDL
	%RSD	3.9	4.06	6.41	11.54	11.45	
MACS1	RV	0.255	*77.68**	84.76	59.56	218.86	*1.67**
N = 18	Mean	0.258	*78.11**	88.27	61.72	207.52	*1.96**
	%RV	101.1	*100.5**	100.9	103.6	94.8	*116.9**

DL = detection limit (in ppt or ng/kg, not ratios); S-gig is *S. giganteus* standard and M-ed is *M. edulis* standard. All data given as µmol/mol except for Sr/Ca and Mg/Ca which are given in mmol/mol; * = data from CCH1 standard; NV = no recommended value; NM = not measured; N = number of replicates, %RV = % recommended value, BDL = below detection limit.

For hemolymph samples, In and Re were used as internal standards to control instrument fluctuations. Samples were diluted 20 times with MilliQ water to assure a salt concentration less than 0.2%. Reproducibility of a large hemolymph sample taken from a clam (*Ruditapes decussatus*) from the Noyalo River, Brittany, France (salinity ~ 17) and digested 10 times is listed in Table 6.

Table 6. Precision for HR-ICP-MS hemolymph samples (*per mol Ca, n = 10).

	Sr/Ca	Mg/Ca	Ba/Ca	Pb/Ca	Mn/Ca	U/Ca	Cd/Ca	Zn/Ca	B/Ca
Unit*	mmol	mol	µmol	µmol	µmol	µmol	µmol	mmol	mmol
Mean	10.37	4.17	66.15	2.59	151.38	4.27	0.44	20.67	10.32
sd	0.17	0.07	3.44	0.13	4.84	0.26	0.02	0.52	0.24
%RSD	1.6	1.6	5.2	5.2	3.2	6.1	5.0	2.5	2.3

The digested tissue samples were analyzed in the same manner as hemolymph. Reproducibility was established by analyzing the NIST 1566a oyster tissue; data are given in Table 7.

Table 7. Precision and accuracy of NIST 1566a oyster tissue (data in µg/kg, n = 5).

	Cd	Ba	Pb	U	B	Mg	Ca	Mn	Cu	Zn	Sr
Mean	3.96	1.50	0.34	0.11	5.45	1294.3	2086.7	11.25	74.8	784.0	12.01
sd	0.05	0.14	0.01	0.00	0.16	30.5	45.5	0.36	0.6	7.45	0.25
%RSD	1.3	9.0	2.9	1.5	2.9	2.4	2.2	3.2	0.8	1.0	2.1
RV	4.15	1.77*	0.37	0.13	NC	1180	1960	12.3	66.3	830	11.1
%RV	95.4	84.9	91.5	85.7	NC	109.7	106.5	91.5	112.8	94.5	108.2

*no certified value, data taken from Buckel *et al*. (2004); NC = not certified. See previous tables for abbreviations.

2.4.2.2 LA-ICP-MS

The LA-ICP-MS system consists of a Fisons-VG frequency quadrupled Nd-YAG laser (λ = 266 nm) coupled to a Fisons-VG PlasmaQuad II+ mass spectrometer. An overview of LA-ICP-MS technology and limitations can be found in Günther and Hattendorf (2005). When applicable, the laser was shot (~50 μm spots) directly in the drill holes of either HR-ICP-MS or stable isotope sampling (Fig. 12), allowing direct alignment of the two elemental profiles, as well as alignment with $\delta^{18}O$ data (cf. Toland *et al*., 2000). Signal intensities of ^{11}B, ^{26}Mg, ^{43}Ca, ^{55}Mn, ^{59}Co, ^{65}Cu, ^{86}Sr, ^{111}Cd, ^{138}Ba, and ^{208}Pb were recorded. Gas blank intensities were recorded every 10^{th} sample. Approximately after every 50^{th} sample, two standards (NIST 610 and MACS1) were analyzed five to six times each. The raw counts per second (CPS) were manipulated off line following Toland *et al*. (2000).

Reproducibility and accuracy for LA-ICP-MS are given in Table 8. Reproducibility is good for all ratios (< 8%), aside from Mg/Ca, due to low Mg concentrations in MACS1 (0.06 mmol/mol in MACS1, compared with 1.09 mmol/mol in the shell). Accuracy is also good, with the data being within 8% of the recommended value, aside from Pb/Ca, which was overestimated by nearly 50%. This overestimation is apparently not a problem of an incorrect recommended value, as this study's HR-ICP-MS data and the LA-ICP-MS data of Munksgaard *et al*. (2004) are within 5% of the recommended value. This discrepancy is probably due to fractionation, as Pb is known to be one of the most problematic elements in this regard (Fryer *et al*., 1995; Longerich *et al*., 1996). Munksgaard *et al*. (2004) used LA-ICP-MS systems with shorter wavelengths (λ = 193 and 213 nm) which produce smaller particles during ablation and reduces elemental fractionation in the plasma (Guillong and Gunther, 2002). However, Pb/Ca results from the LA-ICP-MS are reproducible, thus they are considered as qualitative at this point.

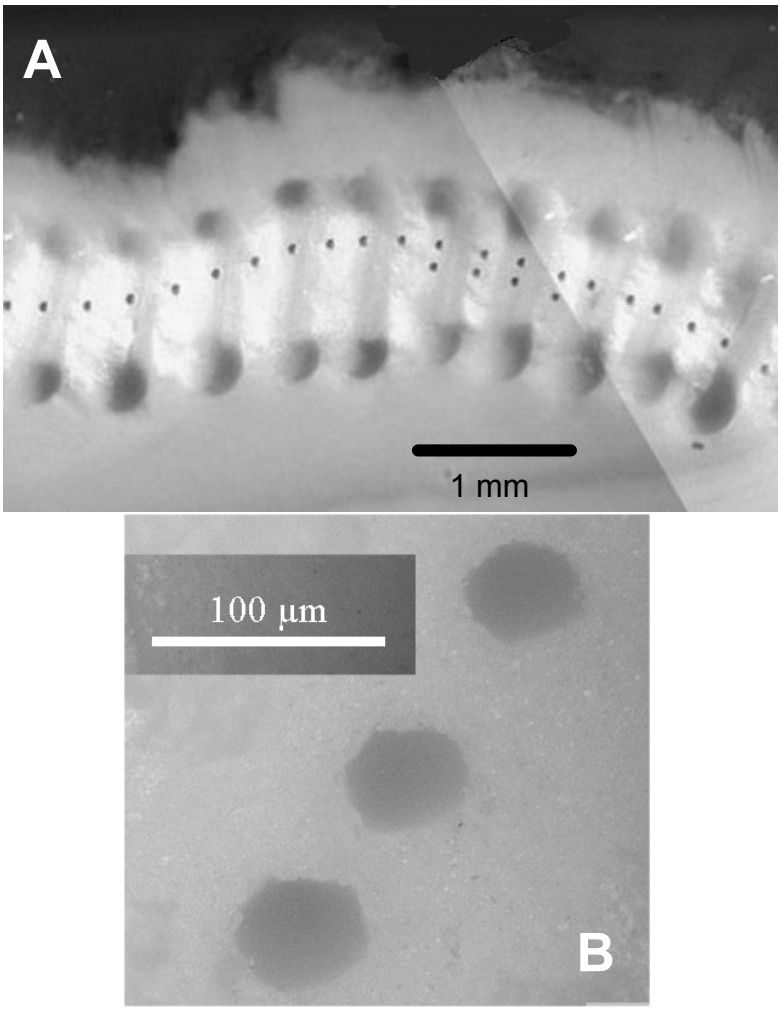

Figure 12. (A) Laser ablation holes in drill holes in a *S. giganteus* shell and (B) a close up of Laser ablation holes in the MACS1 standard.

Table 8. Detection limit, precision, accuracy of LA-ICP-MS for various elemental ratios.

		Sr/Ca	Mg/Ca	Ba/Ca	Pb/Ca	Mn/Ca	U/Ca	B/Ca
DL (3σ)	(ppm)	1.20	3.24	0.04	0.01	1.26	0.01	0.25
MACS1	Mean	0.249	0.06	81.4	87.2	203.1	NP	229.7
	sd	0.005	0.02	3.13	5.95	9.91	NP	17.1
N = 25	%RSD	2.0	30.1	3.8	6.8	4.9	NP	7.5
	%RV	97.6	NV	96.0	146.5	92.9	NP	NV

All data given as µmol/mol except for Sr/Ca and Mg/Ca which are given in mmol/mol; DL = detection limit (in ppm or µg/g, not ratios); NV = no recommended value; NP = not present; N = number of replicates. See previous tables for other abbreviations.

2.4.3 Determination of phytoplankton pigment concentration

In the field 200 to 500 ml of seawater was filtered through a Whatman GF-F filter, which was wrapped in aluminum foil and placed in liquid nitrogen; three replicates

were taken at each sampling. Upon return to the laboratory, samples were transferred to a –85 ºC freezer until analysis. Phytoplankton pigments were analyzed using standard laboratory operating procedures for high performance liquid chromatography (see Gillikin, 2005). The reproducibility of this method was determined to be within 2.7% (or 0.3 µg/l; 1σ) for chlorophyll a, based on seven sediment standards (chlorophyll a = 10.1 µg/l).

2.4.4 Temperature, salinity, pH and dissolved oxygen

Temperature was monitored at certain sites and during laboratory studies using temperature data loggers (± 0.1 ºC; Onset Computer Corporation, StowAway TidbiT), usually set to record temperature every hour. Salinity (± 0.01), pH (± 0.05) and dissolved oxygen (± 0.1 mg/l) were measured either *in situ* or in a bucket (immediately after collection) with a WTW multiline P4 multimeter.

2.5 Modelling

Environmental records are not measured directly as a function of time, but along a growth or accretion axis. Since we are mostly interested in the time series this distance profile has to be transformed into a time profile (Fig. 13), which requires knowledge about growth or accretion rate. In general, it is not possible to estimate the growth or accretion rate and the time profile from the distance grid. So, without extra information or extra assumptions, one has to date at least two observations and assume a constant growth rate to construct a time series. This is illustrated by the dotted line in Figure 13. An example of such extra information are growth bands, present in some corals, bivalves or trees, which can be used to date the record. However, this can induce non-negligible bias. Furthermore, even when growth lines are available, they usually only provide information about variations on annual and multi-annual scales and not on a sub-annual scale.

We have proposed a method to transform the distance series into a time series, based on the assumption that the record is periodic (See De Ridder *et al*., 2004 and 2005). The variations in growth rate are modelled as a distortion of the time base. Once the distortion is known, a more accurate time base can be reconstructed eventually resolving inter-annual variation.

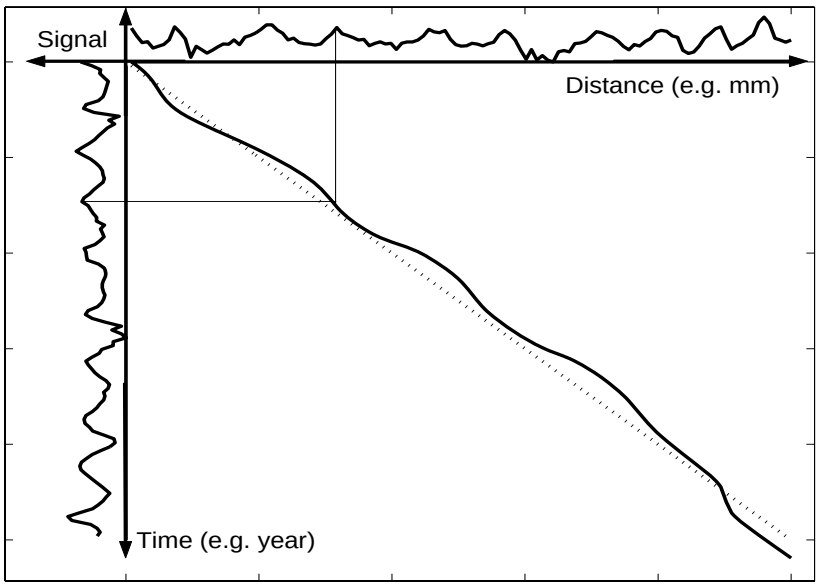

Figure 13. Conceptual graph showing the transformation from a record along a distance grid to time series. The dotted line represents a constant growth rate, while the curved line along the diagonal represents the real growth rate.

The growth rate is not estimated directly. On the one hand we know the distances between subsequent observations and on the other hand we would like to know the time instances between these observations. The ratio of increments of both is the growth rate. To estimate the time instances, we start from an average constant growth rate, where the time instances between the observations are constant. So the time instance at which the nth observation was formed is given by

$$t_n = nT_s$$

In equation (1) T_s is the sample period (dimension: time), which is a measure for the average time instance between two subsequent observations. This constant growth rate model would correspond to the dotted line on the diagonal of Figure 13. Equation (1) will not be valid when the time instances are disturbed, due to variations in growth or accretion rate. This distortion of the time base can be modelled by a distortion term, $g(n)$, which is (i) zero when the growth is equal to the average growth, (ii) negative when the growth is slower than the average and (iii) positive when the growth is greater than the average. So, an improved estimate of the time instant at which observation n was formed is given by

$$t_n = nT_s + g(n)T_s$$

where the first term expresses the constant time step and will be called the time base distortion (TBD) at observation position n (scalar quantity). The TBD is the difference between the dotted and the full line on the diagonal of Figure 13. For annual resolved archives, the TBD can be estimated assuming that the signal is periodic.

3. RESULTS

3.1 Sclerosponges

3.1.1 Growth rate

3.1.1.1 Growth rate of C. nicholsoni

For the specimen used for the specific geochemical analyses, growth measurements indicated a growth rate of 181 µm/yr (n = 60, σ = 15.23 µm/yr) (see Rosenheim *et al*., 2004). Accumulative data for all specimens of *C. nicholsoni* collected and measured showed mean average growth rate to be 198 µm/yr (9 specimens: n = 557, σ = 15.23 µm/yr), while re-growth (growth following specimen damage) was significantly lower, at an average of 93 µm/yr (1 specimen: n = 18, σ = 31.1 µm/yr).

3.1.1.2 Growth rate of P. massiliana

The first set of specimens was labelled twice, for comparison of two consecutive growth periods on the same species. However, the initial calcein incubation was performed too close to plating and was not successful. Annual growth rates obtained from the second staining were highly variable with a mean growth rate of 243 µm/yr (13 specimens, n = 189, σ = 161.4 µm/yr). The second set of specimens was labelled only once, the next day after plating. Although calcein incorporation was successful, the low growth measurements suggest that these specimens had not completely recovered. Measurements taken from these specimens, where calcein labelling was performed soon after plating, were significantly lower (56.66 µm/yr, 8 specimens, n = 229, σ = 23.67 µm/yr). Measurements also varied significantly from one specimen to another, ranging from 9.72 (σ = 3.37 µm/yr) to 70.17 µm/yr (σ = 40.81 µm/yr) for those incubated with calcein soon after plating (Figure 14a), and from 111.60 µm/yr (σ = 57.21 µm/yr) to 676.69 µm/yr (σ = 63.80 µm/yr) for those allowed to recover (Figure 14b). Approximately 10% of the calcein label was at the edge of the skeleton indicating zero growth for these regions. Measurement variation was greater when measurements were taken at the tip rather than from the base or from parallel points along the skeletal form (Figure 14c). The multi-directional growth of the skeletal projections made the growth rate difficult to assess in the 2-dimentional technique adopted (Figure 15). The growth rate of this species falls within the range observed in other hyper calcified sponges (Lazareth *et al*., 2000, Willenz & Hartman, 1999; Rosenheim *et al*., 2004; this study).

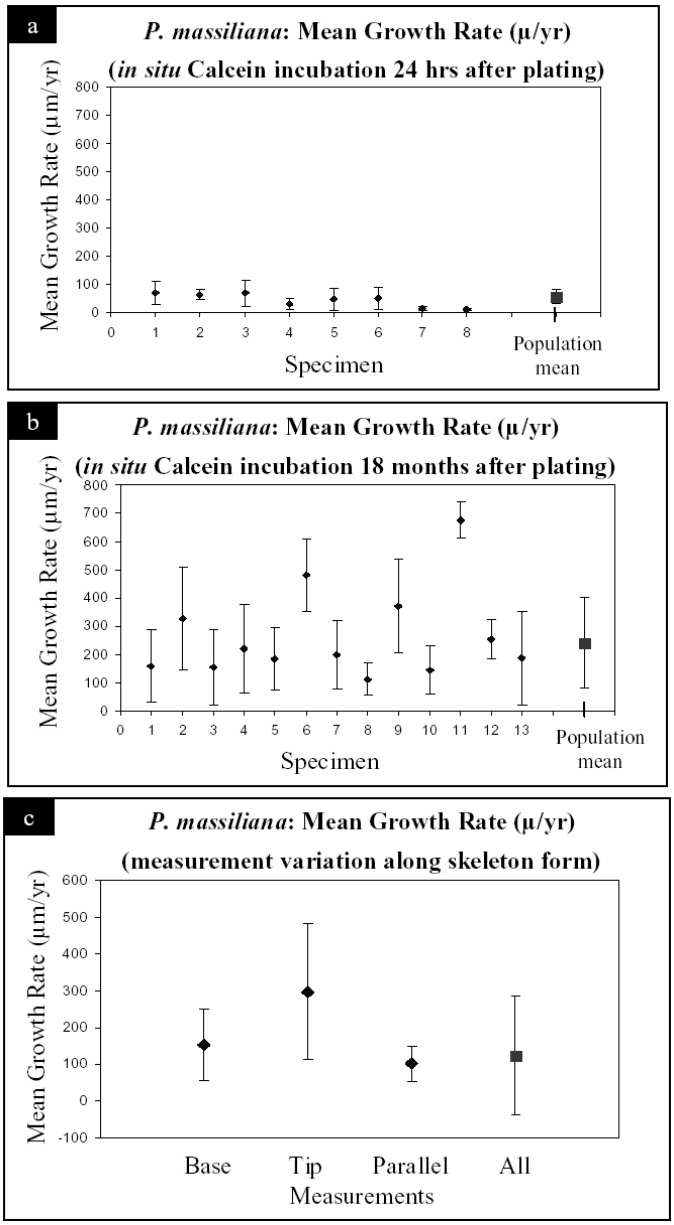

Figure 14. *Petrobiona massiliana*: Scatterplots showing mean growth rate of specimens incubated with calcein soon (a) and 18 months (b) after plating; (c) Scatterplot showing variation in growth rates according to where measured on the skeleton formation.

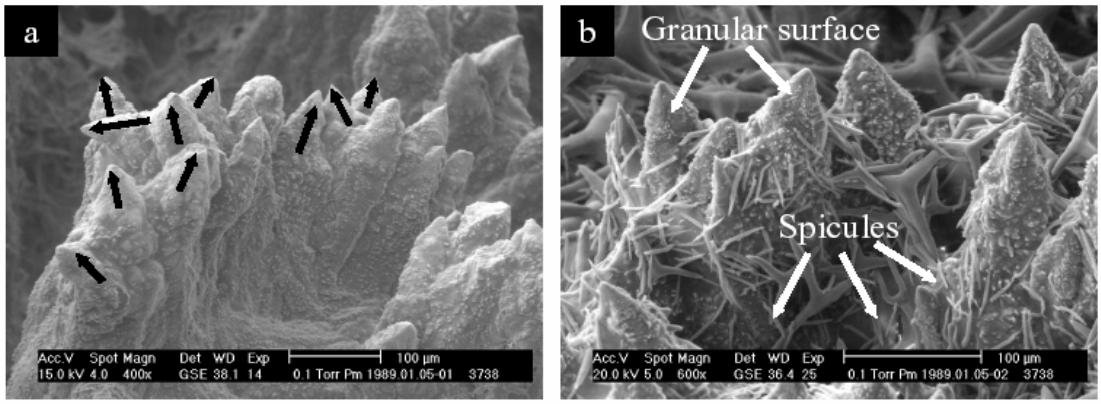

Figure 15. *Petrobiona massiliana*: SEM images of the skeleton after removal of the organic matter using Perhydrol 15% showing multi-directional growth of the larger skeletal projections growth (indicated by black arrows) (a); Spicules and granular surface are evident over and on skeletal projections (b).

3.1.2 Uptake pathway

Transmission Electron Microscopy (TEM) observations showed uptake and accumulation of ferritin particles inside endocytic vesicles of specific cell types (Figure 16b,c,d,e). Bacteria marked with strontium were also accumulated within phagosomes of the same cells (Figure 16f). The incorporated bacteria still contained strontium (Figure 16g). Incubations with the dissolved elements (up to 10 mM) did not allow the location of elements to be determined within the sponge tissue. However, supersaturated incubations (providing particulate ions) allowed element hotspots to be discovered using Scanning Electron Microscopy (SEM) + Energy Dispersive X-ray analysis (EDX) (Figure 17). Focused Ion Beam-cut sections from the element hotspots enabled positive analysis using the Scanning TEM + EDX (Figure 11), but the exact cellular locations are still to be determined at the ultra structural level.

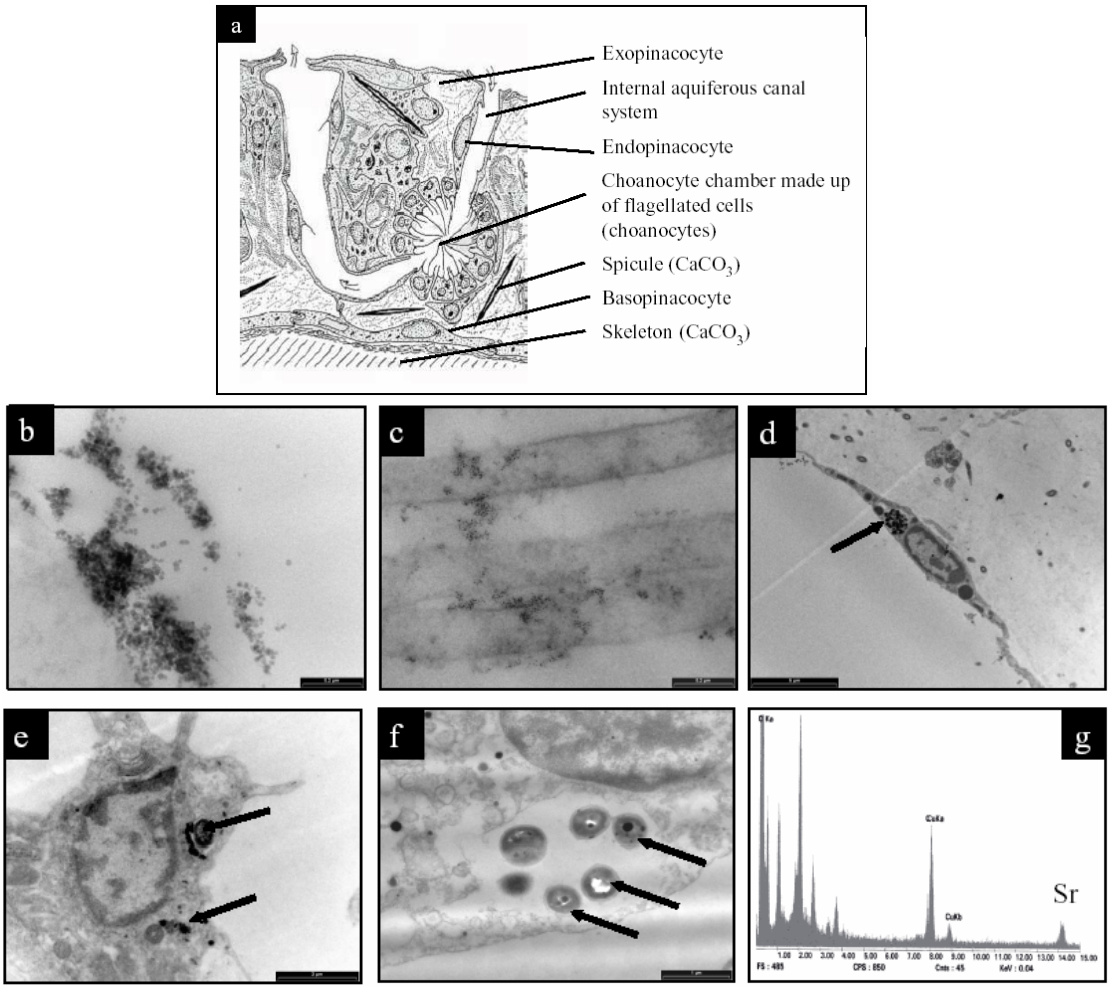

Figure 16. *Petrobiona massiliana*: Cellular organisation in an idealised sponge (a), from Boury-Esnault and Rützler (1997) [3]; TEM images showing uptake of ferritin. Initial accumulation of ferritin at the sponge surface (b), around the microvilli of the choanocytes (c), and in endocytic vesicles in an endopinacocyte (d) and a choanocyte (e). Phagosome, containing bacteria, in a choanocyte (f), and spectra from the incorporated bacteria showing the strontium peak (g).

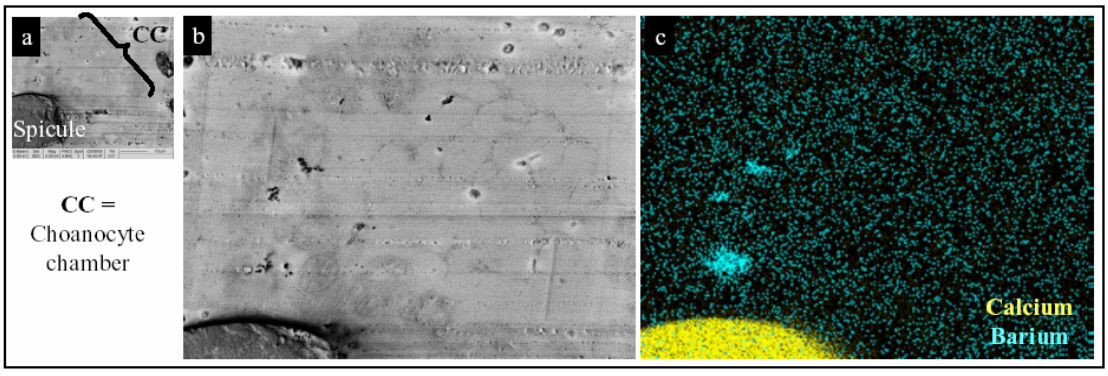

Figure 17. *Petrobiona massiliana*: Choanocyte chamber. SEM image showing cellular arrangement in area of interest (a); SEM image focusing on choanocyte chamber (b) and corresponding element maps for calcium (yellow) overlay barium (blue) (c).

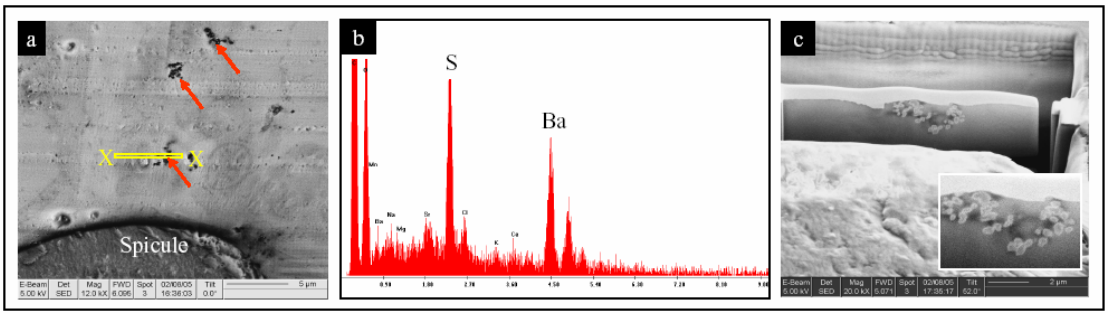

Figure 11. *Petrobiona massiliana*: (a) Part of choanocyte chamber. Barium hotspots are indicated by red arrows; Example spectra from point analysis indicating barium sulphate (b). The yellow transect represents the position of a FIB-milled section across a barium hotspot. Barium sulphate crystals are visible in the FIB-milled section (c) (inset shows crystals enlarged).

3.1.3 Lead in *Ceratoporella nicholsoni* and *Stromatospongia vermicola* skeletons

Figure 19 presents the different sclerosponge lead profiles in Pb concentrations (ppm, or µg/g), as well as ratios to Ca (Pb/Ca, nmol/mol). Data near the surface in RB1, RB2 and RB3 exhibit a rapid increase in lead (Fig. 19), due to element enrichment in the dried tissues after evaporation of the seawater. Therefore, data from the most recently formed skeleton are not considered in the following discussions.

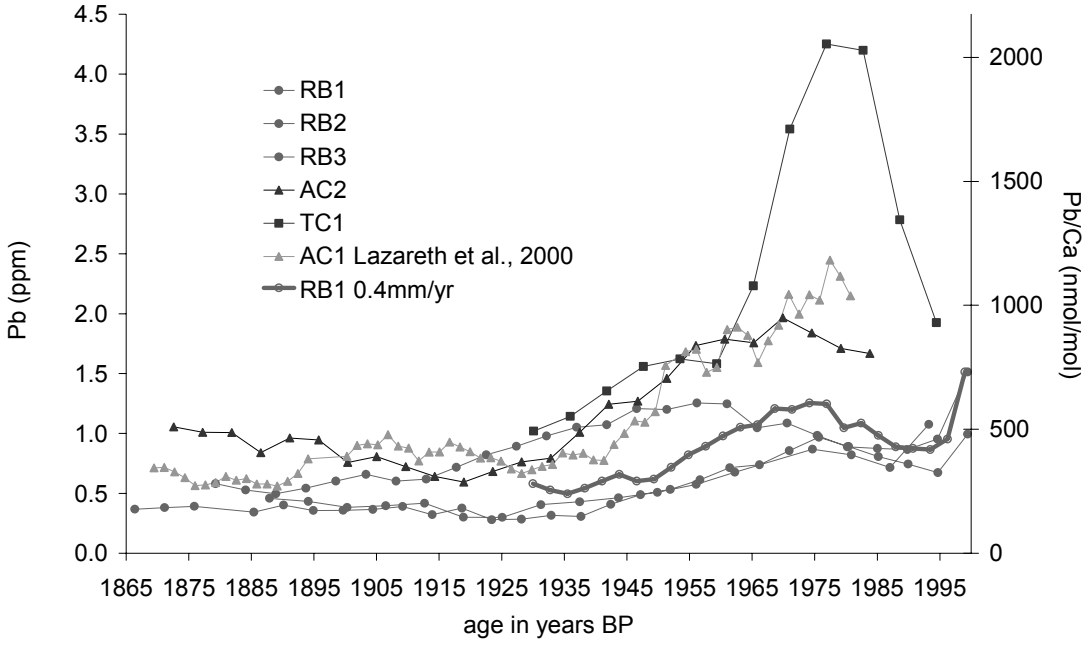

Figure 19. Lead in the different specimens of sclerosponges from Rio Bueno (RB; Jamaica), Lee Stocking Island (LSI; Bahamas), Acklins Island (AC; Bahamas), Turks and Caicos Island (TC; Bahamas) [see also Fig. 8]. Profiles were dated using a constant growth rate of 233 µm/yr (Willenz & Hartman, 1999). All samples are *C. nicholsoni* except sample TC1, which is *S. vermicola*.

3.1.3.1 Intra-specimen reproducibility

The intra-specimen reproducibility from the upper five to nine samples from four *C. nicholsoni* samples is illustrated in Figure 20. The similarity between the lead profiles (BLS: intercept not significant p = 0.77; Slope = 1, CI = 0.87 to 1.17, p < 0.0001, R^2 = 0.96; n = 31), indicates a good reproducibility of the lead signal within specimens. With exception of three data (two values in the AC2 sclerosponge and one value in the TC1 profile), all data of the second profile are similar to those of the first profile within a 10% analytical uncertainty**.**

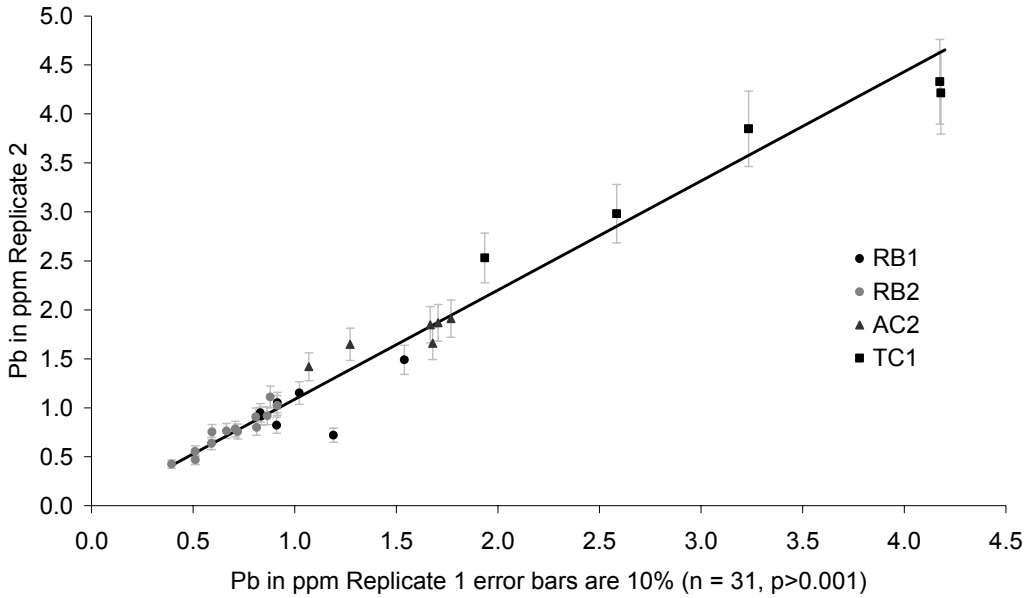

Figure 20. Bivariate least square regression between replicate samples taken along parallel transects on 4 specimens. The intercept is not significant (p = 0.77) and the slope is equal to one (p < 0.0001, R^2 = 0.96; n = 31).

3.1.3.2 Inter-specimen and inter-species reproducibility

An appreciable reproducibility exists in different samples of *Ceratoporella nicholsoni* from the same location (fig. 5a and 5b). Lead profiles from RB2 and RB3 were separated into sections from 1866-1924 (~ flat), 1925-1975 (rise) and 1976-1995. The1866-1934 slope in both samples was not significant (p > 0.05 for both), so the raw data were directly compared and were not significantly different (p = 0.10). The 1925-1975 sections both had significant slopes (p < 0.0001), but the slopes were not significantly different from one another (p = 0.34). There were not enough data points in the 1976-1995 section for proper statistical testing. Specimen RB1 was different than both others for all periods (p < 0.0001).

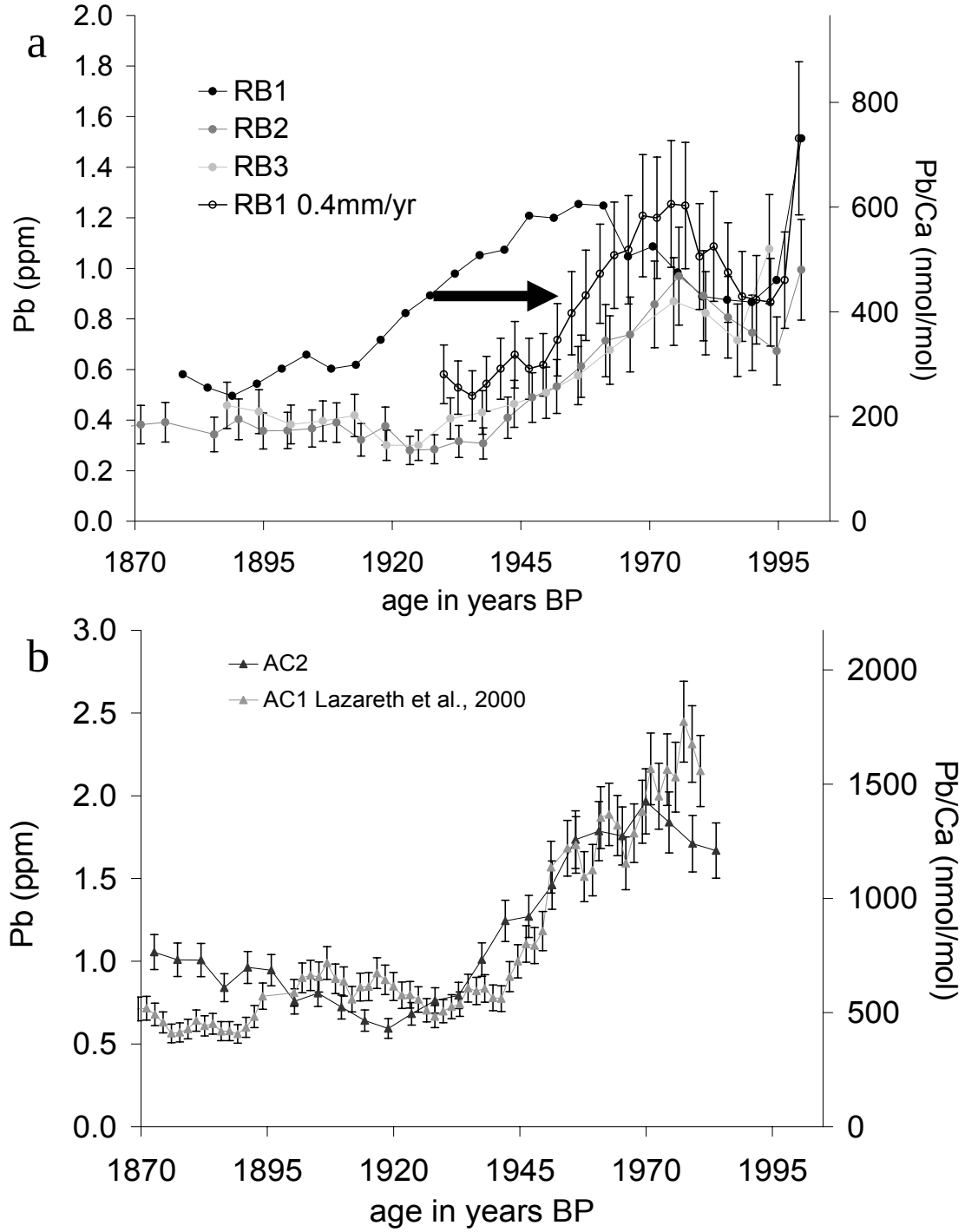

Figure 21. Reproducibility of different specimens of *Ceratoporella nicholsoni* from Rio Bueno (a) and Acklins Island (b). Sample RB1 is plotted assuming a growth rate of 233 µm/yr as well as a growth rate of 400 µm/yr; the arrow shows the shift in the data, matching the rest of the samples.

The similarity between lead profiles of two specimens from Acklins Island, AC1, measured by LA- ICP-MS (Lazareth *et al*., 2000) and AC2, measured by acid dissolution ICP-MS indicates a good reproducibility between different specimens. Additionally, this reproducibility confirms the validity of the laser-ICP-MS technique for measurements of lead concentrations in sclerosponges as previously suggested by Lazareth *et al.* (2000).

All four specimens of *C. nicholsoni* and the *S. vermicola* display comparable lead profile shapes (fig. 19) and present a similar timing of the changes as the *C. nicholsoni* (AC1) studied by Lazareth *et al*. (2000). All specimens of both species exhibit low values before 1925. An increase after ~1930, reaching a maximum value around the mid -1970's (when assuming a higher growth rate for RB1). The lead concentration decreases during the 1980's and the beginning of the 1990's. The main difference between the different sclerosponges studied concerns the absolute lead concentrations. The Sclerosponges from the Bahamas (Acklins Island and Turks and Caicos Island) generally exhibit higher values than the sclerosponges from the Caribbean Sea (Jamaica). The maximum lead values in the Turks and Caicos sample is two times higher than that of the Acklins Island sample and four times that of the Jamaica samples.

3.2 Bivalves

3.2.1 Reproducibility of oxygen isotope profiles in bivalve shells

To test the reproducibility of the signal recorded in *Saxidomus giganteus* shells, the data first need to be fit on the same time axis to correct for differences in growth rate. Oxygen isotope profiles from shells 1 and 3 were fit to the x-axis of shell 2 (shell 2 arbitrarily chosen) using the phase demodulation method described above (section 2.5; see also De Ridder *et al*., 2004). Using this method, there is excellent agreement between the three profiles (shell 1 vs. 2, $R^2 = 0.87$; 1 vs. 3, $R^2 = 0.81$; 2 vs. 3, $R^2 = 0.77$; $p < 0.0001$ for all; Fig. 21).

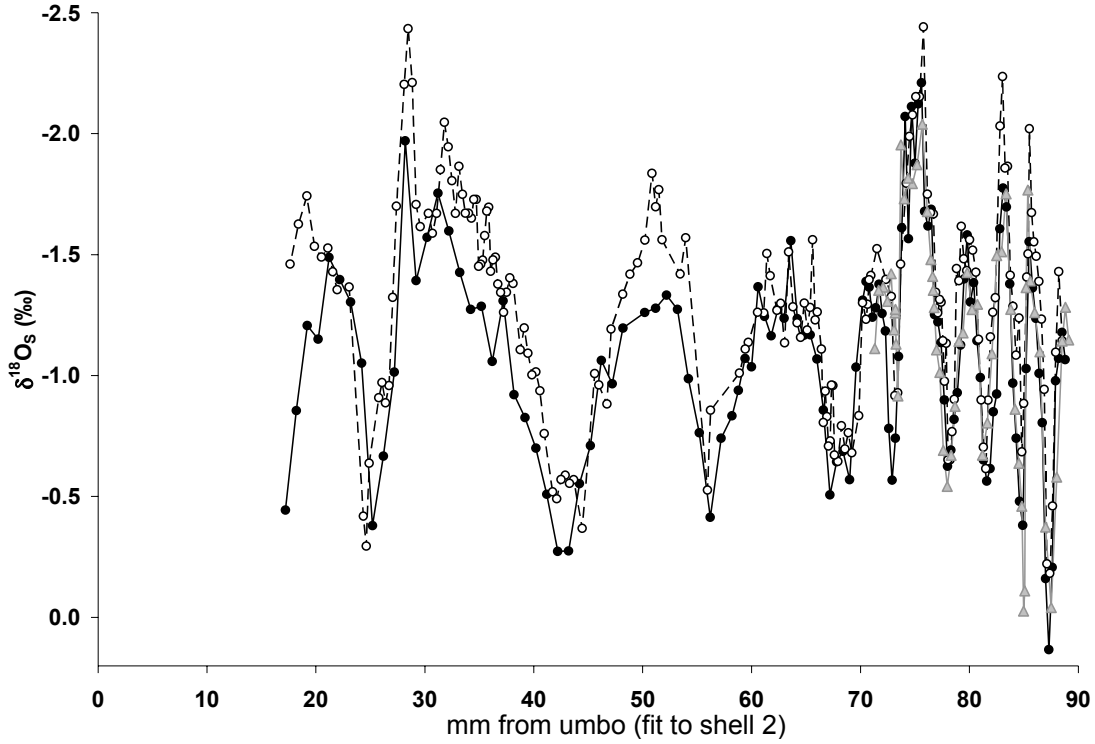

Figure 21. $\delta^{18}O_S$ (y-axis inverted) of the three *S. giganteus* shells fit to the x-axis of shell 2 using the phase demodulation technique (shell 1: open circles, shell 2: solid circles, shell 3: triangles).

3.2.2 Stable carbon isotopes in bivalve shells

All *Mercenaria mercenaria* shells, regardless of collection site or time of collection exhibit a large ontogenic decrease in $\delta^{13}C_S$, up to 4 ‰ (Fig. 22), including a Pliocene shell (data not shown, see Gillikin, 2005).

After removing two outliers, the different tissues from Jarrett Bay clams had significantly different $\delta^{13}C$ values ($p < 0.01$ for all; $n = 10$), except for mantle (-19.1 ± 0.3 ‰; $n = 10$) and muscle (-19.1 ± 0.2 ‰; $n = 10$) tissues ($p = 1.0$), with gills being the least negative (-18.4 ± 0.3 ‰; $n = 10$) and the foot the most negative (-19.5 ± 0.03 ‰; $n = 10$). From the Jarrett Bay samples, the only tissue carbon isotopic signature that was significantly correlated to shell length was the foot, with a weak positive correlation ($R^2 = 0.45$, $p = 0.033$, $n = 10$). In contrast, there was a significant strong positive correlation between muscle $\delta^{13}C$ and length (L) in the Johnson Creek clams ($\delta^{13}C_{muscle} = 0.05$ (± 0.01) * L – 21.09 (± 0.77), $R^2 = 0.98$, $p = 0.0011$, $n = 5$). Three replicate $\delta^{13}C_{DIC}$ samples taken at Jarrett Bay gave a mean of -0.77 ± 0.20 ‰, which is similar to the average of 13 samples taken in the vicinity of this site the year before (-0.5 ± 0.8 ‰). Johnson Creek $\delta^{13}C_{DIC}$ was more negative at -2.40 ± 0.26 ‰ ($n = 3$). The muscle tissues of Jarrett Bay clams were -19.1 ± 0.19 ‰ ($n = 10$) and

muscle tissues of Johnson Creek clams were -18.3 ± 1.2 ‰ (n = 5). Both sediments (-20.3 ± 0.14 ‰) and particulate matter (-21.5 ‰) were within 2.5 ‰ of tissues (~ 19 ‰) at Jarrett Bay.

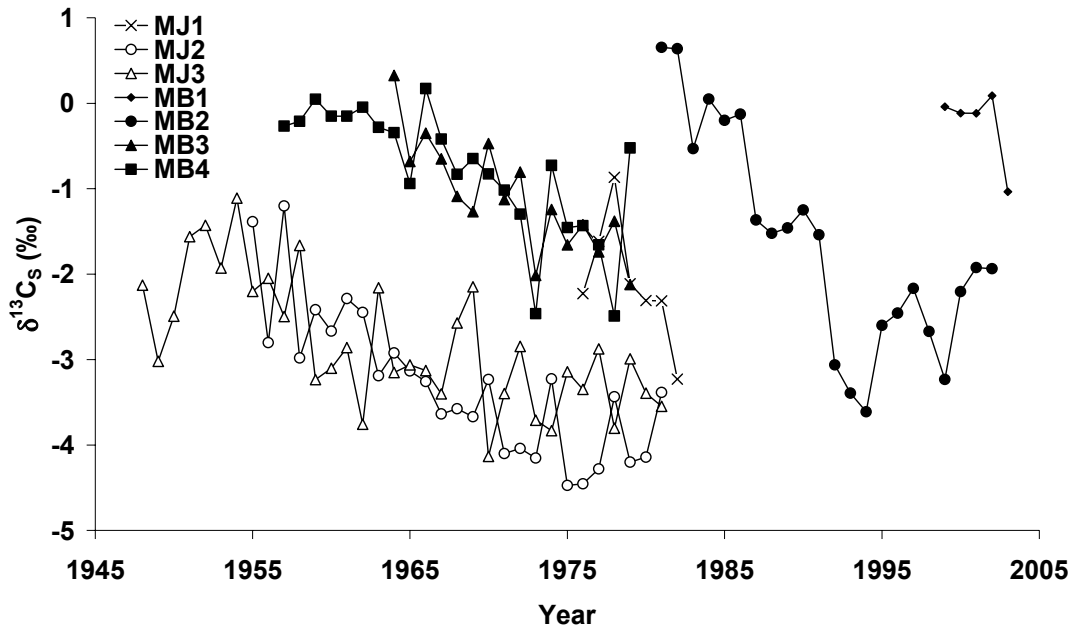

Figure 22. Annual shell $\delta^{13}C$ from *M. mercenaria* shells collected at two sites (Johnson Creek, MJ shells and Back Sound, MB shells) plotted versus year showing the clear ontogenic decrease.

3.2.3 Trace elements in aragonitic bivalves

A suite of trace elements were measured in the aragonitic shells of both *M. mercenaria* and *S. giganteus*. The data from two *S. giganteus* shells are provided in Figure 23, and are discussed in the following sub-sections.

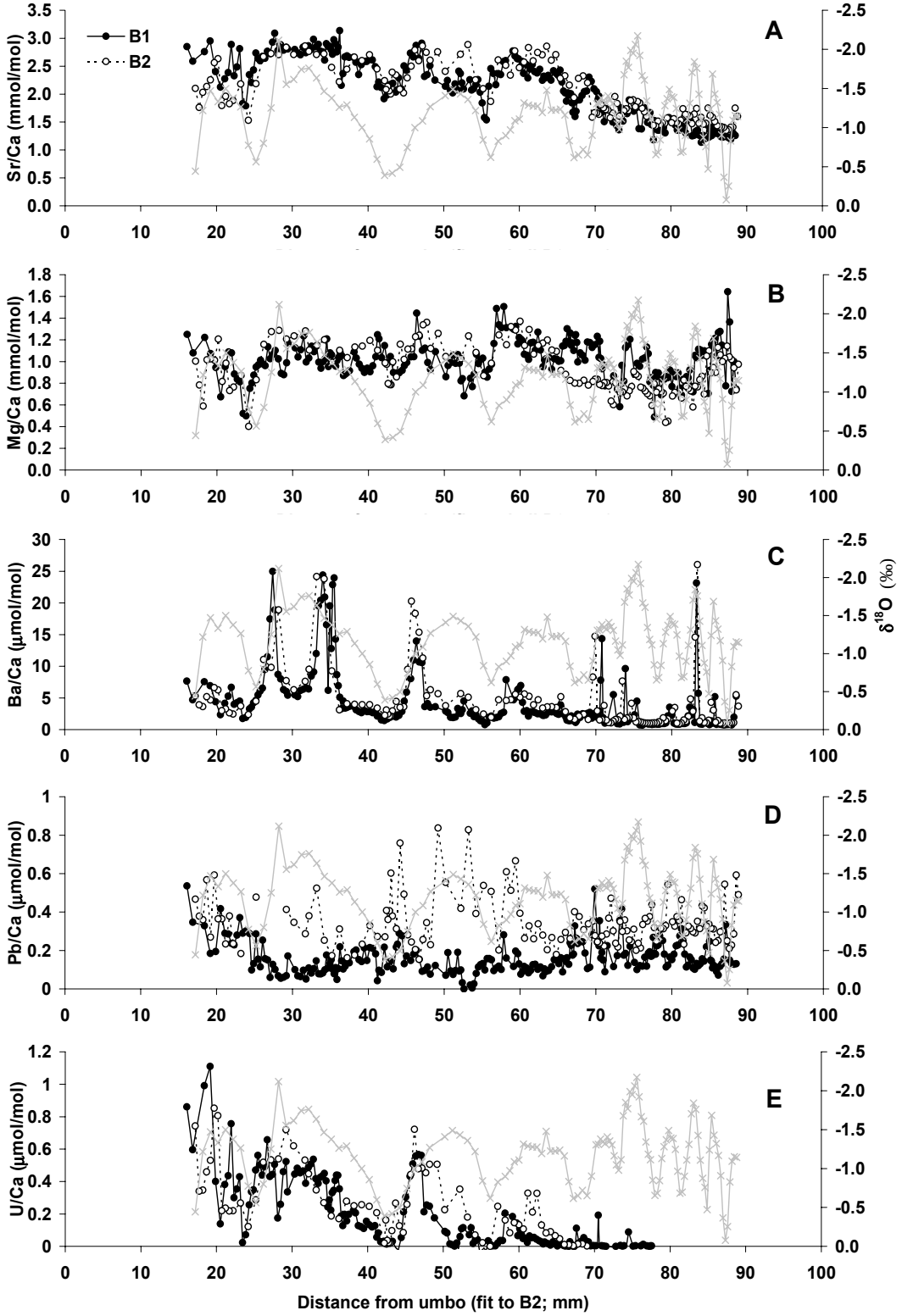

Figure 23. High resolution elemental ratio profiles from the two Puget Sound (Washington, USA) shells measured with LA-ICP-MS fit to shell B2 (see 3.2.1). $\delta^{18}O$ data (grey lines) are from Gillikin *et al.* (*in press*-a) and Sr/Ca data are from Gillikin *et al.* (2005). Note that $\delta^{18}O$ axes are inverted.

3.2.3.1 Sr/Ca ratios

Ratios of Sr/Ca exhibited a clear decrease through ontogeny in *S. giganteus* (Fig. 23A), but not in *M. mercenaria* (data not shown, see Gillikin *et al*., 2005). As bivalve shell growth slows through ontogeny (Schöne *et al*., 2003; Lorrain *et al*., 2004; Gillikin *et al*., *in press*-a), a positive relationship between growth rate and Sr/Ca ratios were observed in *S. giganteus* (Fig. 24A), but not in *M. mercenaria* (Fig. 24B).

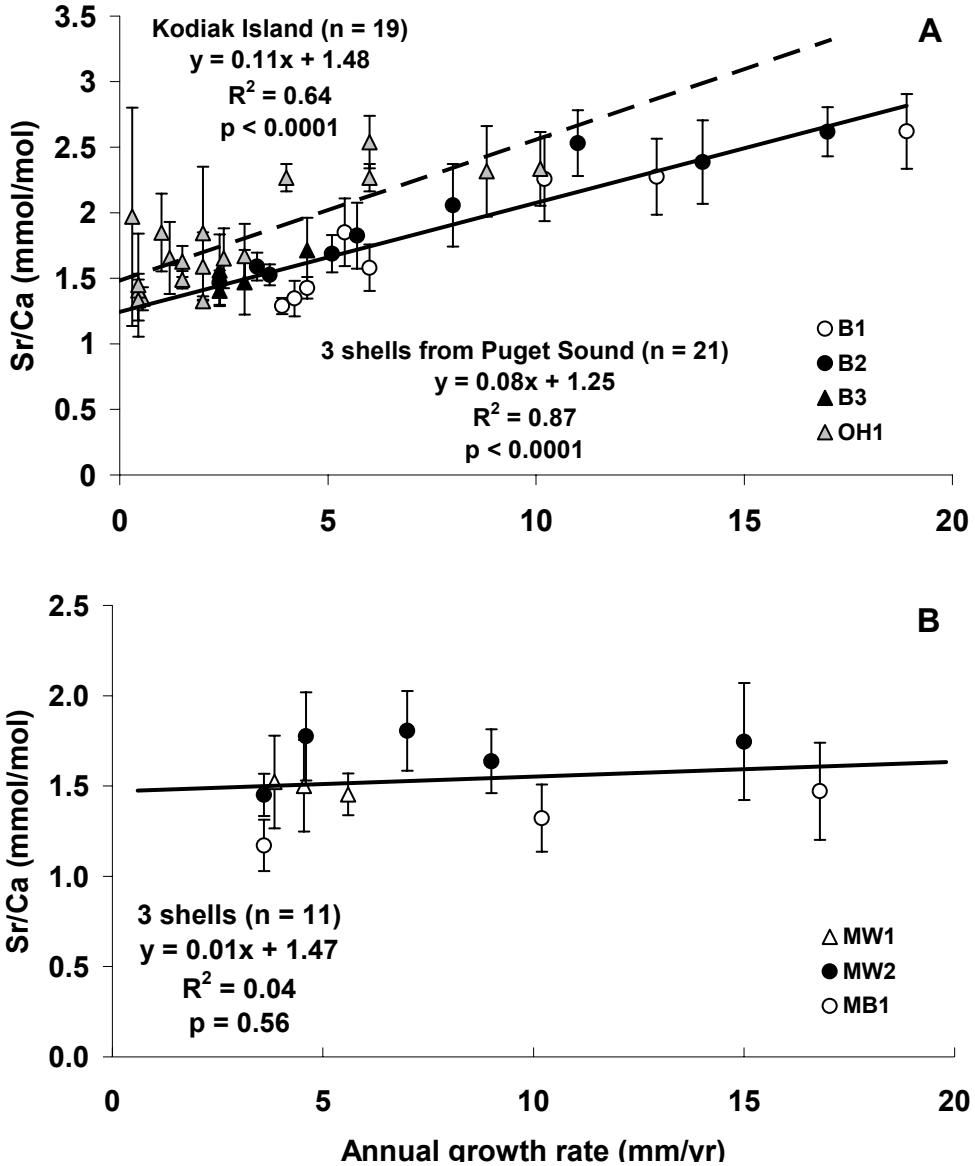

Figure 24. Average annual Sr/Ca ratios versus annual growth rates. The three *S. giganteus* shells from Puget Sound, Washington are included in the same regression (solid line) and are compared with the regression of the 19 year old specimen from Kodiak Island Alaska (dashed line) (A). The three *M. mercenaria* shells are included in the same regression (B). Error bars represent standard deviations; n = number of annual growth increments included in each regression.

3.2.3.2 Mg/Ca ratios

The Mg/Ca profiles exhibit similarities between the two Puget Sound shells, but are clearly not related to SST (Fig. 23B, using $\delta^{18}O$ as a relative temperature scale). Similar results were found in *M. mercenaria* shells (data not shown, see Gillikin *et al*., 2004a).

3.2.3.3 Ba/Ca ratios

The two shells from Puget Sound show a remarkable co-variation, with the Ba/Ca peaks occurring almost exactly at the same time in both shells (Fig. 23C). The sharp episodic peaks generally occur in the spring (using $\delta^{18}O$ as a relative temperature scale).

3.2.3.4 Pb/Ca ratios

Shell B2 (*S. giganteus*) is almost consistently exhibiting higher Pb/Ca ratios than shell B1, especially between 45 to 60 mm from the umbo (Fig. 23D). Upon a closer inspection of the data (see also Fig. 25) there is a clear pattern in the Pb/Ca signal in shell B1 (Puget Sound), with Pb/Ca peaks occurring every winter.

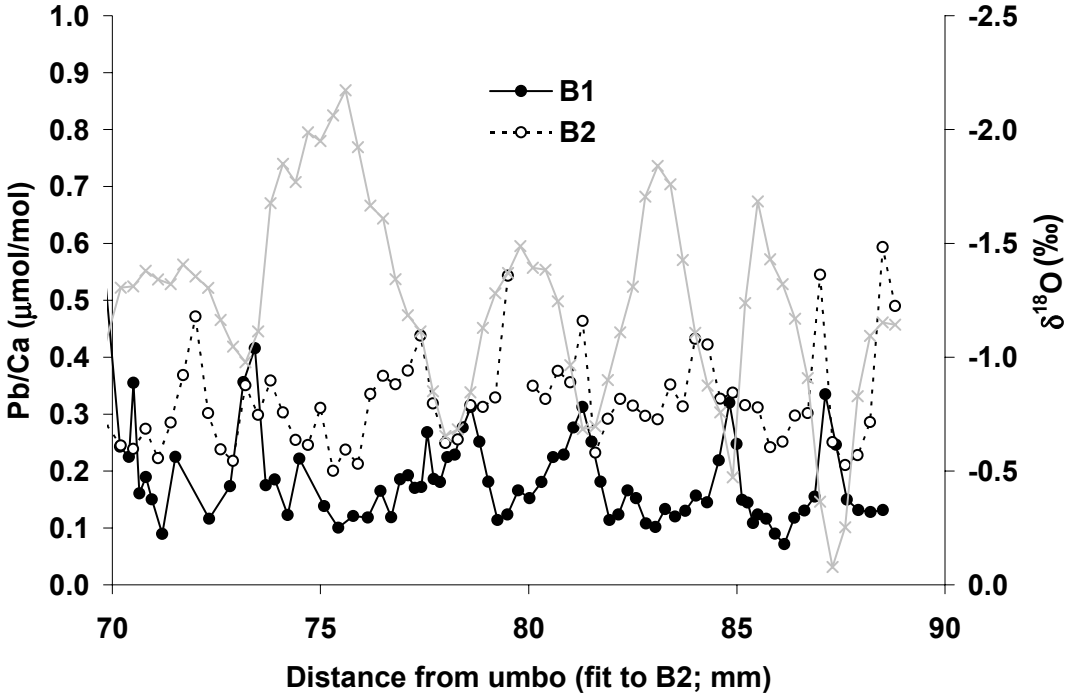

Figure 25. Pb/Ca data from the slow growing region of the Puget Sound (Washington, USA) shells. Data are the same as Figure 23D, but allow a detailed look at the variations in the profile.

Eleven *M. mercenaria* shells were analyzed for Pb/Ca ratios on an annual basis. Overall, the lead concentrations were low and the data appeared 'noisy' (Fig. 26); however, the highest levels were noted around 1980, which could be expected based on other Pb proxies.

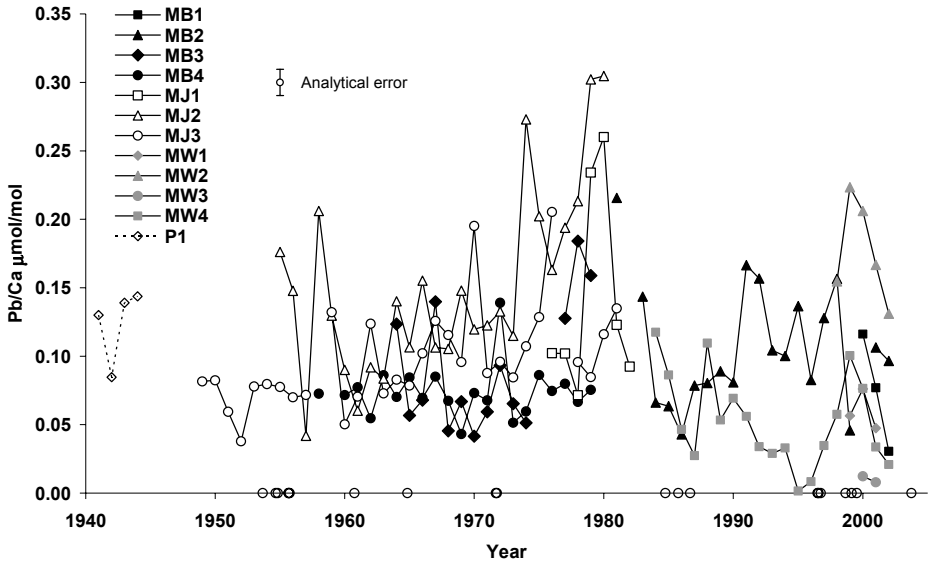

Figure 26. Annually sampled Pb/Ca ratios from the 11 *M. mercenaria* shells. The open symbols on the x-axis represent hurricane years (data from NCSO, 2004). The analytical error is based on 9.8% of the mean Pb/Ca ratio (0.101 ± 0.0099 µmol/mol).

3.2.4 Trace elements in calcitic bivalves

3.2.4.1 Sr/Ca and Mg/Ca ratios

Ratios of Sr/Ca and Mg/Ca in *Mytilus edulis* shells from the Schelde estuary were not simply related to any of the several environmental parameters measured at this site (data not shown); our conclusions were similar to those of Vander Putten *et al*. (2000). Much of the problem in not being about to determine the cause of the variability was because it is difficult if not impossible to date each sample taken from the shells.

Data from the scallop, *Pecten maximus*, however allowed a more detailed examination of potential controlling factors on Sr and Mg incorporation in bivalve shell calcite. Figure 27 provides the Sr/Ca and Mg/Ca data collected from four shells, whereas Figure 28 illustrates temperature and salinity data collected from the same sites as the shells. Considering the daily banding on these shells (Chauvaud *et al*., 1998), exact calendar dates can be assigned to the profiles and daily growth rates can be calculated. These daily growth rates are plotted with Sr/Ca in Figure 29.

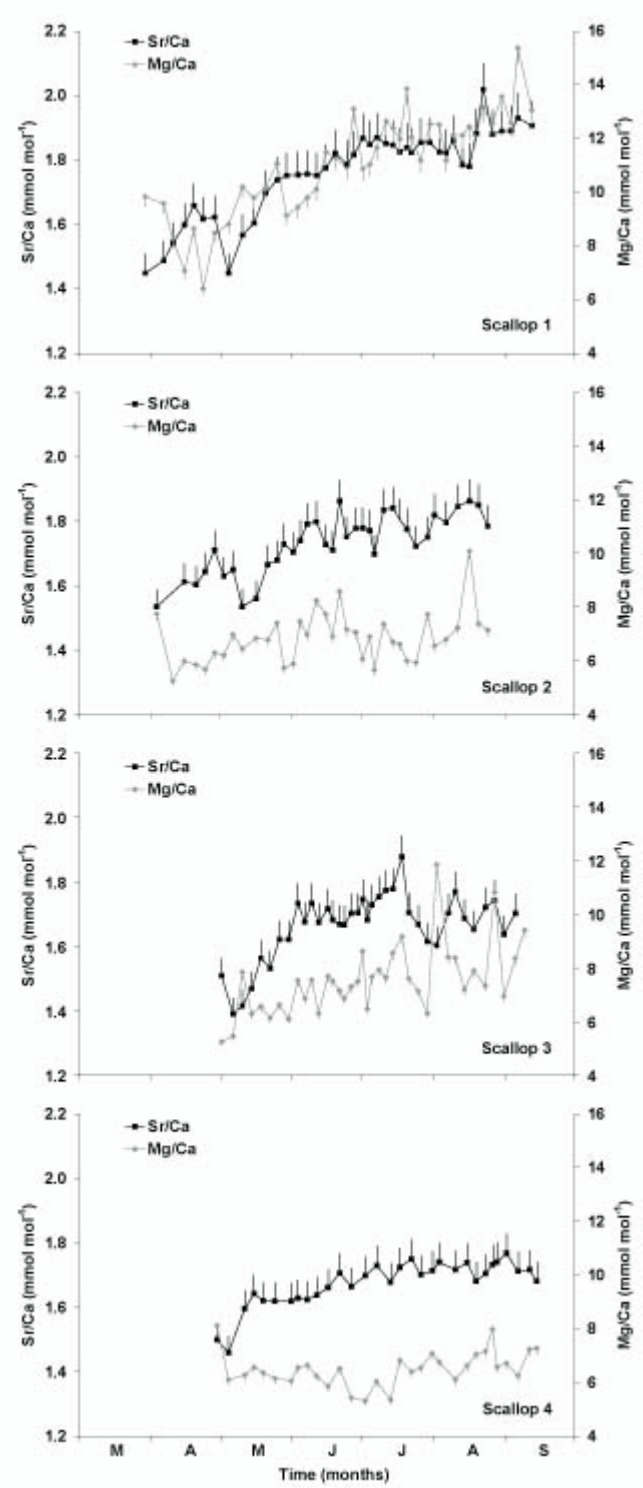

Figure 27. Sr/Ca (black symbols) and Mg/Ca (grey symbols) ratios (mmol/mol) in the calcite shell layer of four age class I *P. maximus* specimens sampled in September 2003 in the Bay of Brest. Metal/Ca ratios correspond to the year 2003.

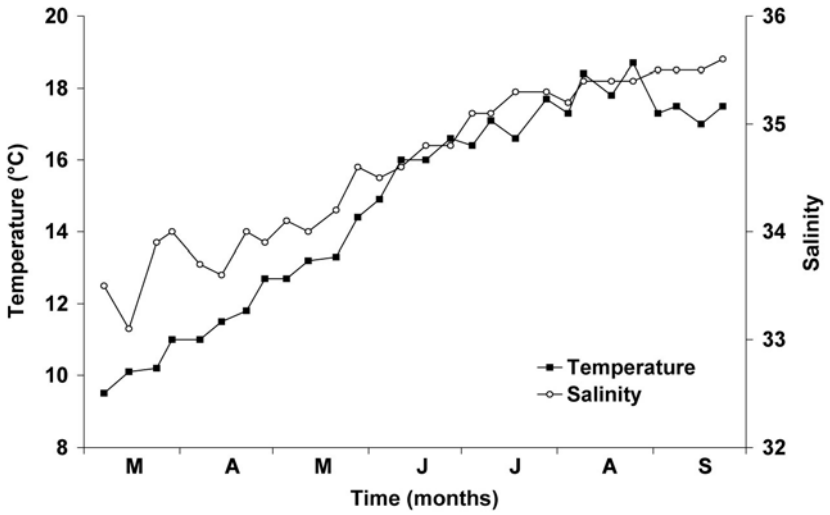

Figure 28. Bottom (30 m) seawater salinity and temperature (°C) variations for the year 2003 in the Bay of Brest (France).

3.2.4.2 Ba/Ca ratios

In the dissolved Ba experiment, *Mytilus edulis* $[Ba/Ca]_{hemolymph}$ was only slightly different from the $[Ba/Ca]_{water}$, with the linear least squares regression

$$[Ba/Ca]_{hemolymph} = 0.86 (\pm 0.04) * [Ba/Ca]_{water} + 2.26 (\pm 1.49)$$

(in µmol/mol; $R^2 = 0.98$, $p < 0.0001$, $n = 36$, in four treatments) (Fig 30). The errors of the regression coefficients reported above (and hereafter) represent the 95% confidence intervals (95% CI), and are based on among individual variation and not among treatment variation. Despite the Ba difference in foods offered (3.35, 5.87 and 14.56 nmol g^{-1} DW Ba), hemolymph was similar between the three treatments of the feeding experiment (Fig. 30, inset).

In the dissolved Ba experiment, tissue Ba/Ca was slightly enriched as compared to $[Ba/Ca]_{water}$ in the ambient treatment but was reduced by almost half in the highest $[Ba/Ca]_{water}$ treatment (Fig. 31). This resulted in an exponential fit between water and tissue

$$[Ba/Ca]_{tissue} = 35.36 (\pm 2.19) * (1-\exp^{(-0.07 (\pm 0.01) *[Ba/Ca]water)})$$

(in µmol/mol; $R^2 = 0.99$, $p < 0.0001$, $n = 11$, in four treatments) (Fig. 31). Although we do not have enough data for statistics, it is clear that there is a trend of increasing tissue Ba/Ca with increasing food Ba (Fig. 31, inset) in the feeding experiment.

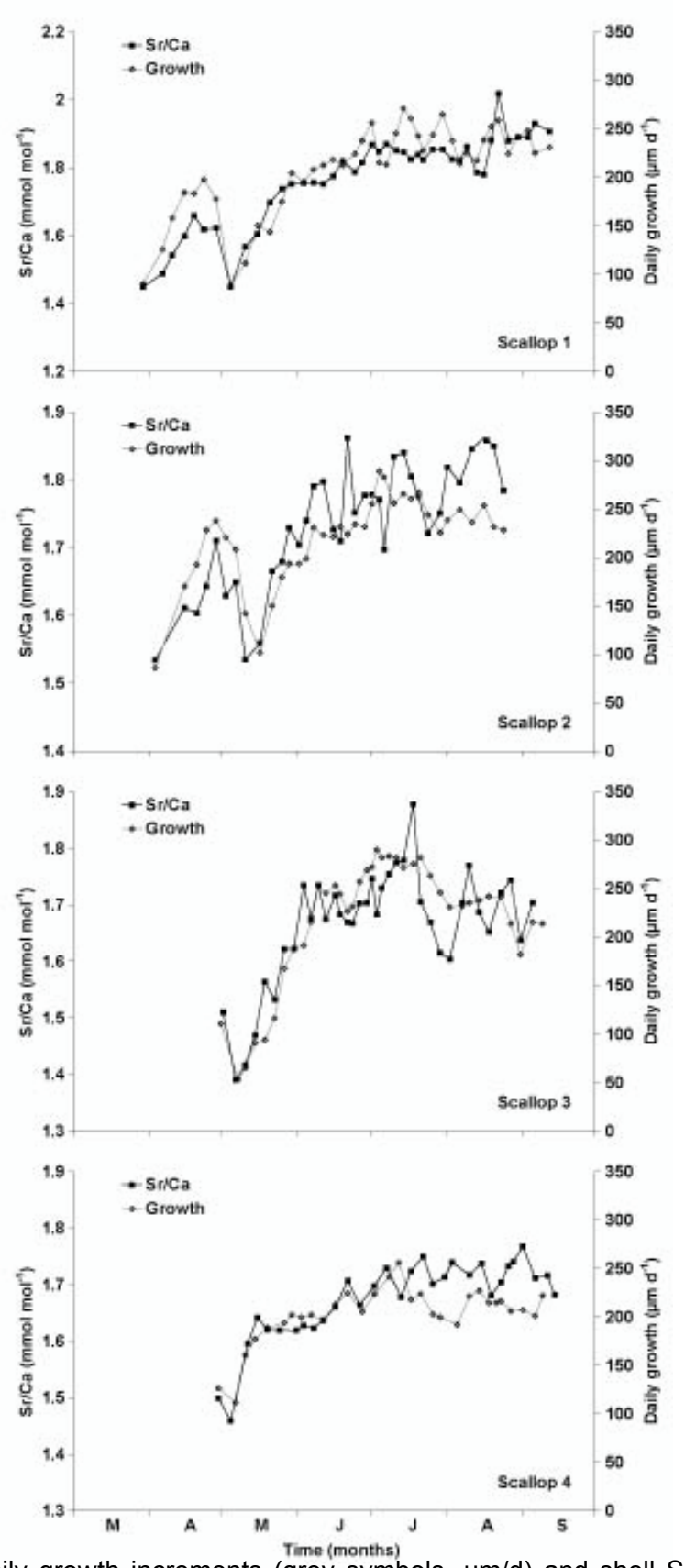

Figure 29. Daily growth increments (grey symbols, µm/d) and shell Sr/Ca ratios (black symbols, mmol/mol) in 2003 for the four age class I *P. maximus* specimens sampled in September 2003 in the Bay of Brest.

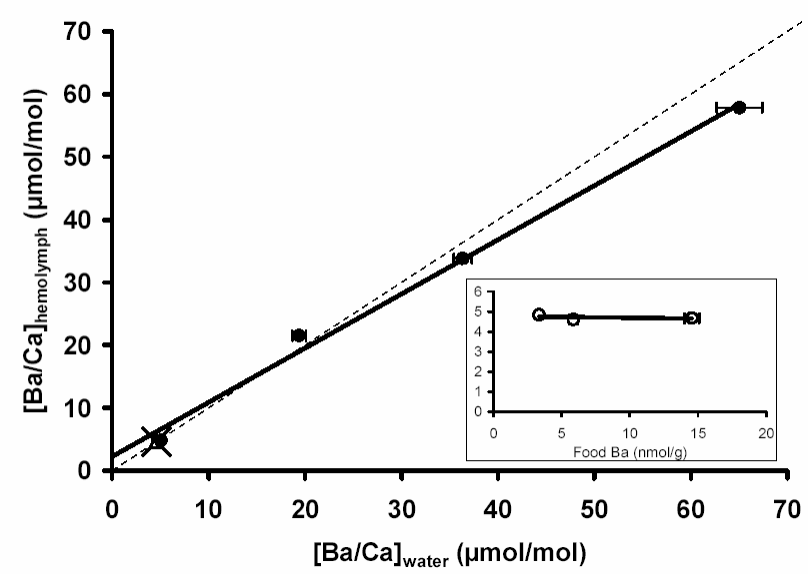

Figure 30. Mean Ba/Ca ratios (± SE) in hemolymph of laboratory grown *Mytilus edulis* versus Ba/Ca ratios of culturing water (± SE; solid circles). Some error bars are smaller than the symbols. The solid line shows the linear least squares regression, with the relationship $[Ba/Ca]_{hemolymph}$ = 0.86 (± 0.04) * $[Ba/Ca]_{water}$ + 2.26 (± 1.49) (R^2 = 0.98, p < 0.0001, n = 36 in 4 treatments). The 1:1 line is also shown (dashed). Data from the feeding experiment, where the mussels were fed food enriched in Ba are shown as the X and diamond. The inset graph illustrates that food [Ba] does not influence hemolymph Ba/Ca ratios (y-axis legend is the same as the main graph).

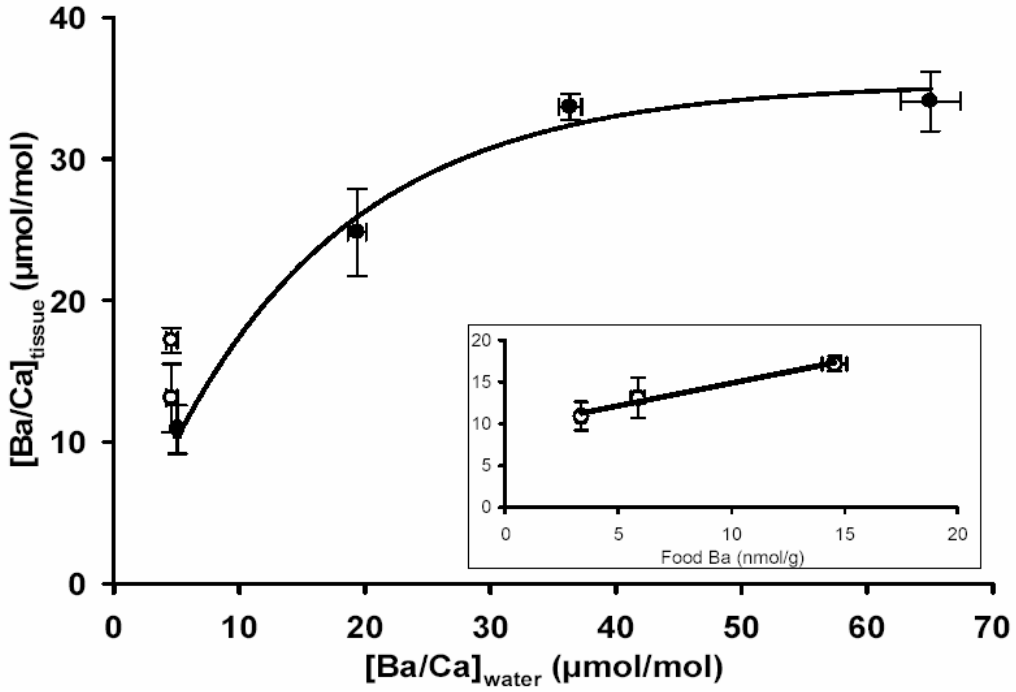

Figure 31. Mean Ba/Ca ratios (± SE) in bulk tissue of laboratory grown *Mytilus edulis* versus Ba/Ca ratios of culturing water (± SE; solid circles). Some error bars are smaller than the symbols. The solid line shows the exponential fit, with the relationship $[Ba/Ca]_{tissue}$ = 35.36 (± 2.19) * (1-$exp^{(-0.07\ (\pm\ 0.01)\ *\ [Ba/Ca]water)}$) ($R^2$ = 0.99, p < 0.0001, n = 11 in 4 treatments). Data from the feeding experiment, where the mussels were fed food enriched in Ba are shown as the open symbols. The inset graph illustrates that food [Ba] clearly does influence tissue Ba/Ca ratios (y-axis legend is the same as the main graph).

Between six to nine shells were analyzed for each Ba treatment. In the dissolved Ba experiment, $[Ba/Ca]_{shell}$ was directly proportional to $[Ba/Ca]_{water}$ with the linear relationship

$$[Ba/Ca]_{shell} = 0.10 (\pm 0.02) * [Ba/Ca]_{water} + 1.00 (\pm 0.68)$$

(in µmol/mol; $R^2 = 0.84$, $p < 0.0001$, $n = 28$, in four treatments) (Fig 32). To calculate the partition coefficient (D_{Ba}), many studies force the regression through zero (see Lea & Spero, 1992; Zacherl *et al*., 2003); yet, considering that our intercept is well above zero, we chose not to force through the origin, resulting in a D_{Ba} of 0.10 ± 0.02 (95% CI). However, it should be noted here that forcing through the origin does not significantly change the D_{Ba} (0.12 ± 0.01; 95% CI) (t-test, $p = 0.38$).

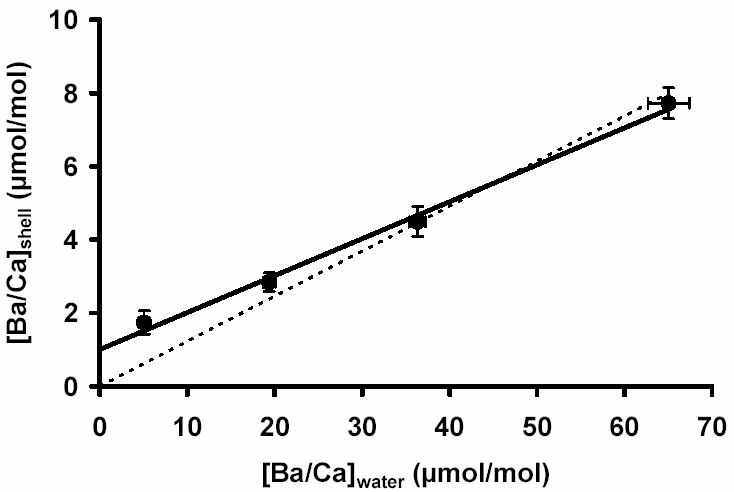

Figure 32. Mean Ba/Ca ratios (± SE) in shells of laboratory grown *Mytilus edulis* versus Ba/Ca ratios of culturing water (± SE). Some error bars are smaller than the symbols. The solid line shows the linear least squares regression, with the relationship $[Ba/Ca]_{shell} = 0.10 (\pm 0.02) * [Ba/Ca]_{water} + 1.00 (\pm 0.68)$ ($R^2 = 0.84$, $p < 0.0001$, $n = 28$ in 4 treatments). The dashed line represents the regression forced through zero.

Although shells were collected in early March, prior to the onset of the spring phytoplankton bloom (see further) and formation of the shell Ba/Ca peak, we analyzed a few shells just behind the calcein mark to assess if the shells were collected during the formation of a 'Ba/Ca peak', but these shell regions did not exhibit elevated $[Ba/Ca]_{shell}$ indicative of the Ba/Ca peak.

In the Field experiment all four sites had significantly different salinity and $[Ba/Ca]_{water}$ values (Fig. 33A, B; ANOVA, $p < 0.0001$; post hoc LSD test, all $p < 0.01$) and there was a highly significant negative relationship between $[Ba/Ca]_{water}$ and salinity (Fig. 34; in µmol/mol; $R^2 = 0.73$, $n = 55$, $p < 0.0001$) with the linear relationship

$$[Ba/Ca]_{water} = -1.22\ (\pm\ 0.21) * \text{Salinity} + 46.05\ (\pm\ 4.57) \qquad (4)$$

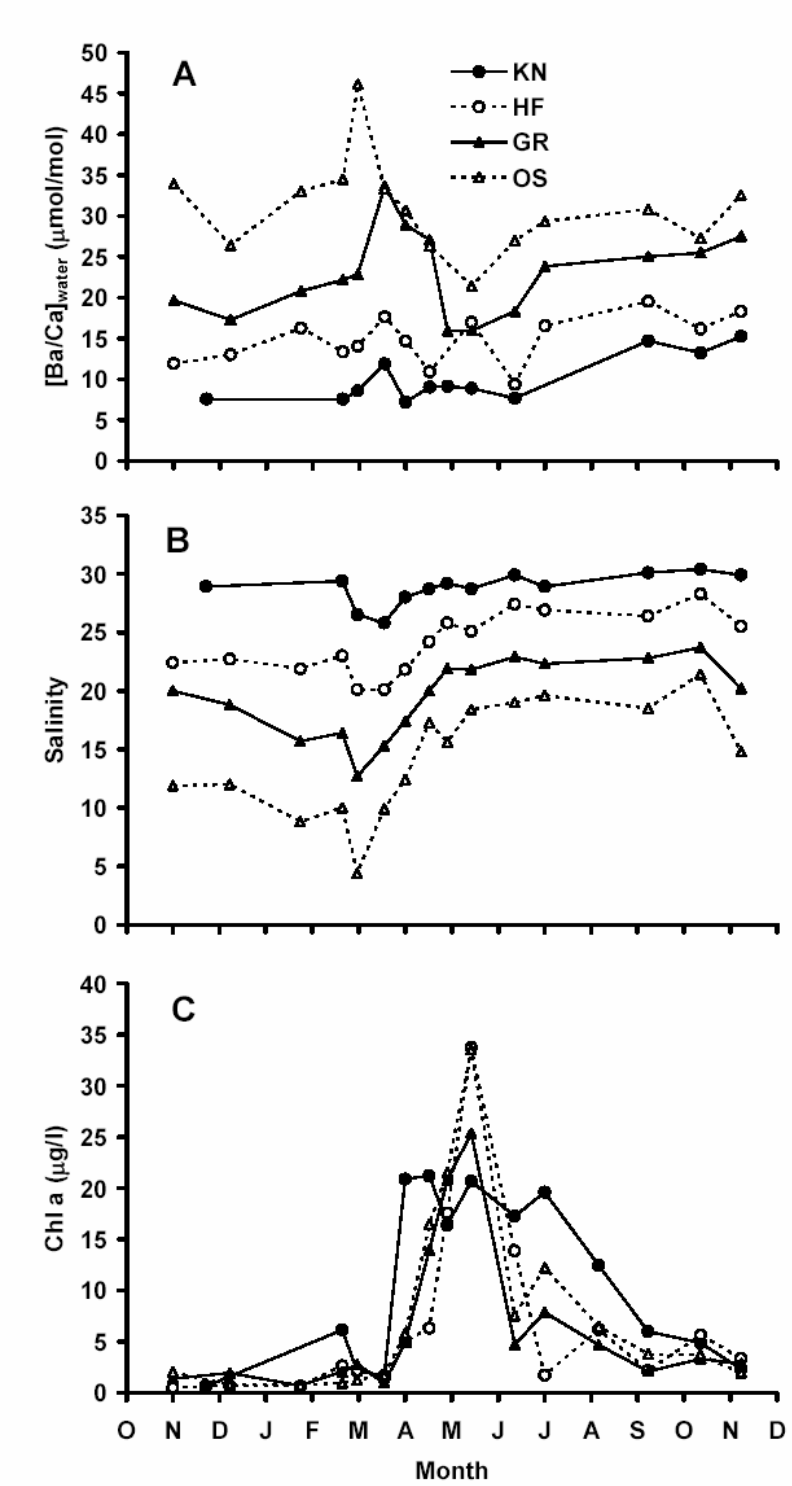

Figure 33. Dissolved $[Ba/Ca]_{water}$ (A), salinity (B) and Chl a (C) at the four Schelde sites measured over one year (Nov. 2001 - Nov. 2002). See Fig. 1 for site abbreviations.

The large scatter in these data is undoubtedly due to changes in the effective river end member as was previously demonstrated for the Schelde estuary (Coffey *et al*., 1997). There was no overall difference between Chl a concentrations at any of the

stations (ANOVA, p = 0.43), with the phytoplankton bloom starting in April and ending in late summer at all sites (Fig. 33C). The temperature profiles from the four sites were remarkably similar, with an annual range of 0 to 20 ºC (data not shown).

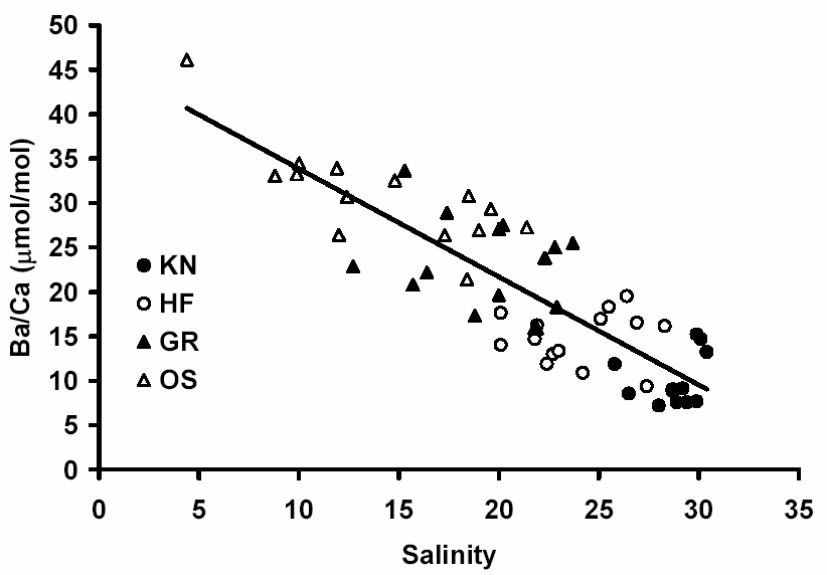

Figure 34. Salinity versus $[Ba/Ca]_{water}$, including data from all sites and sampling dates, with the linear relationship $[Ba/Ca]_{water}$ = -1.22 (± 0.21) * Salinity + 46.05 (± 4.57) (R^2 = 0.73, n = 55, p < 0.0001). See Fig. 1 for site abbreviations.

For the six shells analyzed from the field, $\delta^{18}O$, $\delta^{13}C$ and $[Ba/Ca]_{shell}$ profiles are plotted against distance from the umbo in Fig. 35. All profiles are characterized by the typical low level background $[Ba/Ca]_{shell}$, interrupted by sharp episodic peaks (aside from one shell from OS, Fig. 35). Using the inverted $\delta^{18}O$ scale as a temperature and season indicator (*i.e.*, positive $\delta^{18}O$ in winter), it is clear that these Ba peaks in the shell occur during spring when SST started to rise. The two shells which were transplanted from the Oosterschelde (sites HF and GR) showed clear calcein marks in their shells, which coincided with abrupt changes in the stable isotope profiles. The change in the $\delta^{13}C$ profile is most pronounced in the GR shell as this site has a much lower salinity (Fig. 33B) and hence more a negative $\delta^{13}C$ of dissolved inorganic carbon (DIC), compared to the Oosterschelde, where these animals were collected.

After selecting only the background $[Ba/Ca]_{shell}$ data from the shells (filled circles in Fig. 35), there was a highly significant linear relationship between background $[Ba/Ca]_{shell}$ and average $[Ba/Ca]_{water}$ data from the whole year:

background $[Ba/Ca]_{shell}$ = 0.071 (± 0.001) * $[Ba/Ca]_{water}$

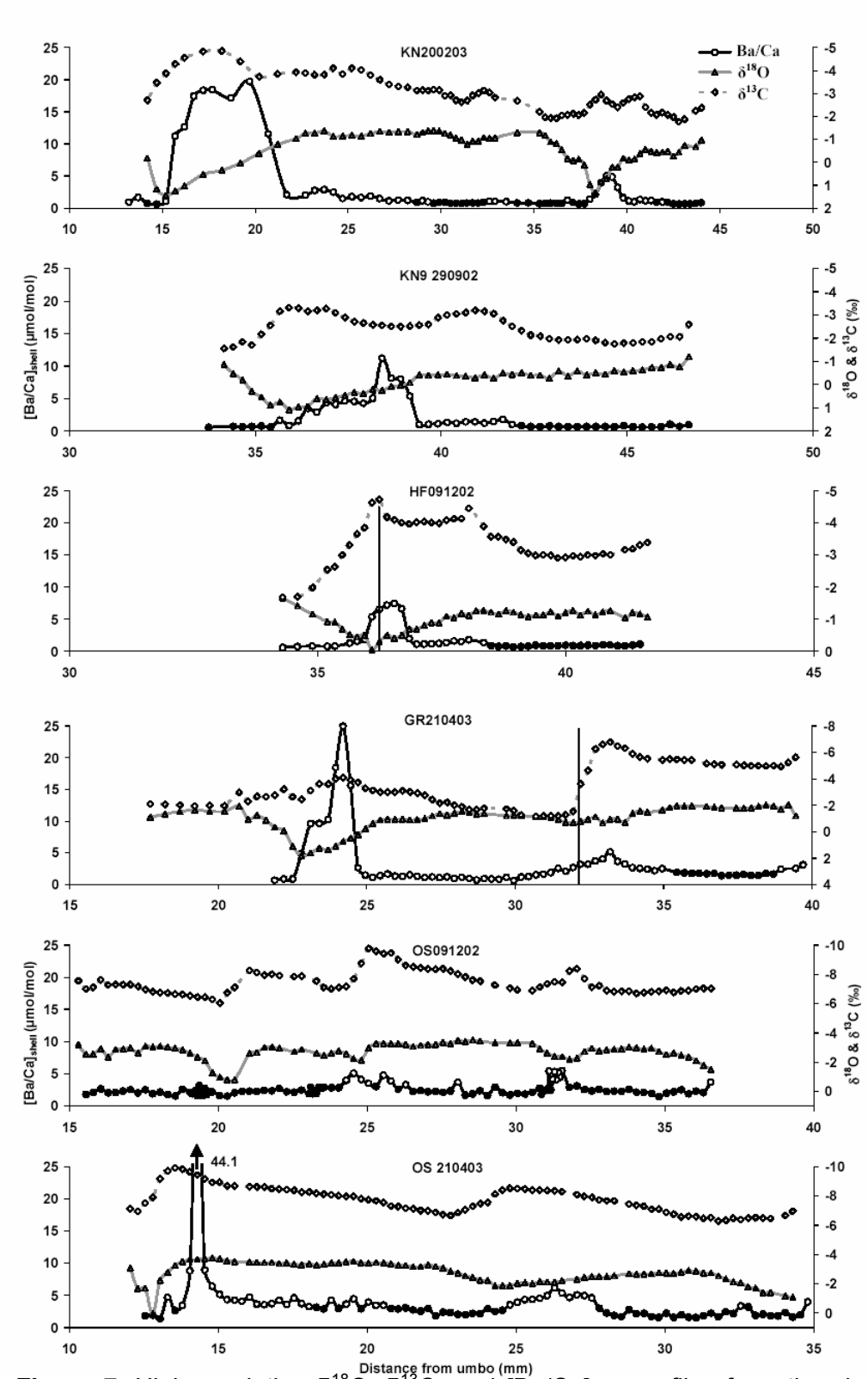

Figure 7. High resolution $\delta^{18}O$, $\delta^{13}C$, and $[Ba/Ca]_{shell}$ profiles from the six shells. Black filled symbols denote data selected as background $[Ba/Ca]_{shell}$ data. Vertical lines correspond to the time of transplantation (HF and GR shells only, see Materials and methods) as determined from the calcein stain. Shell codes represent collection site and date (format: ddmmyy). Note that the isotope axes are inverted.

(in µmol/mol; R^2 = 0.96, p < 0.0001, n = 233 [data of 6 shells from 4 sites]). As opposed to the laboratory data, these data do include zero in the intercept, which was found to be not significant (p = 0.79; 95% CI range = -0.16 to +0.12) and was therefore not included in the regression. Thus the D_{Ba} determined from the field experiment is 0.071 (± 0.001), which is significantly different from the D_{Ba} determined in the laboratory (Fig. 36; t-test, p < 0.001).

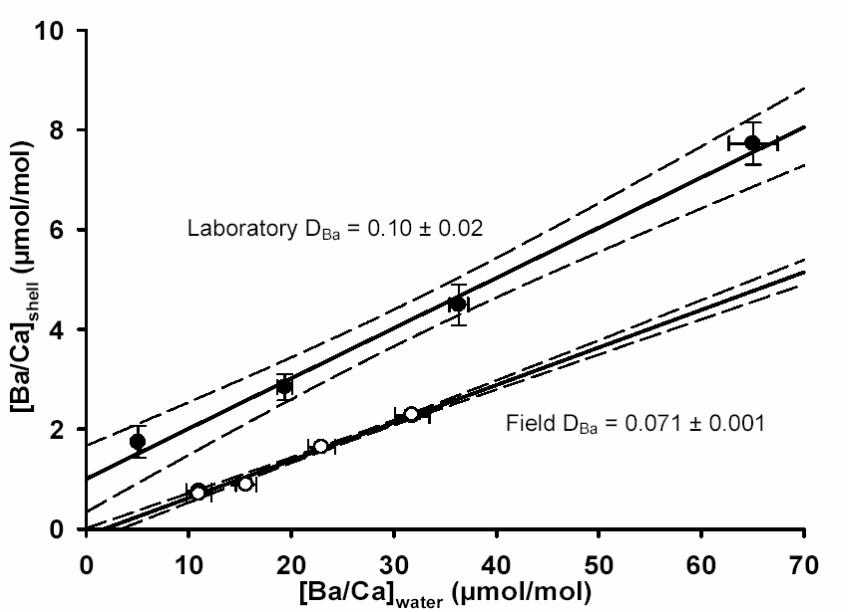

Figure 8. Mean $[Ba/Ca]_{shell}$ (± SE) in shells of laboratory grown (closed symbols; based on 28 shells from 4 treatments) and field grown (open symbols; based on multiple data from 6 shells from 4 sites, background data only) *Mytilus edulis* versus Ba/Ca ratios of water (± SE). The average $[Ba/Ca]_{water}$ over the whole year is used for the field regression (see text, section 4.2). The solid line shows the linear least squares regressions and the dashed lines the 95% CI. Slopes are significantly different (t-test) at p < 0.0001.

3.2.5 Metal uptake in bivalves

3.2.5.1 Uptake kinetics

Results of metal concentrations in the gills as a function of exposure time are presented in Figure 37 and Figure 39a for calcium. The plots were fitted with metal accumulation models [Eq 1] and [Eq 2]. The results of the model fits are presented in Table 9.

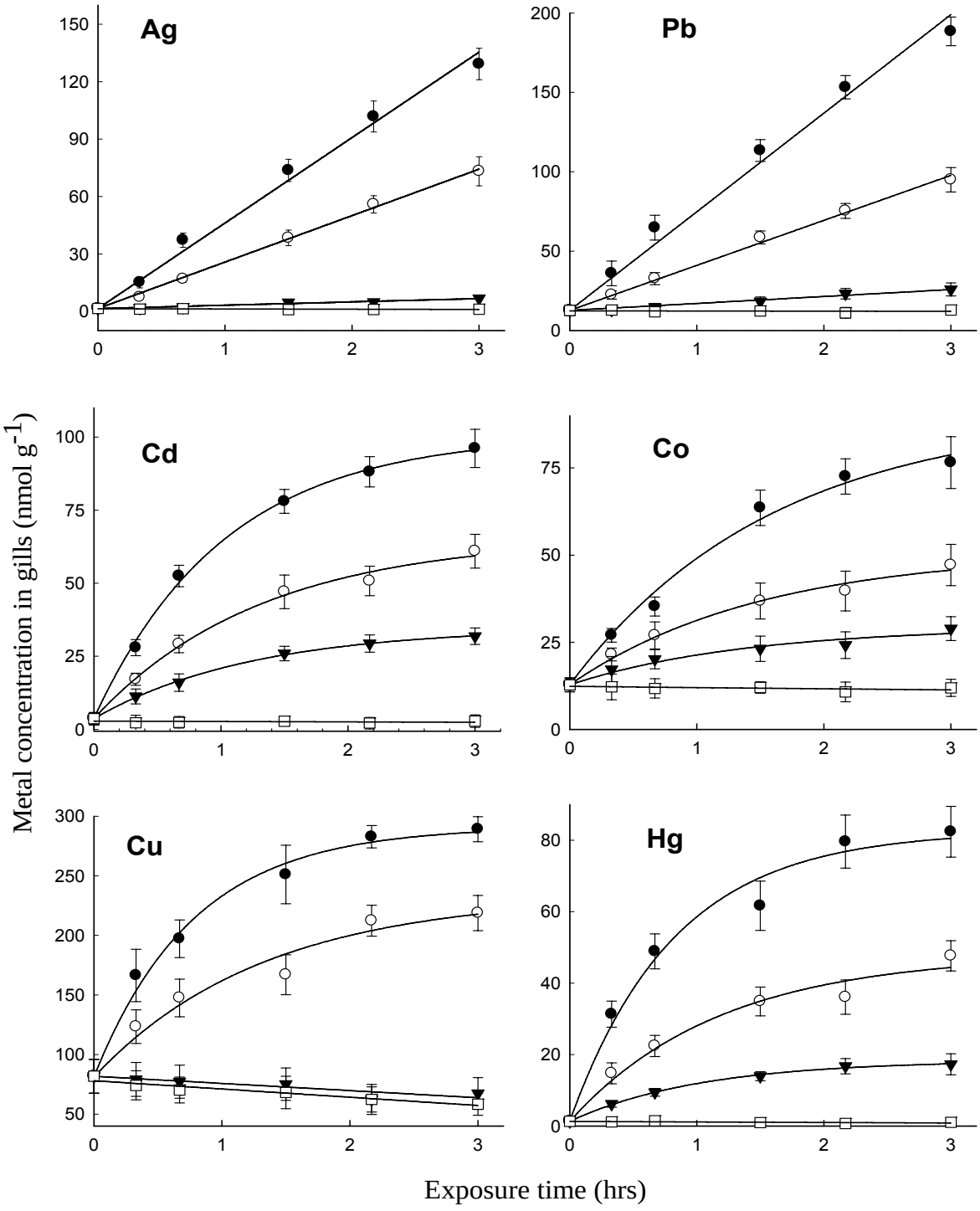

Figure 37. Metal uptake kinetics in isolated gills. The data was fitted with linear uptake model [Eq 1] for Ag and Pb and model [Eq 2] for Cd, Co, Cu and Hg.

Table 9. Results of kinetic modelling of metal uptake and elimination in isolated gills. Marked * rate constants are significantly different (Welch test, p<0.05).

Total	**Free metal ion Free metal**		**Model**	**Regression fitting**			**Uptake**	**Elimination**	
metal (µM)	(µM)	% of total	type	R^2	*p*	k_u (± SE)	*p*	k_e (± SE)	*p*
Ag 1.0	8.5E-06		L	0.9912	<0.001	48.7 (3.2)	<0.001		
0.5	4.3E-06		L	0.9976	<0.001	44.6 (2.6)	<0.001		
	2.1E-06	<<0.	L	0.9641	<0.001	7.2 (1.4)*	<0.001		
0.25		1							
Pb 1.0	0.0568		L	0.9864	<0.001	62.1 (2.0)	<0.001		
0.5	0.0285	5.7	L	0.9958	<0.001	59.6 (2.1)	<0.001		
	0.0143		L	0.9724	<0.001	17.6	<0.001		
0.25						(0.8)*			
Cd 1.0	0.0310		N	0.9982	<0.001	94.5 (4.0)	<0.001	0.87 (0.1)	<0.001
0.5	0.0155	3.1	N	0.9942	<0.001	94.4 (7.2)	0.002	0.79 (0.1)	0.001
	0.0077		N	0.9988	<0.001	100 (3.5)	<0.001	0.81 (0.1)	<0.001
0.25									
Co 1.0	0.5752		N	0.9894	<0.001	48.9 (5.3)	0.001	0.63 (0.1)	0.008
0.5	0.2827	57.5	N	0.9893	<0.001	50.6 (5.2)	0.001	0.66 (0.1)	0.006
	0.1462		N	0.9537	0.001	42.1 (4.0)	0.009	0.62 (0.3)	0.040
0.25									
Cu 1.0	0.0945		N	0.9904	<0.001	315.3 (25)	0.001	1.59 (0.2)	0.001
0.5	0.0473	9.4	N	0.9648	0.001	313.8 (32)	0.006	1.02 (0.2)	0.031
	0.0236		-	-	-	-	-	-	-
0.25									
Hg 1.0	4.3E-15		N	0.9816	0.001	80.6 (5.8)	0.002	1.1 (0.2)	0.004
0.5	2.2E-15	<<0.	N	0.9739	0.001	84.1 (4.6)	0.003	0.89 (0.2)	0.015
	1.1E-15	1	N	0.9978	<0.001	82.6 (3.0)	<0.001	0.96 (0.1)	<0.001
0.25									
Ca	5986	53.4	N	0.9284	<0.001	35.5 (6.8)	<0.001	-	-
			N	0.9827	<0.001	-	-	4.2 (0.7)	
11200									<0.001

3.2.5.2 Uptake pathways

Figure 38 and Figure 39b both shows uptake rates of heavy metals and calcium in mussel gills and the effects of different inhibitors. The uptake rate of after exposure to inhibitors were then compared to the control gills (not exposed to inhibitors) using Kruskal-Wallis Test. Additional experiment (Fig. 39c), was conducted to evaluate the effect of calcium channel blocker diltiazem at two levels of external calcium. Results showed increased effect of diltiazem to inhibit calcium uptake, confirming transport of calcium via this pathway as was expected.

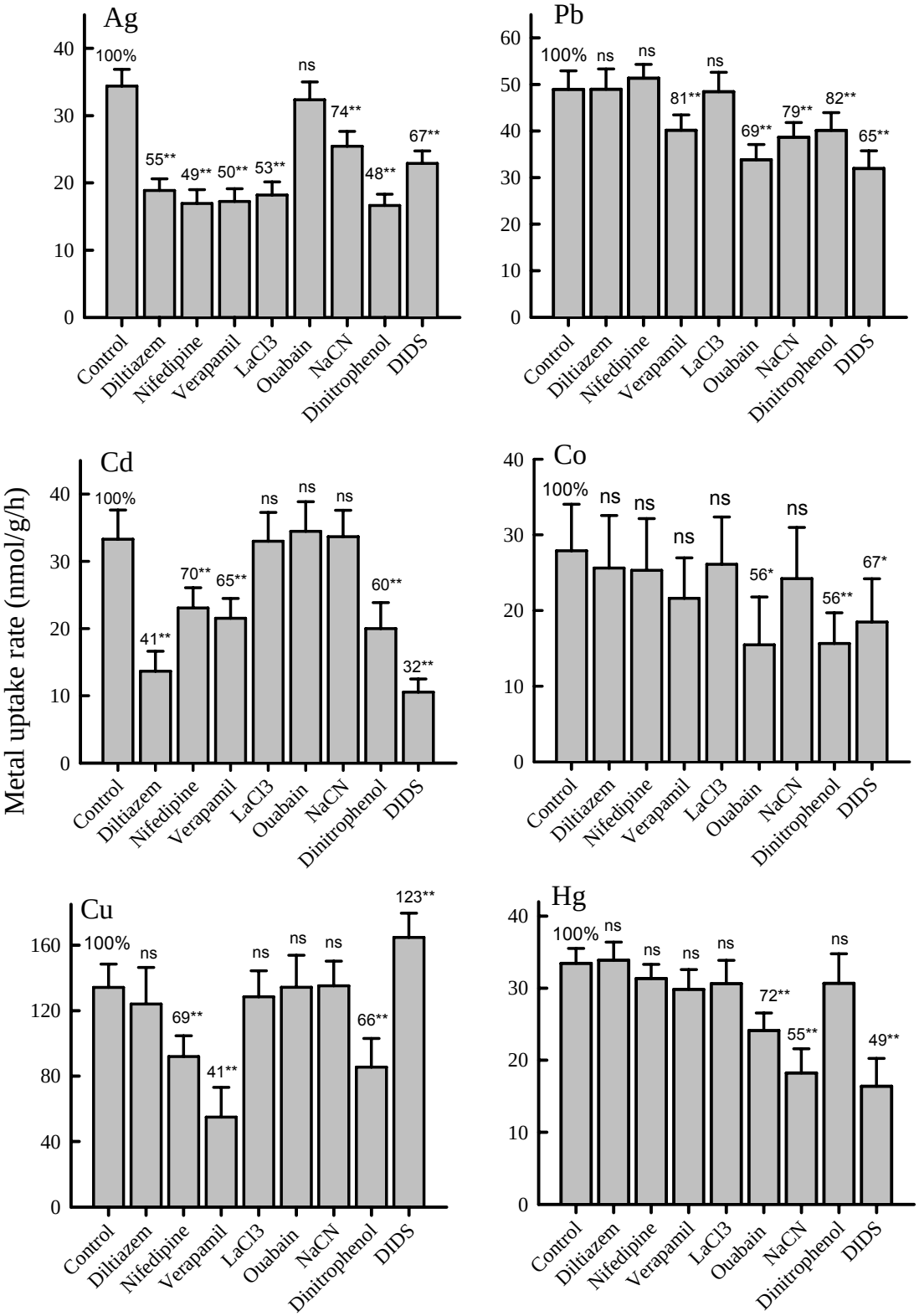

Figure 38. Metal uptake in isolated gills after exposure to metals and the effect of inhibitors on uptake. The numbers on top of bars represent metal concentrations as a fraction of control gills. * = significantly different.

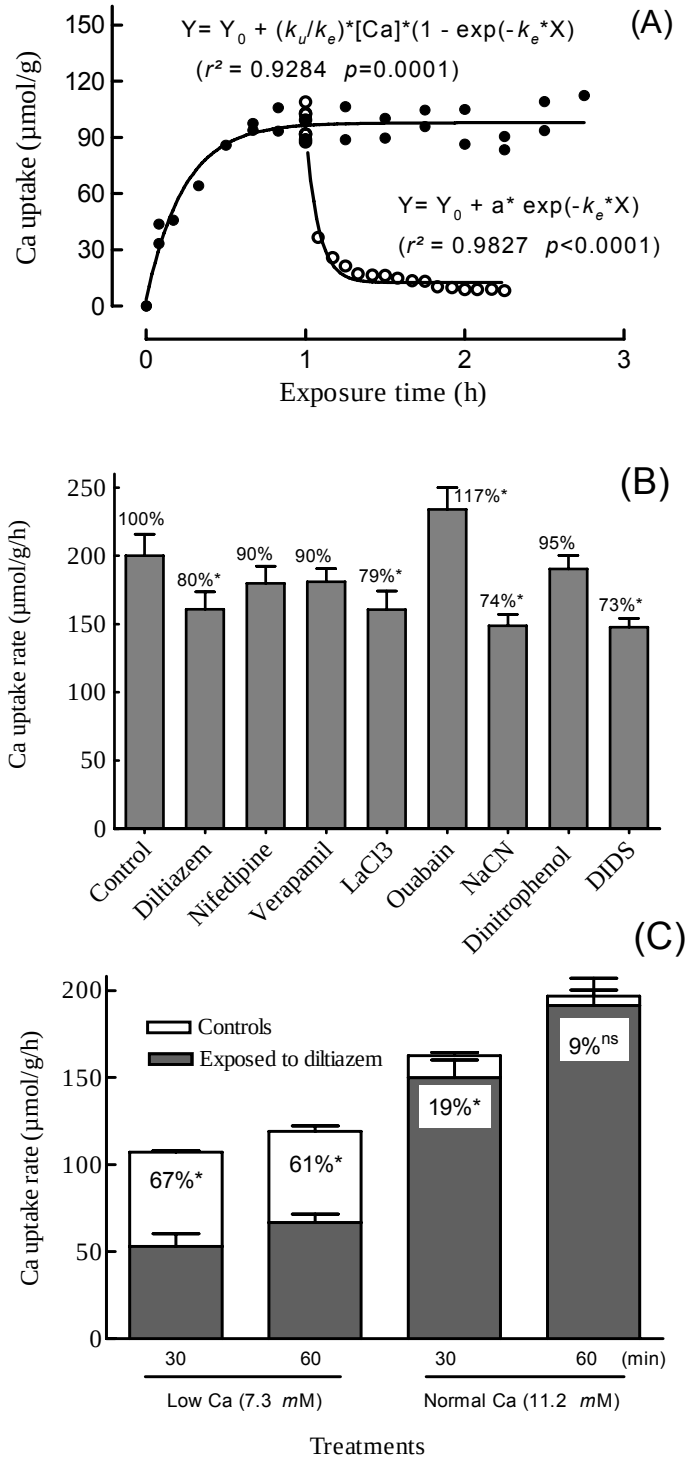

Figure 39. (A) Ca uptake and elimination, data fitted using models indicated, (B) effects of different inhibitors on calcium uptake and (C) Effect of diltiazem at two levels of external calcium and exposure time.

3.3 Echinoderms

3.3.1 Laboratory experiments

3.3.1.1 Mg and trace metals

The ratio of Mg/Ca in the experimental seawater was 3.5 to 4 mol/mol. The ratios of major and trace elements over calcium in the experimental seawater did not vary significantly according to temperature (linear regression, $p \geq 0.463$). The 3 batches of mussels used were not significantly different from each other in respect of Mg/Ca and Sr/Ca ratio (Kruskal-Wallis, $p \geq 0.178$). A highly significant temperature effect was evident on the Mg/Ca and S/Ca ratio in the juvenile *A. rubens* skeletons grown at different temperatures (Figs 40 and 41). Ba/Ca ratios showed a weak relationship with temperature. The Sr, Zn and Cd concentrations in the skeleton showed significant differences between the three temperatures but no linear relationship. Co and Cu incorporation into the skeleton was not influenced by temperature (Table 10).

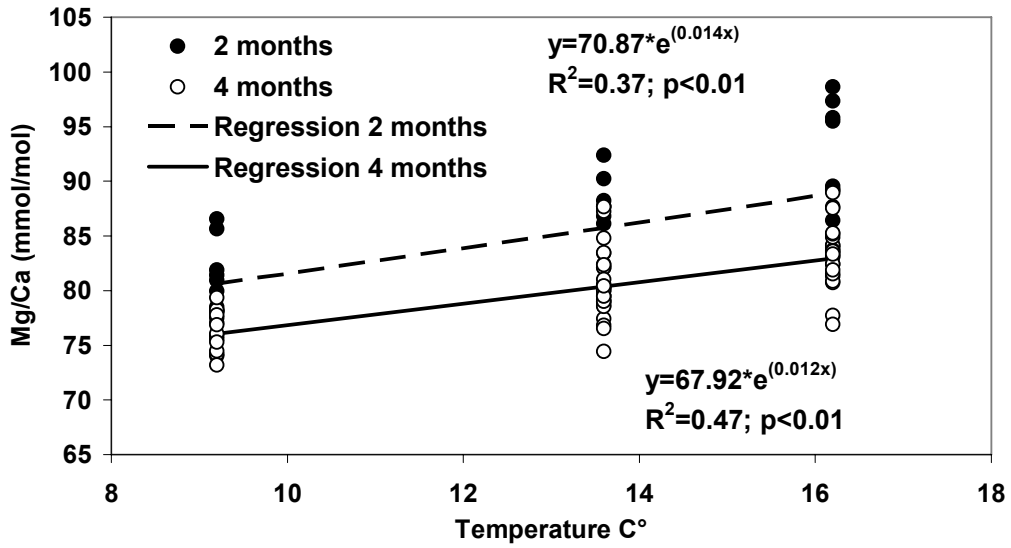

Figure 40. Mg/Ca in the skeleton of *A. rubens* grown at different temperatures.

Table 10. Concentrations of trace metals in juvenile *A. rubens* grown in aquariums at different temperatures (mean ± standard deviation)

T	Co (µg/g)	Cu (µg/g)	Zn (µg/g)	Cd (µg/g)	Ba (µg/g)	Pb (µg/g)
9.2°C	1.20±0.18	1.62±0.32	36.66±6.62	2.91±0.29	16.15±1.33	0.85±0.09
13.6 °C	1.18±0.18	1.70±0.51	49.80±11.63	6.97±0.77	17.17±1.47	0.98±0.15
16.2 °C	1.33±0.19	1.59±0.24	44.04±8.52	2.46±0.35	1.01±1.73	1.01±0.11

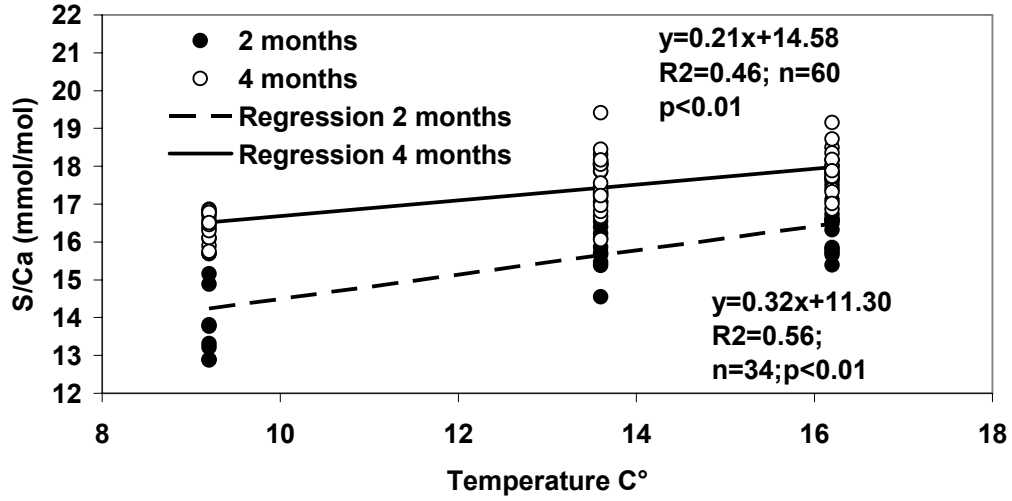

Figure 41. S/Ca in the skeleton of *A. rubens* grown at different temperatures.

No significant temperature effect could be found on the incorporation of Mg, Sr and S into the regenerating spines of *P. lividus* (data not shown).

3.3.1.2 $\delta^{18}O$ and $\delta^{13}C$

The $\delta^{18}O$ of the water in the system at 9.2°C constantly decreased over time whereas the $\delta^{18}O$ of the systems at 13.6°C and 16.2°C constantly increased. A regression carried out on $\delta^{18}O$ values of the three different systems showed an increasing $\delta^{18}O$ with increasing temperature. Thus the $\delta^{18}O$ of the water was subtracted from the $\delta^{18}O$ of the juvenile skeletons following the protocol of Epstein *et al*. (1953) to compensate for differences between the three systems of aquaria. This gives the relative $\delta^{18}O$ of the skeleton. A highly significant temperature effect was evident on the relative $\delta^{18}O$ of the juvenile skeletons (Fig. 42), which decreased with 0.22‰ and 0.37‰ per degree Celsius after 2 months and four months growth, respectively. The $\delta^{18}O$ ratio in regenerated spines of *P. lividus* decreased 0.33‰ per degree Celsius (Fig. 43).

There was no temperature effect on the $\delta^{13}C$ of the water. Significant variation of $\delta^{13}C$ in relation to water temperature was found in the skeleton of the juvenile starfish sampled at the end of the experiment. However, this variation did not yield a simple, linear relation with changes in water temperature. The $\delta^{13}C$ ratios in regenerated *P. lividus* were not linked to changes in water temperature.

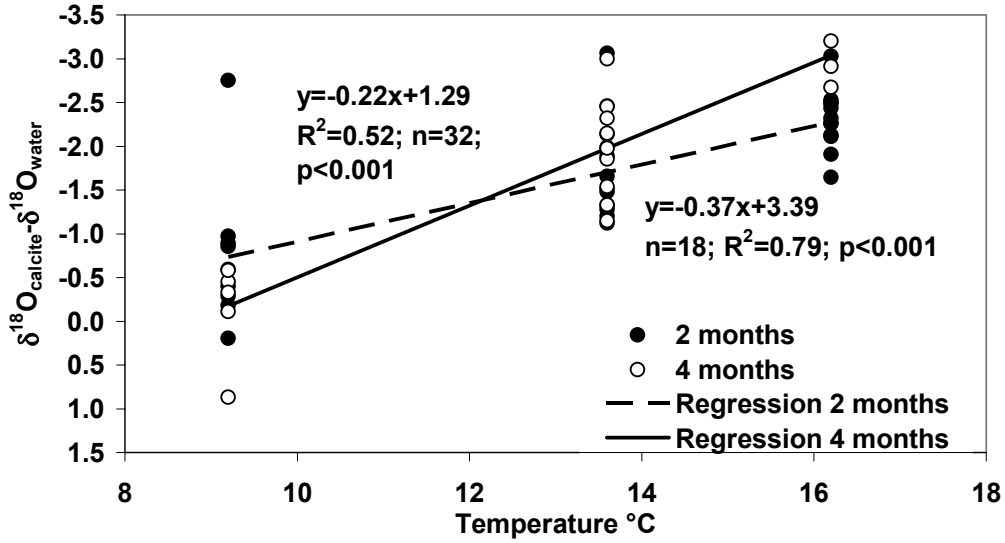

Figure 42. Relative $\delta^{18}O$ in skeletons of juvenile *A. rubens* grown at different temperatures

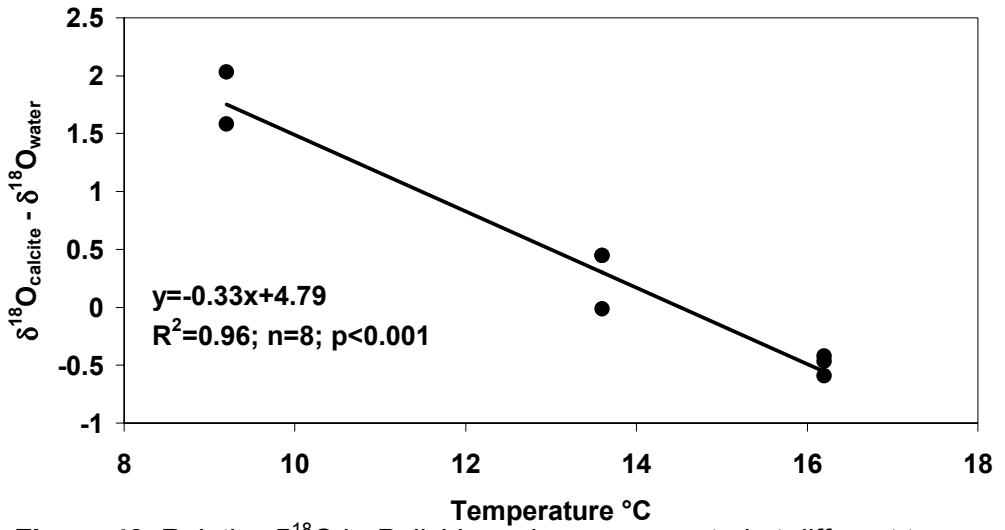

Figure 43. Relative $\delta^{18}O$ in *P. lividus* spines regenerated at different temperatures

3.3.2 Field experiments

3.3.2.1 Mg and trace metals

Modern samples

A significant latitudinal influence was evident on the Mg and S incorporation into the skeleton of starfish and closely related sea urchin species from different latitudes (Figs. 44, 45, 46). Sr, Ba and other trace metals did not show any significant influence of latitude (Fig. 47). All historical samples showed lower Mg/Ca values than modern samples (Fig. 48).

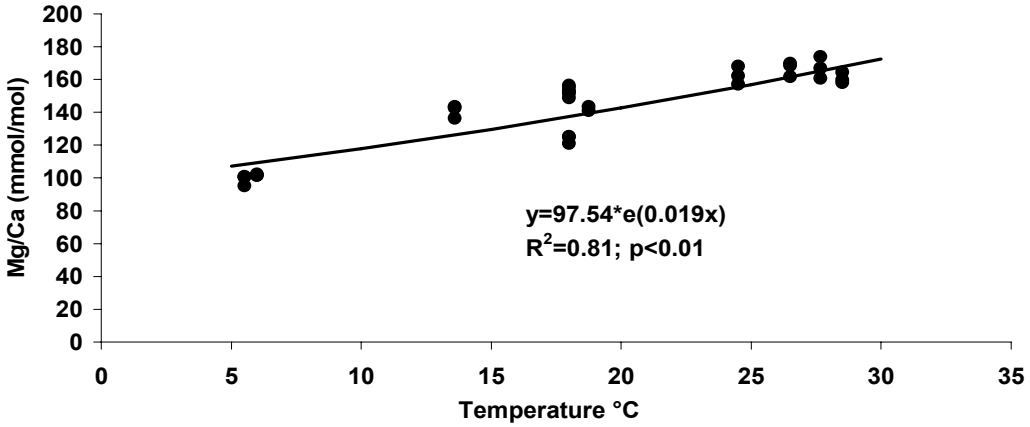

Figure 44. Mg/Ca in modern sea urchin skeletons sampled at different latitudes according to annual mean temperatures of sampling sites.

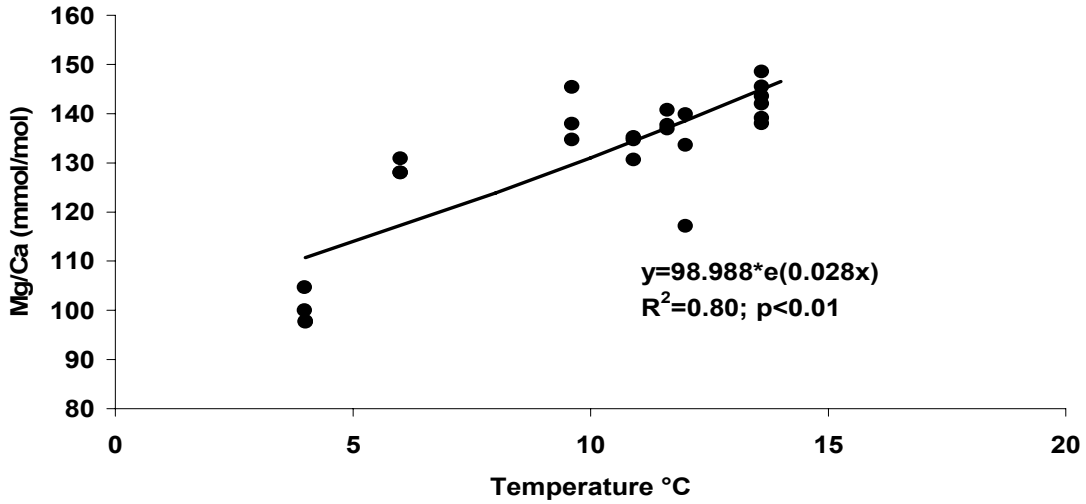

Figure 45. Mg/Ca in modern *A. rubens* skeletons sampled at different latitudes according to annual mean temperatures of sampling sites.

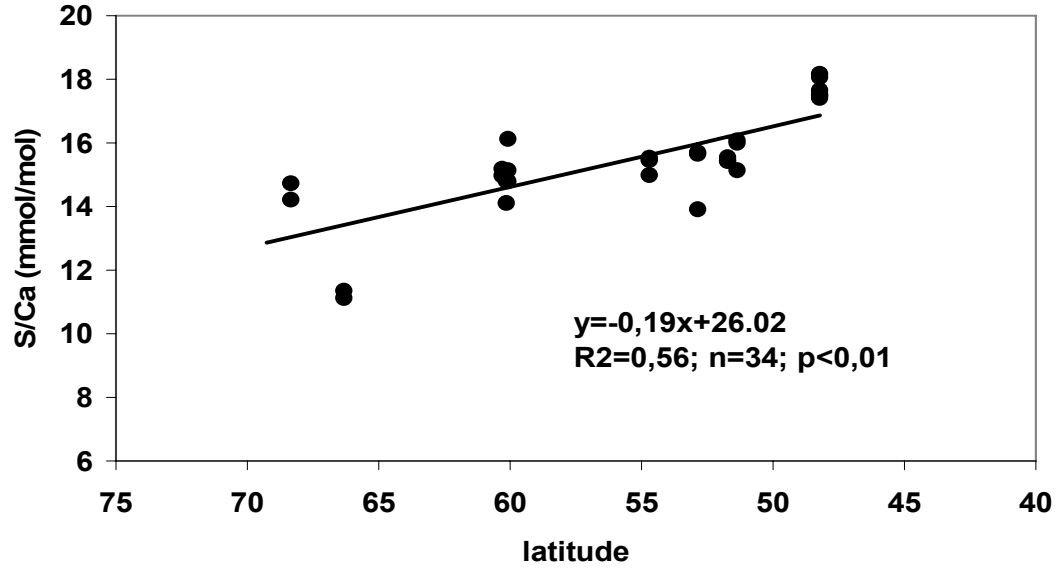

Figure 46. S/Ca in present *A. rubens* skeletons sampled at different latitudes according to annual mean temperatures of sampling sites.

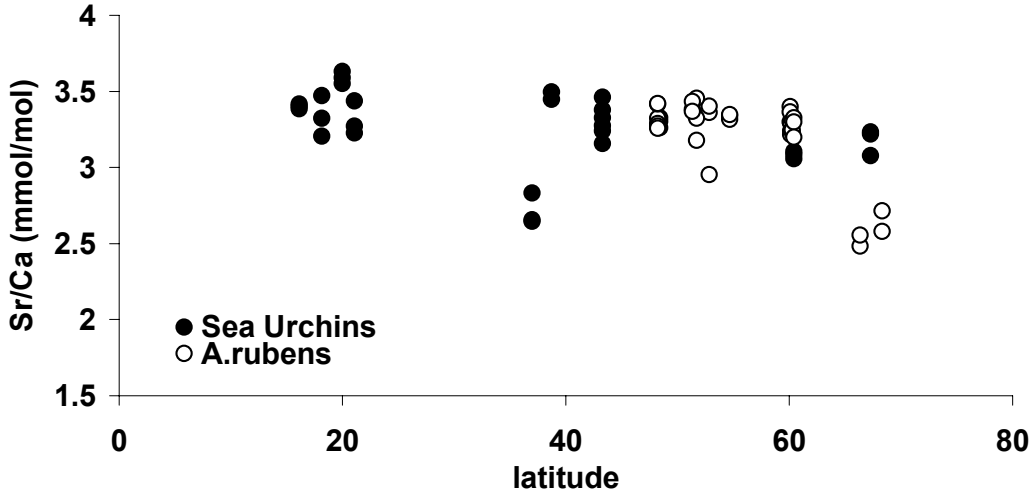

Figure 47. Sr/Ca in present sea urchin and *A. rubens* skeletons sampled at different latitudes according to annual mean temperatures of sampling site

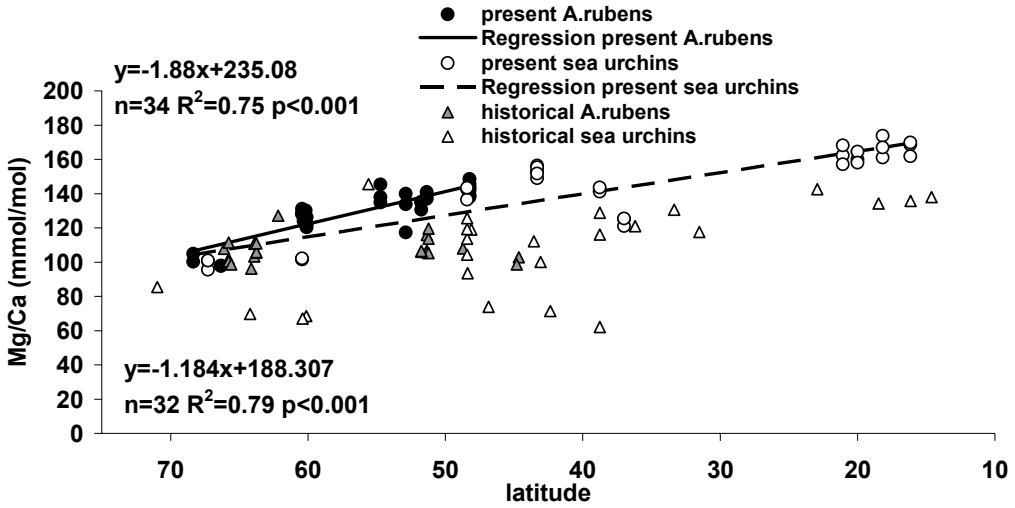

Figure 48. Mg/Ca in modern and historical sea urchin and *A. rubens* skeletons sampled at different latitudes.

3.3.2.2 $\delta^{18}O$ and $\delta^{13}C$

The mean $\delta^{18}O$ of seawater measured in the aquarium experiment was used to calculate the relative $\delta^{18}O$ of starfish and sea urchins sampled at different latitudes. This is less negative with increasing latitude (Fig. 49) and decreasing temperature (Fig. 50). There was no relationship between $\delta^{13}C$ and temperature or latitude (data not shown).

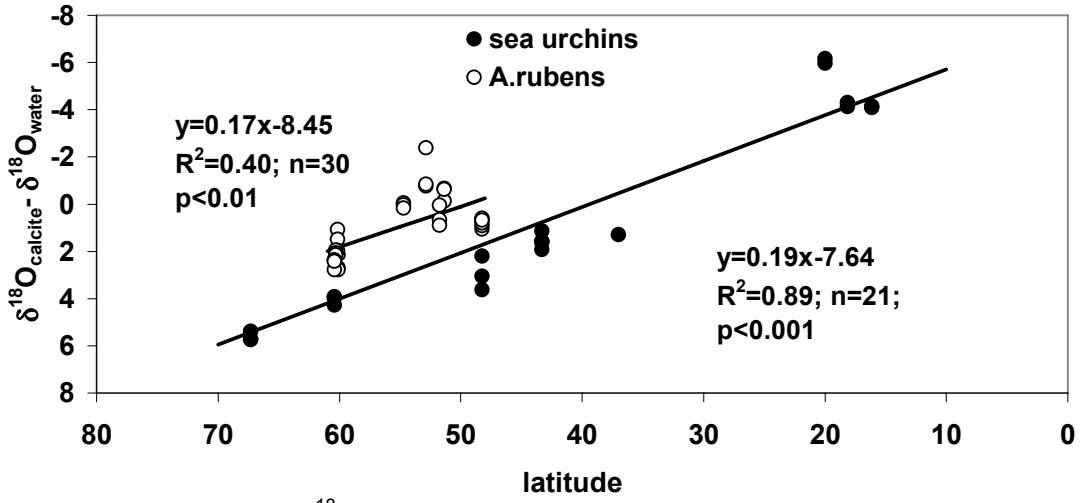

Figure 49. Relative $\delta^{18}O$ in *A. rubens* and sea urchin skeletons sampled at different latitudes.

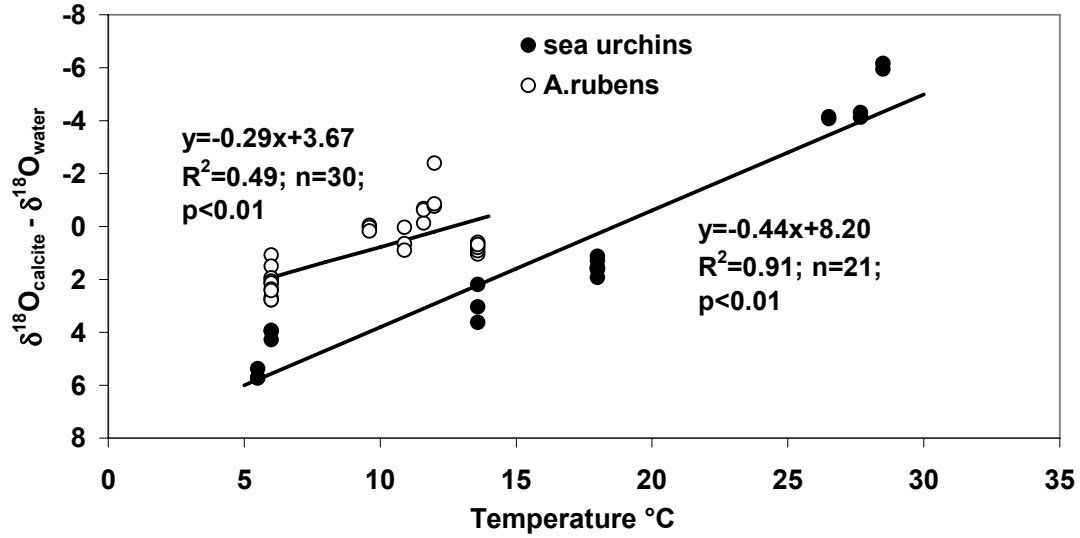

Figure 50. Relative $\delta^{18}O$ in *A. rubens* and sea urchin skeletons sampled at different latitudes according to annual mean temperature of sampling site.

4. DISCUSSION

Considering the size of this project and the limitations imposed on the size of this report, not all data generated in this project are included here. We direct the interested reader to http://www.vub.ac.be/calmar/calmarpubs.htm where peer-reviewed publications and abstracts presented at various meeting can be found.

4.1 Sclerosponges

4.1.1 Growth rate

4.1.1.1 Growth rate of C. nicholsoni

The mean growth rate for *C. nicholsoni* (198 µm/yr) was consistent with previous studies based on calcein measurement (184.2 to 233 µm/yr; Willenz & Hartman, 1985, 1999), but lower than the growth rates detected by other methods such as ^{14}C or ^{210}Pb (270 µm/yr and 220 µm/yr respectively; Benavides & Druffel, 1986). Re-growth (growth following specimen damage) was significantly lower the other calcein-determined specific growth rates at an average of 92.91 µm/yr, but was not so far outside the range specified by Swart *et al*. (2002). Swart *et al*., (2002) compared $\delta^{18}O$, Sr/Ca, ^{210}Pb, and U/Th methods to determine the growth rate of *C. nicholsoni*, and concluded a wide range (100-300 µm/yr) due to variable growth rates. A large inter-specimen variability was also suggested in this study (see section on Pb in sclerosponges; see Fig. 21A).

4.1.1.2 Growth rate of P. massiliana

For *P. massiliana*, the timing of calcein incubation relative to handling of the specimens (collection and cementing to plates) appeared to be very important. Not only was the calcein incorporation poor, but also growth rates were significantly reduced when the incubation was performed within a short time after handling (Fig. 14A). This suggests that this species is very sensitive and requires careful handling and long recovery times prior to actual incubations. When allowed to recover, growth rates were four times higher than the 'handled' specimens.

Growth rate was not easy to determine for this species. Calcein incorporation was not uniform or continuous along the edge of the skeleton when viewed with the fluorescence microscope. Approximately 10% of the calcein label was at the edge of the skeleton indicating that no growth occurred in these regions. The zero growth measurements were not included in the mean growth rate calculations as technically no growth occurred. There were no distinct patterns of calcein absence relating to

tips, parallel surface, or bases between projections of the skeleton suggesting that growth is not organized to the same extent as for *C. nicholsoni*.

The multi-directional growth of the skeleton projections meant that the growth orientation was not easy to determine in the 2-dimensional sections. Greater variation in growth rates occurred at the tip, which may be partly due to the orientation angle relative to growth rather than actual growth variation. However, since all specimens showed huge variation in growth rates (± ~50%; see Fig. 14), within and between specimens, and showed irregular regions of non-growth (~10%), it suggests that the growth rate of *P. massiliana* is highly variable at all points over the skeleton.

The microstructure of the skeletal surface was not investigated fully for *P. massiliana*. The main projections of the skeleton in *P. massiliana* have a granular appearance, possibly due to the presence of nanocrystals on the surface but this has not been confirmed. A recent paper describing skeletal microstructure in the coral *Galaxea fascicularis* (Clode and Marshall, 2003) showed the presence of nanocrystals on the skeleton surface, which have offered insights into the mode of skeletal extension. The preparation (elimination of organic matter) of the skeleton for high-resolution observation of the coral was shown to effect the survival of the crystals thus similar techniques would need to be explored for tissue removal in *P. massiliana*.

Combined experiments performing calcein incubations on living specimens immediately prior to preparation for skeletal observations could indicate growth regions relative to crystal arrangement and may also shed light onto the different growth theories suggested by Vacelet (1991) and Reitner (1989). Ultrastructural studies on the distribution of basopinacocytes, the layer of cells adjacent to the skeleton and therefore potentially involved with calcification, may also shed light onto skeleton growth in *P. massiliana*.

4.1.2 Uptake pathway

The difficulties involved with investigation the distribution and localization of elements in the soft tissues of hypercalcified sponges, notably *P. massiliana,* explains why it has not been studied previously. The thin veneer of tissue, highly integrated with the skeleton and complicated by the presence of spicules, make them not easy specimens to work on.
A number of techniques were used in an attempt to determine the uptake pathway of trace metals through the tissue to the skeleton. EDX on tissues from sponges incubated with dissolved trace metals were not successful. Factors that were investigated include the actual handling and incubation process, fixation method,

tissue dissection, section thickness, and sectioning solutions (on water, saturated calcium solution, and dry) to prevent loss of the divalent ions. Both the cryofixed and the chemically fixed (glutaraldehyde and cacodylate buffer) samples showed excellent preservation and ultrastructural details. The pyroantimonate fixation also produced good results, but the ultrastructural quality was lower due to the black divalent ions precipitated out (the purpose of this fixation). All produced negative analytical results for strontium and barium at this stage, possibly due to concentrations below the limit of detection and vast area for searching the elements under the electron microscope. To focus analytical studies, particulate studies were undertaken to know where to perform the point analyses.

The use of ferritin allowed the initial uptake route to be determined. Exopinacocytes, endopinacocytes and choanocytes functioned as primary cells for uptake of (small) particles across the cell surface. The flagella and microvilli of the choanocytes were surrounded by ferritin, and may help to trap the particles in their surrounding glycocalyx and aid internalisation. Ferritin accumulated in membrane-bound vesicles inside the endopinacocytes and choanocytes, suggested cytoplasmic streaming. Accumulation into vacuoles took place within 30 minutes and remained so after 4 hours. It is not sure if the ferritin would be expelled or assimilated after this time. Further pulse-chase experiments with shorter intervals are required to complete the movement of ferritin with the sponge tissue.

The strontium-labelled bacteria showed a slightly different mode of uptake suggesting that the uptake mode and or route depends on particle size. Bacteria cells were incorporated into the sponge by phagocytosis, accumulating mostly in the choanocytes. They retained their strontium content even after incorporation thus trace metals may be taken up via organic matter.

The accumulation of ferritin and bacteria in the choanocytes focused the EDX studies on these areas. However, increased awareness of specimen handling and knowledge of where to focus EDX analyses did not lead to success in locating the trace metals (strontium or barium) using TEM/EDX. Again, this was considered to be due to the vast areas within the choanocyte chambers to search at TEM magnifications and the low concentrations of dissolved metals used for incubation relative to the detection limits of the instruments, leading to the repeat of experiments using higher concentrations of trace metals. Despite this, further TEM/EDX on the new samples produced more negative results.

SEM/EDX was utilised to analyse larger areas of the sponge. Initial analyses were performed on sections from whole embedded sponges cut with diamond wire, using

minimal water to keep the wire cool and then dried immediately. Only small traces of strontium and barium were located by area analyses. Despite the fact that SEM/EDX analyses is not limited to the surface, and penetrates into the specimen, repeating the analyses after removing the surface of the sections carefully with a dry razor blade improved detection slightly but the element peaks were not significant and the possibility of recognising tissue regions was limited. The presence of small peaks in area analyses and no success in point analyses suggested very low concentrations over large areas, however, later results proved this not to be the case.

Results were improved when SEM/EDX was performed at high resolution directly on the block face of embedded material previously sectioned using a microtome. This provided an ultrastructural map (made from previous sections) correlating with the sample to be analysed in the SEM. Using this technique, choanocytes could be targeted. Despite much searching, strontium and barium were found in only two specimens (one from a sample that was cryofixed, and one fixed using glutaraldehyde in cacodylate buffer).

In both cases, strontium and barium were found at high concentrations in specific locations or hotspots. Despite knowing the exact location, obtaining a second positive analysis at a later date was not easy, highlighting the fact that it is highly localised in very small deposits. TEM/EDX of sections milled from the hotspots confirmed that the barium was present in its particulate form, barium sulphate. In view of the difficulty in locating the trace metals, the fact that they were not found in the pyroantimonate-fixed samples does not mean they were not there.

The presence of strontium and barium in the choanocytes, as predicted from the particulate-uptake experiments (ferritin and bacteria) suggests that they may have similar uptake routes.

4.1.3 Lead in *Ceratoporella nicholsoni* and *Stromatospongia vermicola* skeletons

The excellent intra-specimen reproducibility and similarity between specimens collected from the same site (inter-specimen reproducibility) illustrate that sclerosponges are excellent proxies of environmental Pb, at this resolution. The continuous lead profiles suggest a lack of any important hiatus in the Pb incorporation for all specimens.

Since we analysed Pb/Ca ratios in two different species, *C. nicholsoni* and *S. vermicola,* the question arises whether there is a difference in lead content between both species independent of environmental concentrations. *Stromatospongia*

vermicola displays maximum lead values, which are two- to four-times higher than the values from *C. nicholsoni* during the late 1970's Pb maximum (Fig. 19). However, the Pb level in the *S. vermicola* sample (TC1) is similar to *C. nicholsoni* before the rapid increase starting in 1960 (Fig. 19). This suggests that the differences in maximum lead values are more likely related to location or depth, than being species related. It means that i) if differences in physiological effects exist between *Ceratoporella nicholsoni* and *Stromatospongia vermicola*, they may affect lead incorporation only at higher lead concentrations, or ii) these two species have a similar physiological functioning.

All but sample RB1, display a maximum lead content between 1975 and 1983; with a maximum around 1960. RB1 seems to display a time misfit with regards to the two other RB profiles. This discrepancy is ascribed to a higher growth rate (of approximately 400 µm/year) than the assumed mean 233 µm/yr. Such a rate is significantly larger than those estimated by Willenz & Hartman (1999) (from 173 µm/year to 287 µm/year) and this study (see section 4.1.1.1), but is within those determined by Swart *et al.* (2002) (128 to 400 µm/yr).

A lag of one to two years is expected for the timing of the maximum lead content in sclerosponges taken deeper since the residence time of lead in the upper 100 meters is about two years (Schaule & Patterson, 1983). A maximum lead content within the interval 1975-1983 matches the lead profile published by Lazareth *et al*. (2000), which was calibrated against $\delta^{13}C$. It corresponds to the 1977 lead maximum reported in Florida key corals (Shen & Boyle, 1987) and to the late 1970s-mid 1980s maximum observed in Antarctic snow (Planchon *et al.,* 2003) and bivalve shell (Gillikin *et al*., *in press*-b and section 4.2.3.4). It is slightly delayed with regards to the 1971 and mid-sixties maxima of Bermuda corals (Shen & Boyle, 1987) and Greenland snow (Candelone *et al*., 1995) - early 1970s (Boutron *et al*., 1991), respectively

A higher maximum lead content in sclerosponges was observed in samples collected deeper in the water column. The TC 1 sclerosponge from Turks and Caicos Island (*S. vermicola*) from 130 meters deep displays a Two-fold higher lead maximum than the AC1 and AC2 samples collected at the nearby Acklins Island at a depth of 30 meters. However this is possibly a species specific effect. In contrast, the three RB samples from Jamaica occurring at similar depths do not display important differences in lead content. If a change in the physiological functioning of the sclerosponges linked with depth was responsible for the change in lead uptake, we would expect a lower growth rate for the deeper specimens. This is very unlikely since no important time lag is observed for the lead maxima, when assuming a mean

growth rate of 233 µm/yr, except for one shallow sclerosponge (RB1). The difference in lead content between sclerosponges taken at different depths should therefore reflect changes in the seawater content. However, concentrations of dissolved lead in the Sargasso Sea water are rather constant in the upper 500 meters and vary around 160 pmol kg^{-1} (Schaule & Patterson, 1983) or are only slightly increasing from approximately 80 to 170 pmol kg^{-1} consecutive to a recent decrease in the upper 200 meters (Boyle *et al.,* 1986; Veron *et al.,* 1993 and Wu & Boyle, 1997 and references herein). Therefore, it seems rather unlikely that the two-fold higher lead content of deep sclerosponges is reflecting higher dissolved lead contents of seawater. Lead, in opposition to other metals, mainly absorbs on particulate surfaces, the difference in lead content in sclerosponges is therefore more likely to follow differences in particulate content of the seawater. A three-fold increase in the lead concentration of particulate matter (from 1 to 3 pmol/l) from anthropogenic origin is observed from the surface down to 500 meters (Sherrell &Boyle, 1992) and is a plausible explanation for a recurring higher lead content in deeper sclerosponges for the period 1960-1995. This sheds light on the physiological functioning of these organisms since it favours "particulate filtration" over "dissolved water diffusion" as the major lead uptake mechanism for sclerosponges.

The increase after 1925 lies between +102% and +214% and leads to a maximum around 1980 and is followed by a decrease of -13 to -46%. This trend follows, however strongly smoothed, the evolution of the three to five fold increase in anthropogenic lead deposition from the 1930's through the 1970's (Murozumi *et al.*1969; Shen & Boyle 1988) due to the increase in leaded gasoline use (Nriagu, 1989; Wu & Boyle, 1997). In recent times, the lead concentrations in the sclerosponges tend to return to low values in accord with the 30 to 40% decrease observed in seawater in 1989 (Veron *et al.,* 1993). In 1995, none of the studied sclerosponges had attained pre 1930 values (fig. 2, 7). Other sources than leaded gasoline, such as due to industrial activity, may tend to keep the lead values higher than the pre 1930 values.

Going back in time, the sclerosponge studied by Lazareth *et al.* (2000), tend toward lower lead concentrations of about 0.3 ppm (in 1760). Only one of the Jamaican sclerosponges (RB2) displays this concentration around 1900. The other sclerosponges display slightly higher values, reflecting in large part the increasing lead smelting in the Northern Hemisphere during the industrial period (Murozumi *et al*., 1969).

A good knowledge of the partitioning between water and the studied species would enable reconstructions of lead concentration of ancient seawater and the study of the

past evolution of lead down the water column. Since in the last century, lead concentrations in seawater and in the sclerosponges have changed due to leaded gasoline pollution, we compared the pre "leaded gasoline" period (pre 1925) with the period of maximum lead pollution observed in the sclerosponges. In order to calculate the partitioning (or distribution) coefficient for each period, the lead concentration in the seawater must be known (calcium concentration is approximately 0,01M). Shen & Boyle (1987) estimated a pre industrial dissolved lead concentration of 18 pM in seawater. We calculated the partitioning coefficient (D_{Pb}) by comparing this concentration with the mean lead concentration of the different sclerosponges for the period pre 1925. Concentrations of 170 pM dissolved lead were measured by Schaule & Patterson in 1983 and were compared with maximum lead concentrations in the sclerosponges.

Sclerosponges concentrate much more lead in their skeletons, than corals, which D_{Pb} was estimated at 2.3 (Shen & Boyle, 1988). This is in agreement with the lower growth rate of sclerosponges, accumulating more lead for the same amount of produced carbonate. The ability of sclerosponges to concentrate lead makes them promising proxies to study other heavy metals that are difficult to measure in corals due to their low concentrations such as cadmium.

4.2 Bivalves

4.2.1 $\delta^{18}O$ in bivalve shells

Saxidomus giganteus shell oxygen isotopes are clearly controlled by external environmental factors as indicated by the similarities between the three shells (Fig. 21). Although there were differences up to 0.5 ‰ in high resolution $\delta^{18}O_S$ profiles, the difference in average $\delta^{18}O_S$ was less than half of this (0.19 ‰) and half of what has been reported in corals (0.4 ‰; Linsley *et al*., 1999). This indicates that if $\delta^{18}O_W$ is known, average temperature can be calculated with an uncertainty of ~ 0.8 °C. However, in paleo-environmental studies, $\delta^{18}O_W$ is rarely, if ever, known. Despite the salinity and $\delta^{18}O_W$ data available to us, we were still unable to accurately calculate temperature (more details in Gillikin *et al*. *in press*-a). We were unable to determine if *S. giganteus* precipitates their shell in isotopic equilibrium with surrounding waters, but these data do clearly highlight some of the problems associated with using intertidal estuarine biogenic carbonates as paleotemperature proxies (more details in Gillikin *et al*. *in press*-a). Evidentially, salinity independent proxies, or a salinity proxy, are necessary for more precise paleotemperature determinations.

4.2.2 $\delta^{13}C$ in bivalve shells

4.2.2.1 What is the cause of the decreasing $\delta^{13}C_S$?

All *M. mercenaria* shells investigated showed a clear ontogenic decrease in $\delta^{13}C_S$ (Fig. 22). There are several potential causes for this decrease; however, kinetic effects can most definitely be ruled out. Kinetic effects result in a good correlation between $\delta^{18}O_S$ and $\delta^{13}C_S$ (McConnaughey, 1989, see also introduction), which has not been observed in *M. mercenaria* shells (Elliot *et al*., 2003; Gillikin, unpublished). Other possible causes for the ontogenic decrease in $\delta^{13}C_S$ can be separated into two main categories: changes in environmental $\delta^{13}C_{DIC}$ and biological changes resulting in a change in the internal DIC pool. Environmental changes include the Suess effect, caused by increasing amounts of anthropogenic ^{13}C depleted CO_2 in the atmosphere, which leads to more negative $\delta^{13}C_{DIC}$ in seawater. This phenomenon has been recorded in sclerosponge skeletons (Druffel & Benavides, 1986; Lazareth *et al.*, 2000), but the change over the past 50 years is on the order of 0.5 ‰, far less than the changes observed in these shells (up to 4 ‰). Additionally, similar decreases in $\delta^{13}C_S$ are noted regardless if the clam was collected in 1980 or 2003 (Fig. 22), and the ontogenic decrease is also evident in a Pliocene shell, which grew well before anthropogenic CO_2 inputs were present (data not shown). Thus, changing environmental $\delta^{13}C_{DIC}$ is obviously not the dominant cause. Another possibility is that the clams may live deeper in the sediment as they age and utilize a more negative environmental $\delta^{13}C_{DIC}$ source, as suggested by Keller *et al.* (2002) and Elliot *et al.* (2003). Indeed, strong gradients in pore water $\delta^{13}C_{DIC}$ have been observed within the initial 5 cm of sediment due to the remineralisation of organic matter (up to -1 ‰ cm^{-1}; McCorkle *et al.*, 1985). However, this is probably not a cause as Roberts *et al.* (1989) found that the depth of *M. mercenaria* in the sediment was independent of clam size, and thus different size classes can be considered to use similar water sources. Thus, the most probable cause is a change in the internal DIC pool, which is supported by the negative relationship between shell length and hemolymph $\delta^{13}C$ (Gillikin, 2005).

A change in the internal DIC pool could be due to differences in $\delta^{13}C_R$ caused by food sources with different $\delta^{13}C$ signatures. However, in this study, tissue $\delta^{13}C$ and shell length were generally not correlated. Although some tissues showed a positive relationship (see Gillikin, 2005), this is opposite to what is observed in the shells (Fig. 51). Thus, a change in food as the animal ages is not likely the cause of the $\delta^{13}C$ trend in the shells. Changes in lipid metabolism can also result in changes in $\delta^{13}C_R$, but this would be expected to be reflected in the tissue $\delta^{13}C$, which it is not. Moreover, lipid content has been shown to be low in *M. mercenaria* tissues, changing the $\delta^{13}C$ value of tissues by ~ 0.5 ‰ (O'Donnell *et al.*, 2003). Changing pH can also

affect $\delta^{13}C_S$, with increasing pH resulting in decreasing $\delta^{13}C_S$, as has been observed in foraminifera (Spero *et al.*, 1997) and corals (Adkins *et al.*, 2003). However, internal pH has been shown to decrease in older bivalves (Sukhotin and Pörtner, 2001), which would lead to an increase in $\delta^{13}C_S$. Lorrain *et al.* (2004) proposed that the increased absolute metabolism in larger bivalves relative to their shell growth rate, leads to a larger availability of metabolic C for $CaCO_3$ precipitation. In other words, the increase in CO_2 production is larger than the demand for calcification, resulting in a larger amount of metabolic C in the internal DIC pool. It is therefore expected that the respired to precipitated carbon ratio (Lorrain *et al.*, 2004) will also increase through ontogeny in *M. mercenaria*. This indeed seems probable, as *M. mercenaria* has been shown to have a high metabolic rate compared to other bivalves (Hamwi and Haskin, 1969).

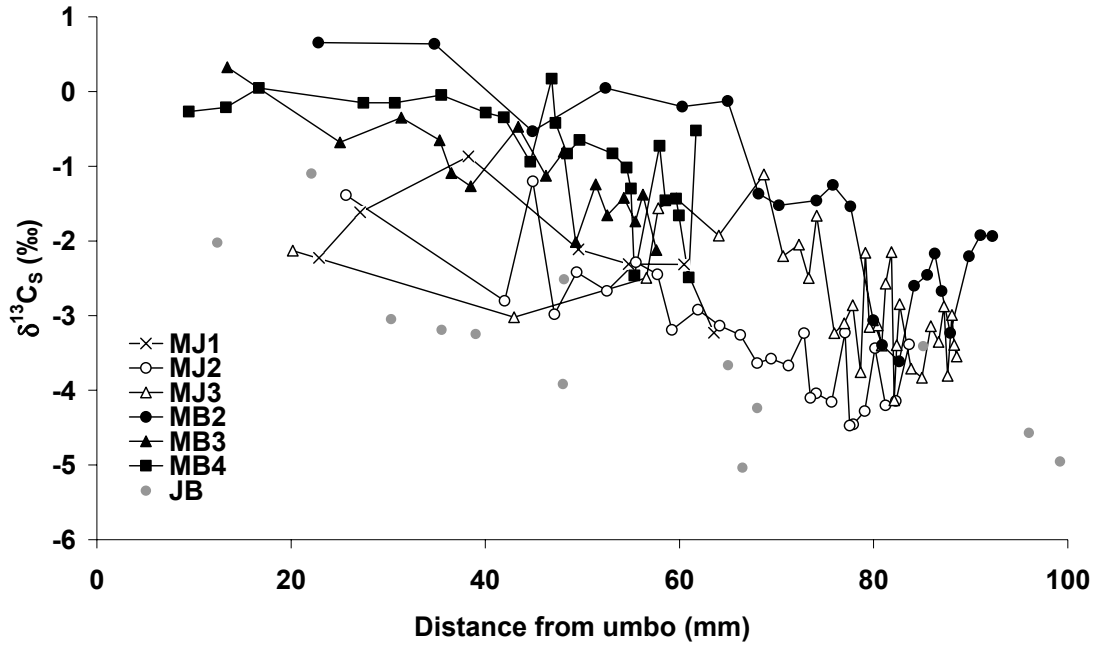

Figure 51. Annual shell $\delta^{13}C$ from *M. mercenaria* shells collected at two sites (Johnson Creek, MJ shells and Back Sound, MB shells) plotted versus shell length. Data from JB shells are also given, but it should be noted that these samples represent less than one year and thus are expected to have a higher variability than the other shells which integrate a full year of growth.

4.2.2.2 How much metabolic carbon is in the shells?

The best standing model to calculate the amount of metabolic C in the shell is given by McConnaughey *et al.* (1997):

$$M * (\delta^{13}C_R) + (1 - M) * \delta^{13}C_{DIC} = \delta^{13}C_s - \varepsilon_{ar\text{-}b} \quad (3)$$

where M is the percent metabolic CO_2 contribution, $\varepsilon_{ar\text{-}b}$ is the enrichment factor between aragonite and bicarbonate (2.7 ‰ in Romanek *et al.*, 1992), and $\delta^{13}C_R$ is

approximated from tissue $\delta^{13}C$ (Elliot *et al.* (2003) have shown that *M. mercenaria* precipitate aragonite shells). At the JB site, where corresponding tissue, water and shell data were available, eq. 3 gave results ranging from 15.8 to 37.8% M, with a linear relationship between shell length and M (Fig. 52). The $\delta^{13}C$ values from the muscle tissue was used for two reasons: 1) it is the same as the mantle tissue, which is closest to the EPF and should have the largest effect on the internal DIC pool, and 2) the muscle has the slowest turn over time, so integrates the longest time (see Lorrain *et al.*, 2002). For the other sites, tissue or water data to match the carbonate samples for each year are lacking, so the sample taken recently at JC was applied to the entire JC dataset. Data for BS was assumed. Water at the BS site exchanges with the open ocean (Peterson & and Fegley, 1986) so should have a $\delta^{13}C_{DIC}$ value close to oceanic values. Thus it was assumed that $\delta^{13}C_{DIC}$ = -0.5 ‰ and tissues = -19 ‰ (*i.e.*, the mean of the JB site) at the BS site. A maximum error of ~1 ‰ can be expected from these assumptions, which would change M by ~5% for a 1 ‰ change in $\delta^{13}C_{DIC}$ and ~1% for a 1 ‰ change in $\delta^{13}C_R$ (*i.e.*, $\delta^{13}C$ of tissues). Using eq. 1 and the assumptions listed above results in M values ranging from 7.4% to 31.4% for the BS and JC clams. Correcting for the changes in tissue $\delta^{13}C$ with shell length in JC clams (see results), only changes M by a maximum of 2.3%. The change in tissue $\delta^{13}C$ with shell length (slope = +0.05 ± 0.01) may be due to larger individuals including microphytobenthos in their diet, which have heavier $\delta^{13}C$ values (~ -15 ‰, Middelburg *et al.*, 2000; Herman *et al.*, 2000) compared to phytoplankton (~ - 20 ‰, see next Chapter). Nevertheless, the change in tissue $\delta^{13}C$ does not greatly contribute to M.

At all sites, the M ranges are substantially higher than the proposed 10% (McConnaughey *et al.*, 1997), even when considering possible errors. Furthermore, there is a linear relationship between M and shell length (Fig. 52), with no significant difference between the slopes or intercepts of the BS and JC sites ($p > 0.05$). The JB site has a similar slope to the other sites ($p = 0.81$), but the intercept is much higher (Fig. 52). This could be the result of different metabolic rates between the sites (cf. Lorrain *et al.*, 2004). Interestingly, the similarity in slopes suggests that the age effect between populations with apparently different metabolic rates is general, with a change in M of +0.19% per mm of shell length.

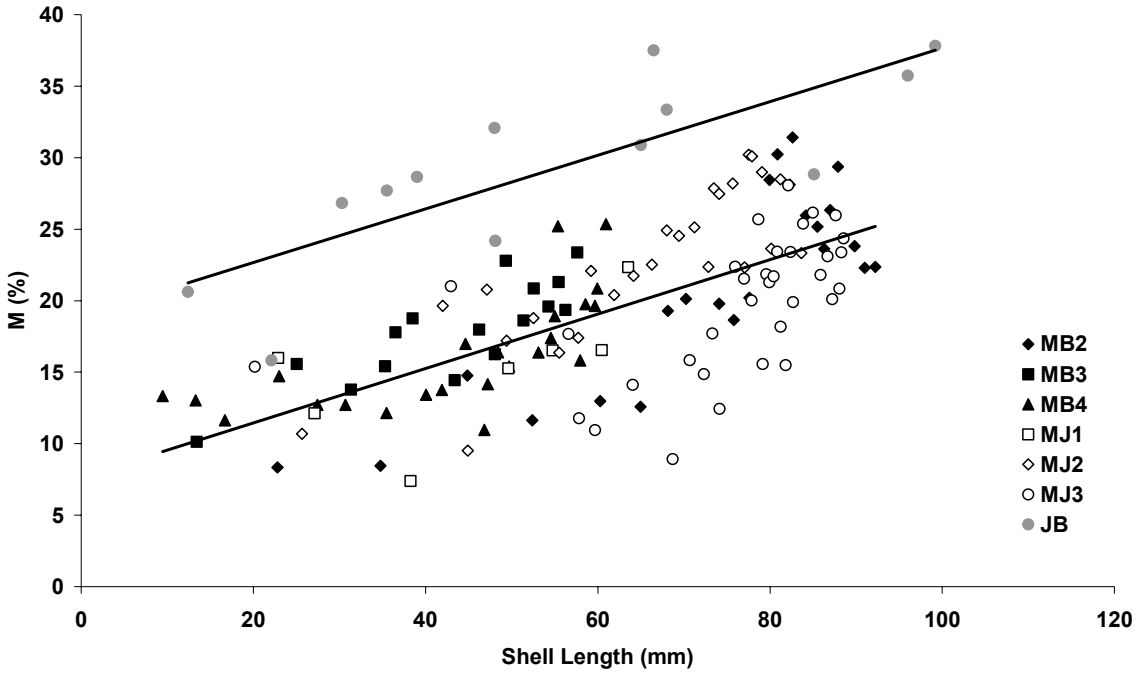

Figure 52. Percent metabolic C (M) from Jarrett Bay clams where tissue, water and shell was sampled for each shell and annual M incorporated into *M. mercenaria* shells collected at two sites (Johnson Creek, MJ shells and Back Sound, MB shells) plotted versus shell length (L in mm). The linear relationship is for the combined Johnson Creek and Back Sound datasets is M (%) = 0.190 (± 0.035) * L + 7.65 (± 2.25) ($p < 0.0001$, $n = 129$, $R^2 = 0.48$). The Jarrett Bay relationship is M (%) = 0.187 (± 0.092) * L + 18.92 (± 5.65) ($p < 0.001$, $n = 13$, $R^2 = 0.64$). The slopes between the two regressions are not statistically different ($p = 0.81$).

4.2.2.3 Can the effect of metabolic carbon be removed?

Being able to predict M would be of great value; with known M, $\delta^{13}C_S$, and tissue $\delta^{13}C$, $\delta^{13}C_{DIC}$ can be calculated using eq. 3. Although tissue $\delta^{13}C$ would not be available for fossil or specimens collected in the past, the shell organic matter $\delta^{13}C$ could be used as a proxy of tissue $\delta^{13}C$. O'Donnell *et al.* (2003) found that the $\delta^{13}C$ value of organic matter extracted from *M. mercenaria* shells was indistinguishable from tissue $\delta^{13}C$. However, the predictability of M from shell length is weak, with an R^2 of 0.48 for JC and BS clams and 0.64 for JB clams (Fig. 52). An attempt to improve the linear model by including several biometric parameters, in addition to total shell length (*i.e.*, a multiple linear regression with annual growth increment length, annual growth increment weight, and age), was made, but they did not improve the model by more than 4%. For example, combining age and length to predict M resulted in the highest R^2 (0.52). Additionally, the large difference in intercepts between the two regressions suggests that there is no general relationship between length and M. Thus, unfortunately, there is too much unexplained variability in the data and apparently large differences in metabolic rate between sites, making M predictions difficult and calculating $\delta^{13}C_{DIC}$ highly uncertain. However, as

suggested by Lorrain *et al.* (2004) $\delta^{13}C_S$ may provide information about metabolic rates for different populations. It would be interesting to understand why the JB clams had higher metabolic rates compared to the other two sites. One possibility is higher organic pollution at this site caused by land run-off, which has been shown to increase respiration rates in bivalves (Wang *et al.*, *in press*).

4.2.3 Trace elements in aragonitic bivalve shells

In the next two sections, aragonite and calcite shells are discussed differently because the two polymorphs of calcium carbonate have different physical properties. These properties result in different trace element partitioning between the two polymorphs.

4.2.3.1 Sr/Ca

Ratios of Sr/Ca in these shells are discussed in more detail in Gillikin *et al.* (2005), where a strong correlation between Sr/Ca and daily growth rate (R^2 = 0.73) was found. Nevertheless, it was hypothesized that growth rate was not the cause of Sr/Ca variations, but that Sr/Ca is controlled by another factor, which is synchronized with growth rate. Although the Sr/Ca profiles are similar between the two Puget Sound shells (Fig. 23A), and Sr/Ca ratios are successfully used as a paleo-temperature proxy in corals (Weber, 1973; Fallon *et al.*, 1999; Cardinal *et al.*, 2001) and sclerosponges (Rosenheim *et al.*, 2004), they could not be related to any environmental parameter in these bivalves (Gillikin *et al.*, 2005). Ratios of Sr/Ca in these shells (~1 – 3 mmol/mol; and most aragonitic bivalves measured to date) are far from Sr/Ca ratios recorded in inorganic aragonite, corals and sclerosponges (~ 8-10 mmol/mol; Weber, 1973; Kinsman and Holland, 1969; Swart *et al.*, 2002) indicating strong biological controls dominate Sr incorporation in marine aragonitic bivalves. Despite the strong biological controls on Sr/Ca ratios, they still can be used to obtain detailed (intra-annual) growth rates in *S. giganteus* with some degree of certainty as suggested by Richardson *et al.* (2004), but this needs to be validated for each species and site (see Gillikin *et al.*, 2005).

4.2.3.2 Mg/Ca

There have been some studies suggesting that Mg/Ca ratios in calcite bivalve shells may be SST proxies (Klein *et al.*, 1996a; Lazareth *et al.*, 2003), and others suggesting that Mg/Ca ratios do not record SST (Vander Putten *et al.*, 2000), or only sometimes do (Freitas *et al.*, 2005). Ratios of Mg/Ca in both corals and foraminifera have been reported to be strongly temperature dependent (Mitsuguchi *et al.*, 1996; Nürnberg *et al.*, 1996), but more recent reports suggest this is not straightforward and

may be problematic (Eggins *et al.*, 2004; Meibom *et al.*, 2004). Despite the large deviation from water Mg/Ca ratios, Mg/Ca ratios in aragonitic bivalve shells (Takesue and van Geen, 2004; this study) are typically within the same range found in corals and sclerosponges (Fallon *et al.*, 1999; Swart *et al.*, 2002).

The Mg/Ca profiles exhibit similarities between the two Puget Sound shells, but are clearly not related to SST (Fig. 22B, using $\delta^{18}O$ as a relative temperature scale). Temperature calculated from shell $\delta^{18}O$ values from Gillikin *et al.* (*in press*-a) for the Puget Sound shells was used to test the Mg/Ca – SST relationship, the resultant regressions slope was not significant (Shell B1: $p = 0.89$, B2: $p = 0.60$). Furthermore, variations in Mg/Ca ratios of the water in which they grew cannot be the cause of the variations observed in the shells; salinity remains above 10 at this site (Gillikin *et al.*, *in press*-a) and thus water Mg/Ca ratios are therefore constant (Klein et al, 1996a). Comparing the data presented here with other studies, all of which measured Mg/Ca ratios in aragonite bivalves that grew in salinities between 18 and 35 (i.e, ~ constant Mg/Ca ratio in the water), presents largely varying results. For example, Toland *et al.* (2000) found Mg/Ca ratios of ~ 0.1 to 0.6 mmol/mol in *Arctica islandica* shells, whereas Fuge *et al.* (1993) obtained much higher values (~ 0.4 to 1.2 mmol/mol) in the same species that grew in similar temperatures. The Mg/Ca ratios ranged from 0.6 to 2.4 mmol/mol in the Puget Sound shells and a similar range was found in an Alaskan shell, which grew in colder waters (data not shown, see Gillikin, 2005). Takesue and van Geen (2004), who analyzed *Protothaca staminea* shells from Humbolt Bay in northern California, USA, found a range of ~ 0.7 to 4.0 mmol/mol, despite the fact that their study site has comparable SST and salinities to the Puget Sound site. These results further substantiate that there is no general correlation between Mg/Ca ratios and temperature in aragonitic bivalve shells.

Another possibility is that Mg/Ca ratios are related to growth rate, as is the case for Sr/Ca ratios. Indeed a significant relationships between growth rate and Mg/Ca ratios in both Puget Sound shells (Shell B1: $p = 0.012$, B2: $p < 0.0001$) was found, however, unlike Sr/Ca ratios the slopes are significantly different between the two shells ($p < 0.01$; Shell B1: slope = 1.49 ± 1.16, n = 181, B2: slope = 7.22 ± 1.81, n = 118) and only explain a fraction of the variability (Shell B1: $R^2 = 0.03$; B2: $R^2 = 0.35$). Although this study could not determine the cause of the Mg/Ca variations in these shells, it does not seem that they are recording environmental information, but that biological controls dominate.

4.2.3.3 Ba/Ca

To date, all published records of high resolution Ba profiles in bivalve shells (both aragonite and calcite) have similar characteristics showing a relatively stable background Ba concentration interspaced with sharp episodic Ba peaks (Stecher *et al.*, 1996; Toland *et al.*, 2000; Vander Putten *et al.*, 2000; Lazareth *et al.*, 2003; Gillikin *et al.*, *in press*-c; section 4.2.4.2). Stecher *et al.* (1996) first proposed that these peaks were the result of the filter feeding bivalves ingesting Ba-rich particles associated with diatom blooms.

The two shells from Puget Sound show a remarkable co-variation, with the Ba/Ca peaks occurring almost exactly at the same time in both shells (Fig. 22C), which strongly suggests an environmental control. Furthermore, this provides an independent proof that the original fitting of the shells, using only $\delta^{18}O$ and the phase demodulation technique of De Ridder *et al.* (2004), is accurate (see Gillikin *et al.*, *in press*-a). To test if there is indeed a relationship between Ba peaks and phytoplankton blooms in *S. giganteus*, the fitting between the $\delta^{18}O$ profile and calendar dates as described in Gillikin *et al.* (*in press*-a) for the Puget Sound shells were used to match the Ba/Ca data with chlorophyll a (Chl a) data (data from Washington State Dept. of Ecology, http://www.ecy.wa.gov/). From Figure 53 is it evident that there is some coincidence between Chl a and Ba/Ca ratios, but it is not consistent. For example, the large Ba/Ca peak in 1994 actually precedes the Chl a peak. Furthermore, the Ba/Ca peak amplitude does not correspond to the Chl a peak amplitude. On the other hand, it is possible that the clams are selective for certain phytoplankton species that contain higher Ba concentrations, however, the only other pigment data available for this site (pheopigments) did not fit the Ba/Ca data better than Chl a (data not shown). These results suggest that there is not a direct relationship between the two. Additionally, no relationship between Ba/Ca in *Mytilus edulis* shells and Ba ingested as food could be found (Gillikin *et al.*, *in press*-c; section 4.2.4.2). Nevertheless, Vander Putten *et al.* (2000) also found a remarkable coincidence of the Ba peaks in several mussel shells that grew at the same location, providing further evidence that an environmental parameter controls their occurrence. Remarkably, a similar phenomenon also occurs in corals, with sharp episodic Ba peaks occurring at the same time each year, which are not related to river discharge (Sinclair, 2005). Thus, as with corals (Sinclair, 2005), there is no suitable hypothesis for these peaks.

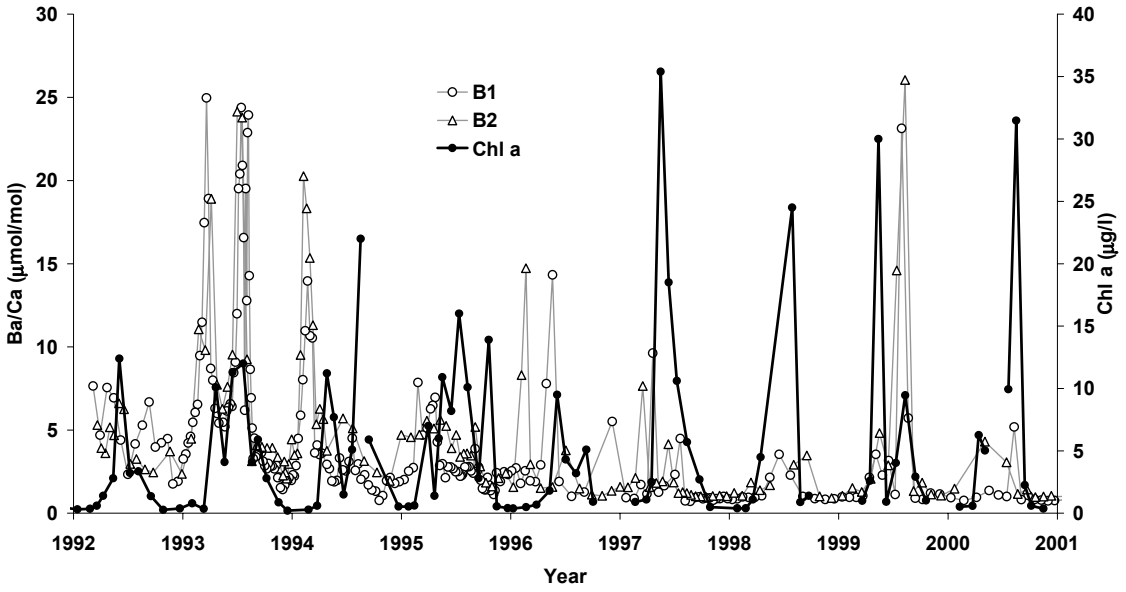

Figure 53. Ba/Ca profiles from the two Puget Sound (Washington, USA) shells and corresponding chlorophyll a data (data from Washington State Dept. of Ecology, http://www.ecy.wa.gov/). The fitting between the $\delta^{18}O$ profile and calander dates, as described in Gillikin *et al.* (*in press*-a), was used to match the Ba/Ca profiles with chlorophyll a data.

While most research has focused on the Ba-peaks, Gillikin *et al.*, (*in press*-c; section 4.2.4.2) found that the background Ba/Ca level in the shells of another bivalve species (*M. edulis*) could be used as an indicator of Ba/Ca ratios in seawater and hence provide an indication of salinity. Unlike Sr/Ca and Mg/Ca ratios, water Ba/Ca ratios may also alter shell Ba/Ca, as Ba/Ca ratios in the water can change dramatically with salinity (e.g., Gillikin *et al.*, *in press*-c; section 4.2.4.2; Fig. 34). Barium is the element most likely to faithfully record seawater Ba chemistry. Ratios of Ba/Ca between the two Puget Sound shells are remarkably similar (Fig. 22C). However, in the two *S. giganteus* shells analyzed here, the background Ba/Ca levels are higher near the umbo. Considering that the $\delta^{18}O$ data do not suggest a reduced salinity when the clams were younger (see Gillikin *et al.*, *in press*-a), this is probably an ontogenic effect. Unfortunately, this complicates the use of Ba/Ca backgrounds in this species, but does highlight the point that species specific differences in elemental incorporation are important. Nevertheless, despite the ontogenic effect, large temporary salinity changes may still be recorded in the shells. Therefore, this could potentially be a cause of the Ba/Ca peaks in the shells. However, if the relationship between Ba/Ca ratios in water and shells were linear, these peaks would require very large drops in salinity, which did not occur (Gillikin *et al.*, *in press*-a).

Finally, water temperature is another factor that can affect aragonite Ba/Ca ratios (Zacherl *et al.*, 2003; Dietzel *et al.*, 2004; Elsdon and Gillanders, 2004). However,

from comparison with $\delta^{18}O$ and Ba/Ca ratios in these shells it is clear that Ba/Ca ratios do not follow temperature.

4.2.3.4 Pb/Ca

Ratios of Pb/Ca in biogenic carbonates have been proposed as a proxy of anthropogenic Pb pollution (Shen & Boyle, 1987; Scott, 1990; Lazareth *et al.*, 2000; Yap *et al.*, 2003; this study, section 4.1.3). In particular, Pitts and Wallace (1994) found a strong linear relationship between dissolved Pb and Pb in shells of the aragonitic clam *Mya arenaria*. Additionally, Pb is preferentially incorporated into aragonite, with a $D_{Pb} > 1$. Considering the large variability between the Puget Sound shells (Fig. 22D), it seems unlikely that the Pb/Ca ratios in these shells are recording only environmental Pb concentrations. Physiology probably plays a role on Pb incorporation, as was suggested by Vander Putten *et al.* (2000) for *Mytilus edulis*. In this study, shell B2 is almost consistently exhibiting higher ratios than shell B1, especially between 45 to 60 mm from the umbo (Fig. 22D). Moreover, there is no statistical difference between the means of an Alaskan shell and shell B1, but both are different from B2 (at $p < 0.05$). The Pb/Ca levels in these shells are similar between the two sites, while Puget Sound is expected to have higher environmental Pb concentrations (Paulson and Feely, 1985; USEPA, 1997) [data not shown].

Upon a closer inspection of the data (see Fig. 54) there is a clear pattern in the Pb/Ca signal in shell B1 (Puget Sound), with Pb/Ca peaks occurring every winter. This could be caused by the animal sequestering Pb in its shell to detoxify tissues coupled with reduced winter shell growth, resulting in higher Pb/Ca ratios in the winter. Indeed, many studies have found higher Pb concentrations in bivalve soft tissues during winter (Boalch *et al.*, 1981; Swaileh, 1996). An alternative hypothesis is that there may be higher resuspension of contaminated sediments in the winter or increased Pb inputs during winter, as many studies have found higher water Pb concentrations in winter (e.g., Baeyens, 1998; Boyle *et al.*, 2005). Nevertheless, this pattern is not found in shell B2, so no conclusions from these data can be drawn. Despite the fact that small temporal and spatial differences in environmental Pb concentrations can probably not be extracted from *S. giganteus* shells, it is not impossible that large scale changes in environmental Pb would be reflected in the shells. The concentrations in these *S. giganteus* shells are generally low, Lazareth *et al.* (2000) measured ratios as high as 1.2 µmol/mol in a sclerosponge. Therefore, shells that experienced a larger environmental Pb concentration may still be useful recorders of anthropogenic Pb pollution (Pitts and Wallace, 1994; Richardson *et al.*, 2001; Gillikin *et al.*, *in press*-b).

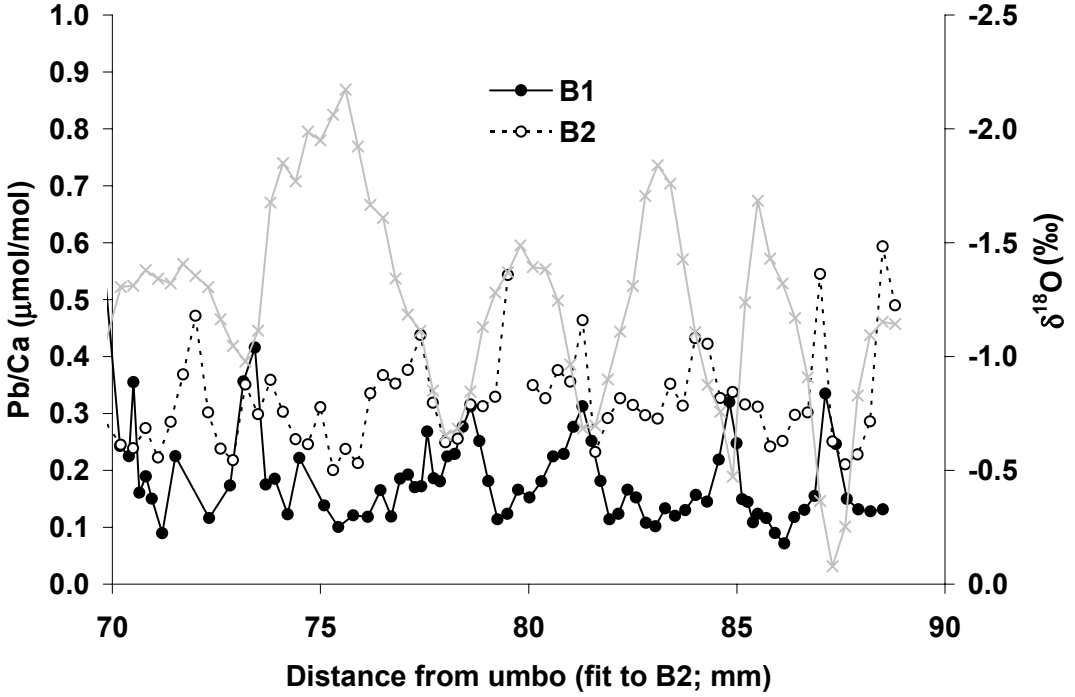

Figure 54. Pb/Ca data from the slow growing region of the Puget Sound (Washington, USA) shells. Data are the same as Figure 2D, but allow a detailed look at the variations in the profile.

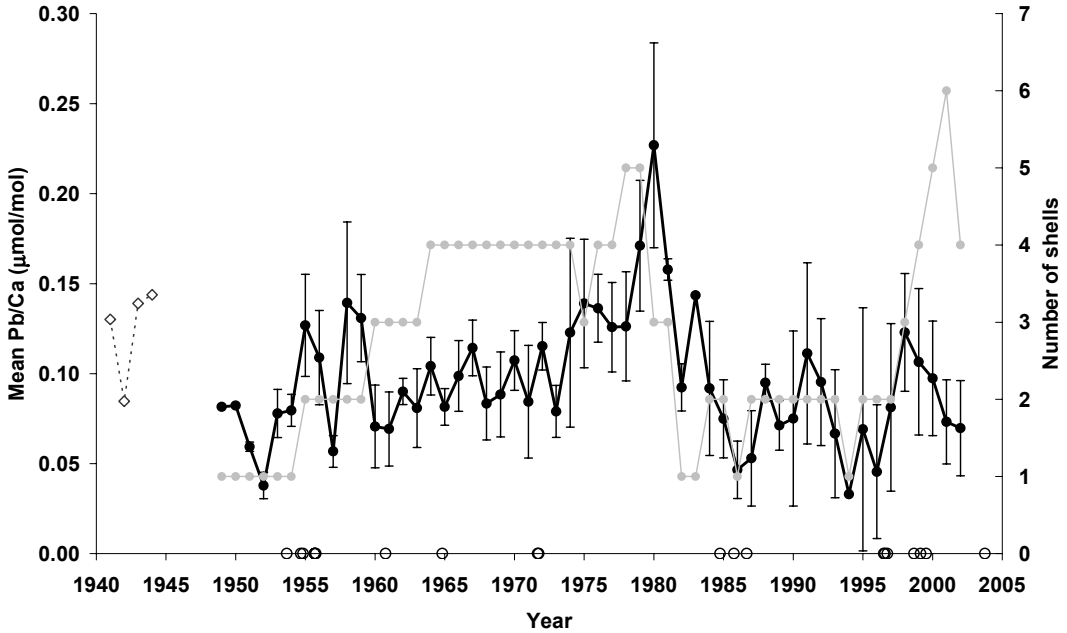

Figure 55. Mean Pb/Ca ratios (black line and circles, data from Fig 26). Error bars represent standard error. The grey line and circles show the number of *M. mercenaria* shells each mean is based on. The open symbols on the x-axis represent hurricane years (data from NCSCO, 2004).

Indeed, despite the large scatter in the Pb/Ca ratios collected from the *M. mercenaria* shells (Fig. 26), when averaged, they clearly show the anthropogenic Pb profile common in other biogenic carbonates (Fig. 55). This indicates that when enough specimens are pooled together, bivalve shells can be used for long term Pb records. The data from this study compare well with other studies of aragonite clams from unpolluted sites. From this it is concluded that the Cape Lookout region of North Carolina has not received extensive pollution over the 1949-2002 period. The 1949-1976 period was not significantly different from the 1982-2002 period, although other proxies suggest that it should be considerably higher. Therefore, the data presented here suggest that there is still a modern source of Pb in the coastal North Carolina environment (see Gillikin *et al.*, *in press*-b for more information).

4.2.4 Trace elements in calcitic bivalve shells

4.2.4.1 Sr/Ca and Mg/Ca

Substantial interindividual differences were found in both the Sr/Ca and Mg/Ca range and variations (Fig. 27). This suggests a minor involvement of environmental factors on Sr and Mg incorporation, since these scallops, sampled at the same location, have all experienced the same environmental conditions. It seems improbable that Sr/Ca and Mg/Ca ratios of seawater can explain seasonal variations of shell Sr/Ca and Mg/Ca ratios, as salinity shows little variations over the entire growth season (between 33.5 and 35.5, Fig. 28). In addition to the inter-individual differences, all Sr/Ca profiles show an increase during the year and one sharp decrease at the beginning of May (Fig. 27), while temperature and salinity steadily increase between March and September, with no drop in May (Fig. 28). From this, it is clear that the Sr/Ca variability cannot be explained only by temperature or salinity but is mostly controlled by individual biological processes.

Figure 29 clearly shows that Sr/Ca variations are generally well correlated with daily growth. In particular, the decrease of Sr/Ca ratios in the beginning of May is precisely correlated with the reduction in growth during this period in all shells. This growth reduction is a common phenomenon in the Bay of Brest and is related to phytoplanktonic blooms that massively sediment on the bottom (Lorrain *et al.*, 2000). Table 1A lists correlation coefficients (R^2) for the four parameters (growth rates, temperature, salinity, and shell Mg/Ca ratios) and reveals that Sr/Ca ratio variations are indeed better explained by daily growth rates (G) than by the other parameters, with:

$$Sr/Ca\ (mmol/mol) = 1.364\ (\pm 0.057) + 0.002\ (\pm 0.0003) * G\ (\mu m/d). \quad (4)$$

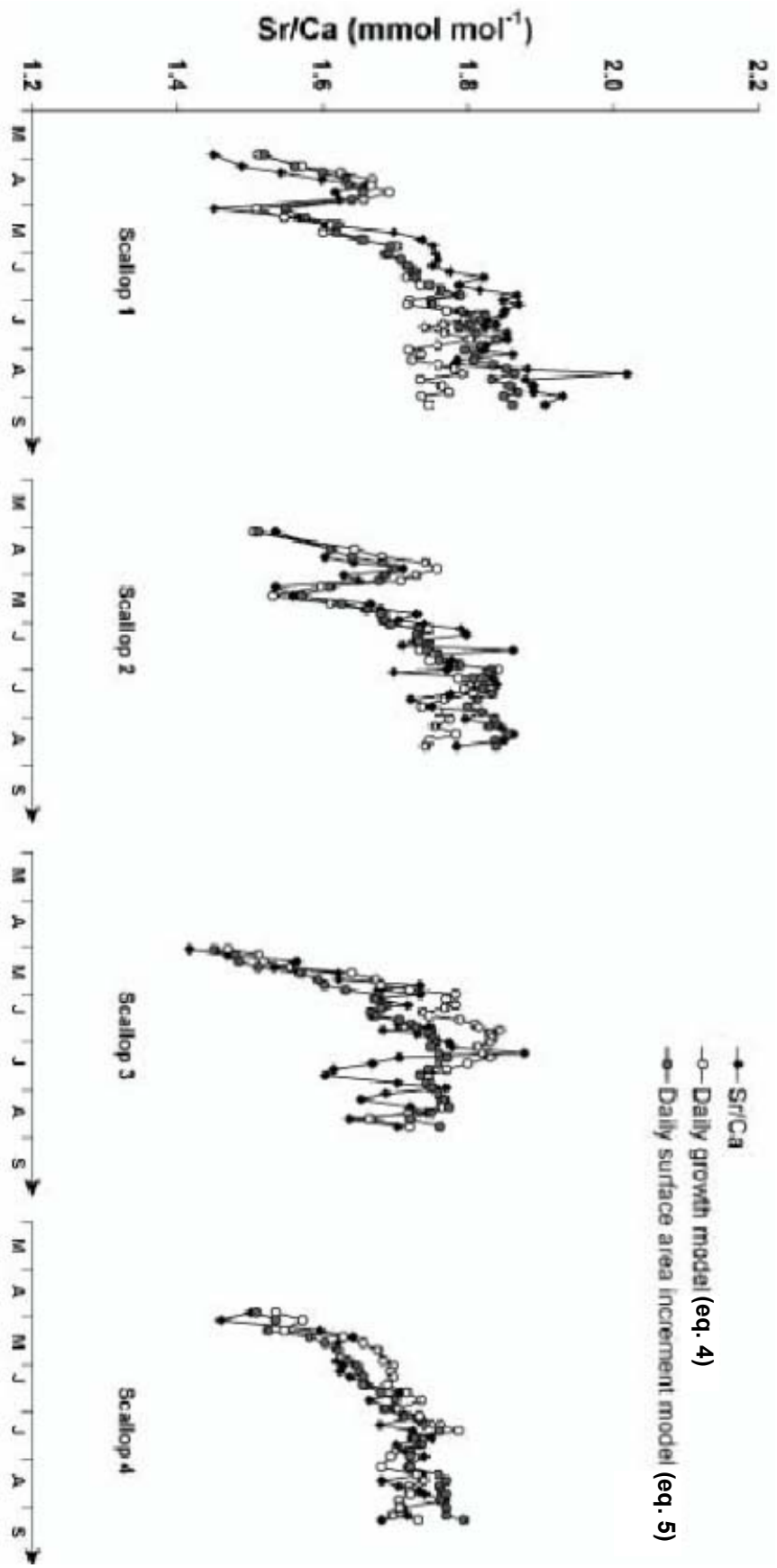

Figure 56. (on previous page) Modelled shell Sr/Ca ratios calculated from daily growth (eq. 4, white symbols) and daily surface area increment (eq. 5, grey symbols) for the four scallops in 2003. Measured shell Sr/Ca ratios (mmol/mol) are shown as black symbols.

When applied to all shells, the model (eq. 4) using only daily growth fits relatively well to the measured Sr/Ca ratios, but some discrepancies remain (Fig. 56). Specifically, predicted values during the summer are lower than expected for scallop 1, whereas they are higher for scallop 3 during the same period. In this sense, the model is not generic; a part of the inter-individual variability is not resolved. However, the four individuals have different shell heights, meaning that the total quantity of carbonate precipitated along the growing edge on a given day is different between individuals. Therefore, Sr/Ca ratios are probably more controlled by total $CaCO_3$ precipitated rather than by linear daily shell growth extension. This quantity can be expressed either by the weight or by the surface of material produced each day. The weight of $CaCO_3$ produced each day can be calculated using an equation relating shell weight (W in g) and shell height (H in cm) modified from Lorrain *et al.* (2004) for the same scallop population: W = 0.195 * H2.726 (R^2 = 0.92, N = 2419, p <0.0001). This daily weight increment explains 69.5% of the Sr/Ca variations (Table 11A). Daily shell surface area increment (DSAI) was then estimated using surface area (S in cm^2) and H in cm (S = 0.802 * H2.045 (R^2 = 0.99, N = 1707, p <0.0001)), which itself explains 74% of the Sr/Ca variations (Table 11A). Therefore both estimates of the total quantity of $CaCO_3$ precipitated provide strong correlations with Sr/Ca ratios. We consider the DSAI as the best explicative variable for Sr/Ca variations, allowing us to establish the predictive model:

Sr/Ca (mmol/mol) = 1.464 (±0.027) + 1.552 (±0.155) * DSAI (cm^2). (5)

This new model reduces the aforementioned gaps between observed and predicted Sr/Ca ratios (Fig. 56). The addition of temperature or salinity does not improve the model, whereas shell Mg/Ca improves it by only 3.5% (Table 11B). Shell Mg/Ca might explain 3.5% of Sr/Ca variability by the mechanism proposed by Mucci and Morse (1983), where incorporation of Mg^{2+} causes a distortion of the crystal lattice, leading to the preferential incorporation of Sr^{2+}, a cation larger than Ca^{2+}. However, this would cause a positive linear correlation between Mg and Sr contents, which although significant, is very weak in *P. maximus* (Table 11A). Therefore, Mg/Ca cannot be considered as an important factor for Sr incorporation in these shells. Further addition of temperature and salinity as a third variable is not significant (Table 11C). This result confirms that kinetic effects predominantly control Sr partitioning in the shell of *P. maximus*.

Table 11. Statistical results (N = 144) of the linear regressions between shell Sr/Ca ratios and possible dependent variables. (A) Simple regression between Sr/Ca and different dependent variables. (B) Multiple regression using DSAI (daily surface area increment) as the first dependent variable. (C) Multiple regression using DSAI and Mg/Ca as the two first dependent variables. R^2 refers to the correlation coefficient.

	Variables	R^2	Overall significance
A	DSAI	0.74	P <0.01
	Daily Weight Increment	0.7	P <0.01
	Daily Growth Rate	0.52	P <0.01
	Temperature	0.49	P <0.01
	Salinity	0.49	P <0.01
	Mg/Ca	0.28	P <0.01

	1st variable	2nd variable			Significance of 2nd variable
B	DSAI	Temperature	0.74	P <0.01	P = 0.8170
		Salinity	0.74	P <0.01	P = 0.3644
		Mg/Ca	0.78	P <0.01	P<0.001

	1st variable	2nd variable	3rd variable			Significance of 3rd variable
C	DSAI	Mg/Ca	Temperature	0.78	P <0.01	P = 0.3113
			Salinity	0.77	P <0.01	P = 0.7723

Ratios of Sr/Ca in abiogenic calcite are controlled by precipitation rate, which is a function of seed crystal surface area (Lorens, 1981) and is therefore difficult to estimate in our bivalves without biomineralization experiments. We do not have a measure of these precipitation rates, but our results suggest that daily surface area increments, as a first approximation, seem to be a good reflection of precipitation rates in *P. maximus*. However the model (eq. 5) still leaves 26% of the variance unexplained, suggesting that a better estimation of precipitation rates could be reached. For example, Sr incorporation could depend on the calcification space, *i.e.*, the volume of extrapallial fluid available for calcification. In bivalves, calcification takes place in the extrapallial space (Wheeler, 1992), and we can suppose that the more volume available relative to daily shell production, the more discrimination is possible at biological membranes. Studies on extrapallial fluids would be necessary to go further in this hypothesis. Unexplained remaining variance and interindividual variability in Sr uptake could also come from variations in the microtopographic properties of the calcite crystals, possibly due to changes in the microdistribution, abundance, or composition of the organic matrix (Vander Putten *et al.*, 2000). Indeed, Paquette and Reeder (1995) showed that Sr had largely different distribution coefficients for different faces in calcite crystals. The overall crystal morphology in these species might differ along the growth axis or between individuals and could explain some of our results.

This study illustrates the importance of having well-constrained growth rates (or calcification rates) when attempting to calibrate proxies in biogenic carbonates. For example, the temperature effect found by Dodd (1965) could be easily explained by the correlation between temperature and growth rates. We also found a significant correlation between Sr/Ca and temperature (Table 11A) but were only able to deconvolve temperature and growth-rate effects because of the growth dip (Fig. 29). The metabolic pumping hypothesis can be also excluded (Klein *et al.*, 1996b), as high metabolic pumping should result in a decrease of Sr/Ca ratios with an increase in growth rate (see Gillikin *et al.*, 2005), whereas growth and Sr/Ca are positively related in our study (Fig. 29). Finally, salinity does not have an effect on Sr/Ca ratios at the range of 33.5–35.5 (Fig. 28), typical of many shelf areas, but we cannot exclude the effects of large salinity changes such as would be encountered in estuaries.

Mechanisms involved in the kinetic effects may be purely mineralogical, *i.e.*, higher growth rates imply less discrimination against Sr, resulting in a partition coefficient (D_{Sr} = $Sr/Ca_{calcite}$ / $Sr/Ca_{solution}$) that becomes closer to equilibrium (*i.e.*, D_{Sr} = 1). The average shell Sr/Ca ratio was 1.7 ± 0.1 mmol/mol (n = 144, Fig. 1), while seawater Sr/Ca had an average value of 8.6 ± 0.4 mmol/mol (n = 7). Therefore the mean D_{Sr} is 0.20 ± 0.01, which is in agreement with other biogenic and abiogenic calcites (Lorens & Bender, 1980; Carpenter & Lohmann, 1992). It is also interesting that *P. maximus* D_{Sr} values are similar to that of other calcitic organisms such as coccoliths (Stoll *et al.*, 2002) and foraminifera (Lea *et al.*, 1999), which have very different biomineralization mechanisms. This could suggest that shell Sr/Ca ratios are independent of these biomineralization mechanisms. However, this is not the case for all trace elements, as Mg/Ca ratios are well correlated with temperature in coccoliths and foraminifera (Lea *et al.*, 1999; Stoll *et al.*, 2001), while we do not find any correlation in *P. maximus* (R^2 = 0.03).

4.2.4.2 Ba/Ca

Biomineralization in bivalves takes place in the extrapallial fluid (EPF), a thin film of liquid between the calcifying shell surface and the mantle epithelium (Wheeler, 1992). The central EPF is where the inner aragonite shell layer is precipitated, whereas the outer calcite shell layer is precipitated from the marginal EPF (*i.e.*, the layer analyzed in this study). The EPF is isolated from seawater and therefore may have different elemental concentrations than seawater. Although there are numerous reports on central EPF elemental concentrations (e.g., Crenshaw, 1972; Wada & Fujinuki, 1976), direct measurements of the marginal EPF are difficult and we know of only one report providing marginal EPF elemental concentrations, but unfortunately Ba

was not measured (Lorens, 1978). However, there does not seem to be a difference in Ba concentrations between hemolymph and central EPF in other bivalve species (A. Lorrain, unpublished data).

Elements move into the EPF through the epithelial mantle cells which are supplied from the hemolymph (Wilbur & Saleuddin, 1983). Ions enter the hemolymph of marine molluscs primarily through the gills, although they may also enter via the gut (see Wilbur & Saleuddin, 1983 and references therein). The relative contributions of Ba to the shell from food versus environment are unknown; however, mollusk guts are known to contain high Ba concentrations (Lobel *et al.*, 1991; A. Lorrain, unpublished data). Therefore, it is possible that the gut is a source of Ba in mollusk shells. However, if food Ba impacted background $[Ba/Ca]_{shell}$, the regression between background $[Ba/Ca]_{shell}$ and $[Ba/Ca]_{water}$ would not go through zero (meaning zero $[Ba/Ca]_{water}$ = zero $[Ba/Ca]_{shell}$). In the field specimens, the regression does go through zero (Fig. 36). This, together with the good correlation with $[Ba/Ca]_{water}$, makes it very unlikely that food is a major source of Ba to the shell during those times when background $[Ba/Ca]_{shell}$ is observed. Nevertheless ingested particulate Ba may be involved in the formation of the $[Ba/Ca]_{shell}$ peaks.

Both the laboratory and field experiments verify that there is a direct relationship between background $[Ba/Ca]_{shell}$ and $[Ba/Ca]_{water}$ in *M. edulis* calcite. A possible reason for the difference in slopes between the laboratory and field experiment $[Ba/Ca]_{shell}$ vs. $[Ba/Ca]_{water}$ (Fig. 36) could be that the stress of handling and the suddenly increased Ba concentration in the laboratory experiments caused a saturation of the ionoregulatory ability of the animal. Lorens & Bender (1980) found that elemental ratios in shells increased in laboratory held *M. edulis* for a short while, then decreased (they termed this section of the shell “transition zone calcite” (or TZC)). They proposed that this was caused by the stress of capture and the adjustment to a new environment. Although we acclimated these animals to laboratory conditions for three weeks, the change to the experimental conditions may have caused stress and we may have included TZC in our analyses. This could explain the higher D_{Ba} in the laboratory cultured mussels. Furthermore, the fact that the regression does not go through the origin supports this. As in the field population, it can be expected that when there is zero Ba in the water, there should be zero Ba in the shell. Interestingly, as the hemolymph can be expected to represent the crystallization fluid better than seawater, when a regression between hemolymph and shell is performed (laboratory experiment), the regression does go through the origin (intercept not significant, $p = 0.07$). The D_{Ba} calculated using hemolymph, 0.134 (± 0.006) ($R^2 = 0.95$, $n = 25$, $p < 0.0001$), is also more similar to that for planktonic foraminifera (see further).

Alternatively, the field D_{Ba} may also not be accurate, we averaged the $[Ba/Ca]_{water}$ from the whole year, while it is clear that the background $[Ba/Ca]_{shell}$ is formed from approximately mid-summer to the end of the growing season. Selecting only the $[Ba/Ca]_{water}$ from July to November changes the regression slightly, but significantly to background $[Ba/Ca]_{shell}$ = 0.091 (± 0.006) * $[Ba/Ca]_{water}$ – 0.52 (± 0.17) (R^2 = 0.76, $p < 0.0001$), and when only selecting September to November it changes to background $[Ba/Ca]_{shell}$ = 0.081 (± 0.006) * $[Ba/Ca]_{water}$ – 0.26 (± 0.15) (R^2 = 0.76, $p < 0.0001$). Therefore, considering both the laboratory and field data, we propose that the D_{Ba} for *M. edulis* lies within the range of 0.07 to 0.12. Furthermore, the algorithm used to select the background $[Ba/Ca]_{shell}$ data used here may be excluding some $[Ba/Ca]_{water}$ data stored in the shell. It is possible that all $[Ba/Ca]_{shell}$ data between large $[Ba/Ca]_{shell}$ peaks are recording $[Ba/Ca]_{water}$. If this was the case, seasonal $[Ba/Ca]_{water}$ could be reconstructed; however, this could only be determined from more detailed experiments. Nevertheless, these data do illustrate that average $[Ba/Ca]_{water}$ can be estimated from *M. edulis* shells using the proposed algorithm to select the background $[Ba/Ca]_{shell}$ data.

It should be noted that incorporation of elements in calcite with ionic radii larger than calcium (such as Ba) are expected to be strongly affected by external factors, such as temperature or salinity (Pingitore & Eastman, 1984; Morse & Bender, 1990). We are unable to determine if salinity has an effect or not. The strong relationship in the field between $[Ba/Ca]_{water}$ and salinity makes it difficult to deconvolve the effects, whereas in the laboratory salinity was similar in all treatments. Therefore, this could be another reason for the difference in intercepts between the two experiments. Considering the seasonal 20 ºC temperature range at these sites (from ~0 to 20 ºC), and the stable background [Ba/Ca] ratios observed in these shells, it does not seem likely that there is a major temperature effect on background D_{Ba} in *M. edulis*. This is most probably true for all bivalves as well, as the stable Ba background in all published data is evident and temperature almost always has a seasonal cyclicity. Similarly, Lea & Spero (1994) did not find an influence of temperature on D_{Ba} in foraminifera, and no temperature effect has been reported for inorganic calcite. However, definitive experiments should be carried out to confirm that temperature does not affect bivalve background [Ba/Ca] ratios.

Abiogenic experiments on the D_{Ba} in calcite have provided a range of values, which is probably due to unconstrained precipitation rates in many of the experiments (Tesoriero & Pankow, 1996). For the range of *M. edulis* shell precipitation rates estimated by Lorens (1981), D_{Ba} is expected to range between 0.03 and 0.05 according to the abiogenic calcite experiments of Tesoriero & Pankow (1996). Pingitore & Eastman (1984) provided an inorganic D_{Ba} of 0.06 ± 0.01, which is very

similar to the low end of the range we estimate for *M. edulis* D_{Ba} (*i.e.*, 0.07). Planktonic foraminifera, on the other hand can have higher D_{Ba} than *M. edulis*, ranging from 0.09 to 0.19 (Lea & Boyle, 1991; Lea & Spero, 1992; 1994), whereas benthic foraminifera have an even higher D_{Ba} in both laboratory (0.2 – 0.5; Havach *et al.*, 2001) and field based studies (0.37; Lea & Boyle, 1989). It can generally be considered that when the partition coefficient of a particular element (D_{Me}) is far from inorganically determined D_{Me}, then other factors most likely influence D_{Me}, such as the physiology of the organism or other biological factors. For example, Sr/Ca in corals has been shown to be a good SST proxy and the D_{Sr} is close to one (Weber, 1973), which is similar to abiogenic aragonite (Kinsman and Holland, 1969), whereas in aragonitic bivalve shells the D_{Sr} is around 0.25 and there is no link with SST (Gillikin *et al.*, 2005). The fact that foraminiferal Ba/Ca has successfully been used as a proxy of dissolved Ba/Ca, and that the foraminiferal D_{Ba} is farther from expected values than *M. edulis*, further implies that Ba/Ca in *M. edulis* has great potential as a robust proxy of dissolved seawater Ba/Ca, as there should be an even smaller biological effect in *M. edulis* calcite.

To test this proxy further, we use the shell GR210403 data for the period preceding transplantation. These data should be representative of Oosterschelde conditions with salinity above 30. The background $[Ba/Ca]_{shell}$ before transplantation is 0.98 ± 0.05 (n = 13), which corresponds to a $[Ba/Ca]_{water}$ of 13.8 ± 0.7 when using a D_{Ba} of 0.07 and 8.2 ± 0.4 when using a D_{Ba} of 0.12. A range of $[Ba/Ca]_{water}$ of 8 to 14 is reasonable for a salinity of about 30 (Fig. 34) and provides additional evidence that even at low $[Ba/Ca]_{water}$, this is a good proxy.

Our results confirm the general Ba profiles recorded in other bivalves (e.g., Stecher *et al.*, 1996; Toland *et al.*, 2000; Vander Putten *et al.*, 2000; Torres *et al.*, 2001; Lorrain, 2002; Lazareth *et al.*, 2003; Gillikin, 2005), with a stable background signal interrupted by sharp episodic peaks, generally occurring in the spring (using $\delta^{18}O$ as a relative temperature scale). The unstable background Ba in OS shells probably reflects the highly variable salinity at this site. Another striking feature of the profiles is that the peak amplitude seems to be correlated to the mussels' age, with younger shell sections having larger peaks. For example, shell KN200203 has a large Ba/Ca peak ~ 20 µmol/mol at 15 – 22 mm of growth, while in the same shell at 38 – 40 mm the peak only reaches ~ 5 µmol/mol (Fig. 35). This is reproduced in the other shells as well, with a large peak around 24 mm in shell GR210403 and small peaks around 35 – 40 mm in shells KN9 290902 and HF091202 (Fig. 35). This trend was also found by Vander Putten *et al.* (2000), who collected their *M. edulis* shells from the same estuary in 1997, suggesting that peak amplitude is not environmentally controlled. However, this could be an averaging effect, with the sample size

integrating more growth time as shell growth slows with age (see Goodwin *et al.*, 2001). Considering the width of the peaks, this does not seem probable and is more likely a physiological effect of ageing (see further).

There are several hypotheses which could explain the $[Ba/Ca]_{shell}$ peaks. The hypothesis of Stecher *et al.* (1996), that either Ba-rich phytoplankton or barite formed in decaying phytoplankton flocs are ingested by the filter feeding bivalve and eventually the Ba is sequestered in the shell, is plausible. However, our data do not support a direct incorporation of Ba from phytoplankton ingestion into the shell. Although we could not measure Ba in the shell in the feeding experiment, it can be assumed that ingested Ba would have to pass through the hemolymph to get to the EPF and be taken up in the shell. We fed mussels food with different Ba concentrations, which was taken up in the bulk tissues (Fig. 31 inset), but hemolymph Ba concentrations did not increase (Fig. 32 inset). However, it is possible that Ba concentrations in the food offered in this study were not high enough to have an effect (maximum ~ 15 nmol/g). Although many marine phytoplankton species contain barium concentrations similar to that of the food used in this study, certain species can have barium concentrations as high as 420 nmol/g (dry weight; Dehairs *et al.*, 1980) (see Fisher *et al.* (1991) for review). Therefore, as previously suggested by Stecher *et al.* (1996), the $[Ba/Ca]_{shell}$ peaks can still be related to phytoplanktonic events in some way; for example, barite ingestion (see further) or uptake of specific phytoplankton species containing high levels of barium. However, the lack of a $[Ba/Ca]_{shell}$ peak in the shell OS 091202 (Fig. 35) and the large Chl a peak at this site (Fig. 33C) suggest that phytoplankton blooms are not the direct cause. Nevertheless, this does not exclude barite ingestion as a cause. Indeed, invertebrates are known to directly ingest barite crystals (Brannon & Rao, 1979). It is possible that barite formation only occurs downstream from the OS site (see Stecher & Kogut, 1999), explaining the lack of a $[Ba/Ca]_{shell}$ peak at this site. This would also explain the large sharp $[Ba/Ca]_{shell}$ peak in the KN shells (Fig. 35), despite the lower broad Chl a peak at this site (Fig. 33C). However, particulate Ba data from the Schelde, which show a peak in the spring only at mid-salinities (Zwolsman & van Eck, 1999), do not agree with this scenario; but a more detailed sampling campaign is needed to be conclusive. Clearly, more work is needed to understand the relationship between these $[Ba/Ca]_{shell}$ peaks and phytoplankton. Therefore, further experiments for longer time periods using a larger range of [Ba] in food and possibly even barite would be useful.

An increase in $[Ba/Ca]_{water}$ is highly unlikely to be the cause of $[Ba/Ca]_{shell}$ peaks, as the 20 – 25 µmol/mol $[Ba/Ca]_{shell}$ peaks would require $[Ba/Ca]_{water}$ to be around 300 µmol/mol, which is clearly not the case (Fig 33A). An alternative hypothesis may be

that Ba is remobilized from tissue stores during spawning, which also occurs in the spring. Indeed, *M. edulis* tissue dry weight also exhibits sharp episodic peaks throughout the life of the animal (Kautsky, 1982). The lack of a $[Ba/Ca]_{shell}$ peak in the OS shell could possibly be due to this mussel not spawning. Osmotic stress may have required a large part of this animals' energy budget, leaving no energy for spawning (cf. Qiu *et al.*, 2002; Gillikin *et al.*, 2004). It is also interesting to note that the $\delta^{13}C$ profiles coincide with changes in $[Ba/Ca]_{shell}$. This is most evident in shells KN9 290902 and HF092102, where the $\delta^{13}C$ values are more negative when the $[Ba/Ca]_{shell}$ deviates from background concentrations and are more positive when the $[Ba/Ca]_{shell}$ is at background levels (Fig. 35). Bivalve shell $\delta^{13}C$ values are known to be influenced by the incorporation of metabolically derived light carbon (*i.e.*, ^{12}C) (McConnaughey *et al.*, 1997). Furthermore, it has been shown that increased metabolism in larger bivalves, relative to growth rate, leads to a larger availability of metabolic C for $CaCO_3$ precipitation and therefore results in a more negative $\delta^{13}C$ in the shell (Lorrain *et al.*, 2004). Using this rationale, higher metabolic rates from either spawning or seasonally increased growth, caused by an increase in food supply, would also result in a more negative shell $\delta^{13}C$. This could explain the pattern we see in these shells, and also agrees with a metabolic control on $[Ba/Ca]_{shell}$ peak amplitude as described above. However, data from the scallop, *Pecten maximus*, do not corroborate this hypothesis, with their $[Ba/Ca]_{shell}$ peaks not being correlated with spawning (Lorrain, 2002). Alternatively, the higher $[Ba/Ca]_{shell}$ could be a kinetic growth rate effect, which has been noted in inorganic calcite (Tesoriero & Pankow, 1996). Higher growth rates would also increase metabolic rates and thus lower shell $\delta^{13}C$. Finally, it can be argued that the $[Ba/Ca]_{shell}$ peaks can be caused by higher organic matter content in the shell. Bivalve shells can contain up to 5% organic matter (see Marin & Luquet, 2004, and references therein) and Ba is known to be associated with organic matter (Lea & Boyle, 1993). However, neither Hart *et al.* (1997) nor Sinclair (2005) found a relationship between organic matter and Ba concentrations in other biogenic carbonates (*i.e.*, corals), and Rosenthal & Katz (1989) suggest that Ba is bound to the crystal in molluscs. Thus it is unlikely that the Ba peaks are associated with shell regions containing higher organic content.

Remarkably, a similar phenomenon also occurs in corals, with sharp episodic Ba peaks occurring at the same time each year, which are not related to river discharge (Sinclair, 2005). However, unlike bivalves, Sinclair (2005) found that the timing of the peaks differed between coral colonies, even when they grew within 20 km of each other. The main conclusion of Sinclair (2005) regarding the cause of these peaks in corals was that there is currently no satisfactory hypothesis to explain them. This is also the case for bivalves. However, the similarities between coral and bivalve Ba/Ca peaks may suggest a common cause for these peaks. This in itself would be amazing

considering the large difference in biology, ecology, and biomineralization mechanisms between these two phyla of invertebrates.

Our data suggest that *M. edulis* shells have potential as a proxy of dissolved $[Ba/Ca]_{water}$. However, it should be clear that only high resolution profiles covering an adequate amount of growth may be used to assure the correct background $[Ba/Ca]_{shell}$ is selected. This selection can also be aided using the $\delta^{18}O$ and $\delta^{13}C$ profiles. Selecting the mid-summer growth region (or the most negative $\delta^{18}O$) along with the most positive $\delta^{13}C$ should result in a good selection of background $[Ba/Ca]_{shell}$. Obviously whole shell analyses are not suitable to determine $[Ba/Ca]_{water}$, because peaks would be integrated. Once the correct background $[Ba/Ca]_{shell}$ is obtained, the $[Ba/Ca]_{water}$ may be approximated using a D_{Ba} of about 0.1. These data can be useful for giving a relative indication of salinity (different estuaries can be expected to have different salinity - $[Ba/Ca]_{water}$ relationships (Coffey *et al.*, 1997)), which could assist with $\delta^{18}O$ interpretations (see Gillikin *et al.*, *in press*-a for more explanation). Furthermore, if $[Ba/Ca]_{water}$ was extended back through geologic time for the world's large estuaries, the overall change in the oceanic Ba budget could be better constrained. However, we stress that this proxy needs to be further refined before it should be used as a proxy of environmental conditions.

4.2.5 Metal uptake in bivalve tissues

4.2.5.1 Uptake kinetics

Biomineralization of obviously a biological process; therefore, understanding the pathway of elemental incorporation is vital to understanding proxy incorporation. Results showed uptake of Ca, Cd, Co, Cu and Hg that resembled saturation of kinetics, however, because steady-state was observed at all the three metal exposures, it was therefore unlikely that either internal metal binding sites or membrane transporters were saturated under those conditions. Foulkes (2000) indicated that apparent saturation of metal transfer at higher metal concentrations is not necessarily indication of saturation of membrane transporters involved. Therefore, the observed steady-state was probably a result of kinetics dominated by equilibrium between metal uptake and elimination processes and not saturation of transporters or internal binding sites.

The uptake kinetics of essential (Ca, Cu, Co) and non-essential metals (Ag, Cd, Pb, Hg) did not reveal differences that can be linked to biological significance of the elements. The distinction between uptakes of essential and non- essential metals especially at higher exposures may be unclear due to breakdown of internal metal

regulation (Foulkes, 2000). Most organisms are capable to internally regulating body burdens of biologically essential metals (Wright, 1995; Simkiss and Taylor, 1989). However, it is difficult to predict critical body burdens (Rainbow, 2002) and in this study it is not certain whether critical body burdens were reached. According to Wang and Rainbow (2005), tissue body burden and the detoxificatory fate of metals in animals seem to be even more important in affecting metal accumulation than the nature of the exposure routes or of the exposure regimes.

Kinetics of calcium in the gills showed the lowest uptake rate constant but a higher elimination rate constant. Calcium is an important essential element and is the main constituent of mussel shells. Therefore, it was expected to have a higher turn-over compared to trace metals. Overall, obtained uptake rate constants did not reflect a ranking of metals according to free metal ion concentrations in the exposure water as predicted by FIAM which predicts metal availability in terms of free metal ion activity in the exposure solution. According to FIAM, the expected bioavailability in decreasing order will be Co > Ca >> Cu > Pb > Cd >> Ag >> Hg. However, according to obtained ku values, the observed order was Cu > Cd > Hg > Pb > Co > Ag > Ca. These results suggests that uptake of metals is not only dependent on the form(s) in which the metal exist (chemical speciation) but also on other factors, among the important ones is the characteristics of available membrane transporters (Simkiss and Taylor, 1989).

4.2.5.2 Uptake pathways

As shown in Figure 38 and Figure 39b, all seven metals were influenced by more than one type of inhibitor and since the inhibitors used are known to affect different mechanisms, the results suggest metal uptake of these metals can occur through different pathways. Though studies are still few, in *M. edulis* examples of transport of some non- essential metals like Cd via different routes including those intended for essential elements have been reported. For example, calcium channel blockers were also shown to decrease the uptake of non- essential metals Ag and Cd (Vercauteren & Blust, 1999; Wang and Fisher, 1999). Indication of uptake of Zn an essential metal via the calcium channels has also been reported in literature (Vercauteren & Blust, 1999). In this study, in addition to Cd and Ag, two other metals, Cu (essential) and Pb (non- essential) also showed results that suggest uptake via the calcium channels.

It is generally assumed that most ion channels are intended for the homeostasis of common ions such as Ca2+, Cl-, K+, Mg2+ and Na+. It seems reasonable, since most ion channels are shown to be selective for specific ions. However, opportunistic entry for other ions with similar size or charge is possible (Simkiss & Taylor, 1989,

2001). In the case of calcium channels, it is suggested that metals that act as Ca analogues such as Ag, Cd, Co and Pb can also be transported through calcium channels. Many studies especially involving freshwater species have consistently shown competitive inhibition of uptake between calcium and several metals, particularly those with similar ionic size to calcium like cadmium. Therefore, common uptake route probably through the calcium channels is often assumed between calcium and these metals. However, in seawater it is probable that high calcium concentration will out-compete other metal ions for uptake through calcium channels (Wright, 1995).

The metabolic inhibitors NaCN and 2,4-dinitrophenol decreased the uptake of all seven metals. These results indication that metal uptake that directly use metabolic energy or id depended on processes that utilize energy. The involvement of active transport for many metals is still debated. For example, Carpene & George (1981) concluded that Cd uptake in mussel gills was largely by passive diffusion requiring no metabolic energy, but Vercauteren & Blust (1999) showed Cd uptake in whole mussels that was sensitive to metabolic inhibitors. Roesijadi and Unger (1993) also presented results that indicate active transport for the uptake of Cd in oysters. It has been suggested that when metabolic inhibitors are used to test involvement of active transport, caution must be taken since many metabolic inhibitors are known to form complexes, which in turn may cause secondary effects (Foulkes, 2000). This may be unlikely since exposures to inhibitors were stopped prior to metal exposures. Generally, the results reported here are consistent with previous studies showing the involvement of active transport for the uptake of Cd, Se and Zn in whole mussels (George & Coombs, 1977; Wang & Fisher, 1999; Vercauteren & Blust, 1999), Cd in isolated mussel gills (Carpene & George, 1981) and Cd in gills of oysters (Roesijadi & Unger, 1993).

The effects of ouabain on the uptake of Co, Hg and Pb into the gills, suggests transport that involve an ATP -dependent Na-K pump. There is not much literature concerning the effect of ouabain on metal uptake in mussels. In one study Vercauteren & Blust (1999) reported decreased uptake of Cd and Zn after exposure to ouabain, but in related species, Roesijadi and Unger (1993) found no significant effect of ouabain on Cd uptake in isolated gills of oysters. In other cell types, Endo et al (1996) found inhibition of Cd uptake in epithelial cell lines after exposure to ouabain. The possible role of Na-K pump in metal transport requires further investigations.

The last pathway tested was DIDS sensitive anion exchangers. Though nothing is reported on mussels, DIDS sensitive metal uptake pathway for As, Cd, Co and Zn

has been demonstrated in fish and other cell types (*i.e.* Endo, 1998). According to our results, inorganic anion exchangers may be involved in the uptake of several metals (Ag, Ca, Cd, Co, Cu, Hg and Pb) in isolated gills of mussels. This pathway requires further investigation to corroborate these findings.

4.3 Echinoderms

The aquarium experiments indicate a possible relation between Mg/Ca ratios in the echinoderm skeletons and temperature of the water they live in. Similarly, Mg/Ca in the skeletons of field collected specimens also showed a positive relation with temperature. Using an exponential model (see Lea, 2003 for rationale), laboratory experiments yielded an exponential increase in Mg/Ca of 1.2-1.4% per °C while field collected samples provided a 2.8% figure. It should be noted however, that this is only due to one group of data from the Barents Sea where salinity issues can be raised. Clearly this aspect deserves further research. Benthic foraminifera possess a high magnesium calcite skeleton like echinoderms (Lea 2003) Mg/Ca ratios in their skeleton depend on the water temperature (Toyofuku *et al.* 2000, Lear *et al.* 2002). This relation compares nicely to Mg/Ca relations obtained from starfish and sea urchins (benthic foraminifera 1.8% (Lea 2003), starfish 2.8%, sea urchins 1.9%). Relations with temperature in pelagic low magnesium calcite foraminifera are steeper than those of benthic foraminifera (9-10%, Lea *et al.* 1999) and do not compare to echinoderm relations. This illustrates the need for different regional recorders.

Surprisingly, Mg/Ca ratios in spine regenerates were not linked to sea water temperature. This is in agreement with the results reported by Davies *et al.* (1972) for regenerating spines of *Arbacia punctulata*. In comparison with normal growth of the whole skeleton, spine regeneration is a rather fast process and spine skeleton is a rather low-magnesium calcite (Mg/Ca ratio is 25-50mmol/mol in comparison with 95-175mmol/mol in the whole skeleton). Now, Erez (2003) reported that the distribution coefficient of Sr in foraminifera shells decreased with increasing calcification rate. This suggests that fast growing parts of the skeleton or specific processes like regeneration could have different fractionation coefficients for Mg and are not reliable recorders of sea water temperature.

Echinoderm skeletons have already been used to track Mg/Ca ratio changes in the phanerozoic ocean (Dickson 2002). Several taxa within the phylum were used, which could result in a high degree of uncertainty caused by physiological differences between the organisms and different uptake rates. In the present study our focus was on a single starfish species and on a group of closely related sea urchins to compare historical with modern samples. A difference in the Mg/Ca ratios is discernable as

historical ratios are always lower than modern ones. This shows that echinoderm specimens preserved in museums are useable when preserved in a dry state. However, even a short time immersion of the animal in a preserving agent can alter the chemistry of the skeleton (Renaud *et al.* 1995).

Similar to bivalves (Gillikin *et al.*, 2005; Lorrain *et al.*, *in press*), Sr/Ca ratios in starfish and sea urchins are not controlled by temperature, as opposed to results obtained for corals (Weinbauer *et al.* 2000) and sclerosponges (Rosenheim *et al.* 2004). This can be related to the different crystalline forms: coral and sclerosponge skeletons are made of aragonite whereas those of echinoderms are composed of calcite.

S/Ca ratios seem to be dependent on temperature changes. The sulphur most likely comes from sulphur bearing glycoproteins within the organic matrix (Cuif & Dauphin 2005). More research is needed to understand the behaviour of sulphur in relation to sea water temperature.

The slope of relative $\delta^{18}O$ values of starfish and sea urchin skeletons versus temperature is highly significant and the starfish slopes neatly match slopes measured in corals and molluscs. Using the slope of sea water $\delta^{18}O$ from the aquarium experiment we calculated the theoretical $\delta^{18}O$ of sea water at the different sampling locations, using mean water temperatures from the sampling site. This allowed us to calculate the relative $\delta^{18}O$ for the specimens collected at different latitudes. It is noteworthy, that the slopes of aquarium (4 months) and field relations between relative $\delta^{18}O$ and temperature closely match, indicating the robustness of the relation. $\delta^{18}O$ is a valid proxy of temperature in the skeleton of starfish and sea urchins, but its use should be a cautious one. As in other taxa, without information about the $\delta^{18}O$ of sea water at different times in the ocean history we cannot develop its full potential. Weber & Raup (1966, 1968) showed that different skeletal elements of the echinoderm skeleton have different $\delta^{18}O$ but if one only uses the same type of element, for example ambulacral plates, or a bulk sample of the whole skeleton this problem can be avoided.

5. CONCLUSIONS AND RECOMMENDATIONS

In this project we studied three taxa, sclerosponges, bivalves and echinoderms. Each has their strengths and weaknesses as potential proxies of environmental conditions. Sclerosponges have been shown to be excellent recorders of their environment (see aforementioned references), but are slow growing and are difficult to apply exact ages to geochemical profiles obtained from them, which can lead to difficulty in interpreting the data. This was a major problem we ran into with Pb/Ca profiles. More detailed information about growth structures and rates are desperately needed form this proxy substrate.

Bivalves are fast growing and many provide easy methods for dating geochemical profiles obtained form their shells. Furthermore, they occur around the world in many environments. Clearly this study has shown the difficulties in obtaining environmental information from many proposed proxies such as $\delta^{13}C$, Sr/Ca, Mg/Ca, and to a lesser extent Pb/Ca. On the other hand Ba/Ca ratios seem the most promising proxy. However, this does not exclude bivalve shells from being potential recorders of their environment. New proxies are constantly being developed and need to be tested on bivalves. With their large geographical and ecological range, bivalve shells would be very useful if they proved to record different aspects of their environment.

Echinoderms are also widespread and this study has shown that there is a great potential to use them as environmental recorders. Similar to foraminiferal calcite, the Mg/Ca ratios in echinoderm skeletons is providing data on the water temperature in which it formed.

Overall this project has answered many questions posed by the geochemical proxy community. We have published 17 peer reviewed papers on various topic and have several more coming. However, there are many questions that remain unanswered as well as new questions that have arisen. Clearly, the use of alternative marine calcareous skeletons as recorders of global climate change demands further study.

6. ACKNOWLEDGEMENTS

We are grateful for the HPLC expertise offered by J. Sinke and J. Nieuwenhuize (NIOO-CEME, Yerseke, NL). M. Elskens assisted with statistics and together with N. Brion collected the many liters of North Sea water for the barium experiment. C.H. Peterson (University of North Carolina, Chapel Hill), who kindly provided the *Mercenaria mercenaria* shells collected in the early 1980's; L. Campbell (University of South Carolina) who kindly provided the Pliocene *M. mercenaria* shell; and K. Li and S. Mickelson of the King County Department of Natural Resources and Parks, Water and Land Resources Division, Marine Monitoring group (WA, USA) and J. Taylor (U. Washington) who supplied the *Saxidomus giganteus* shells and water data. W.C. Gillikin and L. Daniels both kindly assisted with sample collection in North Carolina and C. Setterstrom collected the Puget Sound water samples. We also wish to thank J. Dille and R. DeHaens (Service Science des Matériaux et Electrochimie, Université Libre de Bruxelles), S. Fally **(**Université Libre de Bruxelles, Service de Chimie Quantique et Photophysique, B-1050 Brussels**)**, H. Zandbergen and V. Sivel (Technische Universiteit Delft), G. Borgonie and M. Claeys (Department of Biology, Ghent University), X. Turon (Universitat de Barcelona), M. Uriz (Centre d'Estudis Avançats de Blanes), D. Cardinal (African Museum), K. Ryan (Marine Biological Association, UK), The staff of the Discovery Bay Marine Laboratory (University of the West Indies), J. Vacelet, N. Boury-Esnault and C. Marschal (Station Marine d'Endoume), P. Swart and B. Rosenheim (Rosenstiel School of Marine & Atmospheric Science, University of Miami, FL). Historical echinoderm samples were kindly provided by Dr. Ameziane-Cominardi (Muséum national d'Histoire naturelle, Paris) and Dr. C. Massin (Institut royal des Sciences naturelles de Belgique). Some echinoderms were collected by Dr. Buschbaum (AWI-Bremerhaven), Dr. Belyaena (Zoology Institute Moscow), Dr. Charbonnel (Maison de la Mer, Sausset-les-Pins) and MSc. Cardoso (Nederlands Instituut voor Onderzoek der Zee). We thank R. Colwell (National Science Foundation Director), D. Santavy (USEPA NHEERL/GED, Gulf Breeze, FL), S. Pomponi and the crew of the R/V Edwin Link and Johnson-Sea Link I (Harbor Branch Oceanographic Institution, FL) for assistance in the collection of some sclerosponge samples.

We also thank the numerous MSc students who helped on this project: Hans Ulens (VUB-ANCH), C. de Jonghe (ULB), Dirk Steenmans (VUB-ANCH), Li Meng (VUB-ANCH), Ivy Meert (VUB-ANCH); as well as various other researchers that worked on the project: Baharak Bashar (GEOL-Ph.D.), Sophie Verheyden (MRAC), and Denis Langlet (MRAC).

7. REFERENCES

Adkins, J.F., Boyle, E.A., Curry, W.B. and Lutringer, A. (2003). Stable isotopes in deep-sea corals and a new mechanism for "vital effects". *Geochimica et Cosmochimica Acta* 67: 1129-1143.

Andreasson, F.P. and Schmitz, B. (1998). Tropical Atlantic seasonal dynamics in the early middle Eocene from stable oxygen and carbon isotope profiles of mollusk shells. *Paleoceanography* 13 (2):183-192.

Baeyens, W., van Eck, B., Lambert, C., Wollast, R. and Goeyens, L. (1998). General description of the Scheldt estuary. *Hydrobiologia* 366, 1-14.

Baeyens, W. (1998). Evolution of trace metal concentrations in the Scheldt estuary (1978-1995). A comparison with estuarine and ocean levels. *Hydrobiologia* 366, 157-167.

Benavides, L.M. and Druffel, E.M. (1986). Sclerosponge growth rates as determined by ^{210}Pb and $\Delta^{14}C$ chronologies. *Coral Reefs* 4: 221-224.

Boalch, R., Chan, S. and Taylor, D. (1981). Seasonal variation in the trace-metal content of *Mytilus edulis*. *Mar. Poll. Bull*. 12, 276-280.

Bouillon, S. (2002). Organic carbon in a southeast Indian mangrove ecosystem: sources and utilization by different faunal communities. PhD Thesis, Vrije Universiteit Brussel, 334 pp.

Boury-Esnault, N. and Rützler, K. (EDS). (1997). Thesaurus of Sponge Morphology. Smithsonian Contributions to Zoology 596: i-iv, 1-55.

Boutron, C.F., Görlach, U., Candelone, J.-P., Bolshov, M.A. and Delmas R.J. (1991). Decrease in anthropogenic lead, cadmium and zinc in Greenland snows since the late 1960s. *Nature* 353: 153 156.

Boyle, E.A., Chapnick, S.D., Shen, G.T. (1986). Temporal variability of lead in the western north Atlantic. *Journal of Geophysical Research* 91(C7): 8573 8593.

Boyle, E.A., Bergquist, B.A., Kayser, R.A. and Mahowald, N. (2005). Iron, manganese, and lead at Hawaii Ocean Time-series station ALOHA: Temporal variability and an intermediate water hydrothermal plume. *Geochim. Cosmochim. Acta* 69, 933-952.

Brannon, A.C. and Rao, K.R. (1979). Barium, strontium and calcium levels in the exoskeleton, hepatopancreas and abdominal muscle of the grass shrimp, *Palaemonetes pugio* - relation to molting and exposure to barite. *Comparative Biochemistry and Physiology A-Physiology* 63, 261-274.

Buckel, J.A., Sharack, B.L. and Zdanowicz, V.S. (2004). Effect of diet on otolith composition in *Pomatomus saltatrix*, an estuarine piscivore. *J. Fish Biol.* 64, 1469-1484.

Candelone, J.-P., Hong, S., Pellone, C. and Boutron, C.F. (1995). Post-Industrial Revolution changes in large-scale atmospheric pollution of the northern hemisphere by heavy metals as documented in central Greenland snow and ice. *Journal of Geophysical research* 100(D8): 16605 16616.

Cardinal, D., Hamelin, B., Bard, E. and Patzold, J. (2001). Sr/Ca, U/Ca and $\delta^{18}O$ records in recent massive corals from Bermuda: relationships with sea surface temperature, *Chem. Geol.* 176, 213-233.

Carpene, E. and George, S.G. (1981). Absorption of cadmium by gills of *Mytilus edulis (L.)*. *Mol. Physiol*. 1, 23-34.

Carpenter, S.J. and Lohmann, K.C. (1992). Sr/Mg ratios of modern marine calcite - empirical indicators of ocean chemistry and precipitation rate, *Geochim. Cosmochim. Acta* 56, 1837-1849.

Chauvaud, L., Thouzeau, G. and Paulet, Y.M. (1998). Effects of environmental factors on the daily growth rate of *Pecten maximus* juveniles in the Bay of Brest (France): *Journal of Experimental Marine Biology and Ecology* v. 227, p. 83–111.

Clode, P.L. and Marshall, A.T. (2003). Skeletal microstructure of *Galaxea fascicularis* exsert septa: A high-resolution SEM study. *Biological Bulletin* 204 (2): 146-154.

Coffey, M., Dehairs F., Collette O., Luther G., Church, T. and Jickells, T. (1997). The behaviour of dissolved barium in estuaries. *Est. Coast. Shelf Sci.* 45, 113-121.

Crenshaw, M. A. (1972). Inorganic composition of molluscan extrapallial fluid, *Biol. Bull*., 143 506-512.

Cuif, J.P. and Dauphin, Y. (2005). The Environment Recording Unit in coral skeletons – a synthesis of structural and chemical evidences for a biochemically driven, stepping-growth process in fibres, *Biogeosciences* 2, 61-73.

Davies, T.T. Crenshaw, M.A. and Heatfield, B.M. (1972). The effect of temperature on the chemistry and structure of echinoid spine regeneration *Journal of Paleontology* 46: 874-883.

De Ridder, F., Pintelon, R., Schoukens, J., Gillikin, D.P., André, L., Baeyens, W., de Brauwere, A. and Dehairs, F. (2004). Decoding nonlinear growth rates in biogenic environmental archives, *Geochem. Geophys. Geosyst*. 5, Q12015, doi:10.1029/2004GC000771.

De Ridder, F., Pintelon, R., Schoukens, J. and Gillikin, D.P. (2005). Modified AIC and MDL model selection criteria for short data records. IEEE *Transactions on Instrumentation and Measurement* 54 (1): 144-150.

Dehairs, F., Chesselet, R. and Jedwab, J. (1980). Discrete suspended particles of barite and the barium cycle in the open ocean. *Earth Planet. Sci. Lett.* 49, 528-550.

Dickson, J.A.D. (2002). Fossil echinoderms as monitor of the Mg/Ca ratio of phanerozoic oceans *Science* 298: 1222-1224.

Dietzel, M., Gussone, N. and Eisenhauer, A. (2004). Co-precipitation of Sr^{2+} and Ba^{2+} with aragonite by membrane diffusion of CO_2 between 10 and 50 ºC, *Chem. Geol*. 203, 139-151.

Dodd, J.R. (1965). Environmental control of strontium and magnesium in Mytilus: *Geochimica et Cosmochimica Acta* v. 29, p. 385–398.

Druffel, E.R.M. (1997). Geochemistry of corals: Proxies of past ocean chemistry, ocean circulation, and climate. *Proc. Natl. Acad. Sci*. 94, pp. 8354-8361.

Eggins, S.M., Sadekov. A. and De Deckker, P. (2004). Modulation and daily banding of Mg/Ca in *Orbulina universa* tests by symbiont photosynthesis and respiration: a complication for seawater thermometry? *Earth and Planetary Science Letters* 225: 411-419.

Eisenman, E.A. and Alfert, M. (1982). A new fixation procedure for preserving the ultrastructure of marine invertebrate tissues. *Journal of Microscopy-Oxford* 125: 117-120

Elliot, M., deMenocal, P.B., Linsley, B.K. and Howe, S.S. (2003). Environmental controls on the stable isotopic composition of *Mercenaria mercenaria*: potential application to

paleoenvironmental studies. *Geochemistry Geophysics Geosystems* 4, 1056, 10.1029/2002GC000425.

Elsdon, T.S., Gillanders, B.M. (2004). Fish otolith chemistry influenced by exposure to multiple environmental variables. *J. Exp. Mar. Biol. Ecol*. 313, 269-284.

Endo, T., Kimura, O. and Sakata, M. (1996). Effects of zinc and copper on uptake of cadmium by LLC-PK1 cells. *Biol Pharm Bull*. 7, 944-8.

Endo, T., Kimura, O. and Sakata, M. (1998). Cadmium uptake from apical membrane of LLC-PK1 cells via inorganic anion exchanger. *Pharmacol. Toxicol*. 82, 230-235.

Epstein, S. and Mayeda, T. (1953). Variation of ^{18}O content of waters from natural sources. *Geochimica et Cosmochimica Acta* 4: 213-224.

Epstein, S., Buchsbaum, R., Lowenstam, H.A. and Urey, H.C. (1953). Revised carbonate - water isotopic temperature scale. *Bulletin of the Geological Society of America* 64, 1315-1326.

Erez, J. (2003). The source of ions for biomineralization in foraminifera and their implications for paleoceanic proxies. Vol.54 Pp. 115-144 In: J.J Rosso (ed.) *Reviews in Mineralogy & Geochemistry*. Mineralogical Society of America, Washington, DC.

Fallon, S.J., McCulloch, M.T., van Woesik, R. and Sinclair, D.J. (1999). Corals at their latitudinal limits: laser ablation trace element systematics in Porites from Shirigai Bay, Japan. *Earth Planet. Sci. Lett*. 172, 221-238.

Fisher N.S., Guillard R.R.L. and Bankston D.C. (1991). The accumulation of barium by marine-phytoplankton grown in culture. *Journal of Marine Research* 49: 339-354.

Foulkes, E. C. (2000). Transport of Toxic Heavy Metals Across Cell Membranes. *Proc. Soc. Exp. Biol. Med*. 223, 234-240.

Freitas P., Clarke L. J., Kennedy H., Richardson C. and Abrantes, F. (2005). Mg/Ca, Sr/Ca, and stable-isotope ($\delta^{18}O$ and $\delta^{13}C$) ratio profiles from the fan mussel *Pinna nobilis*: Seasonal records and temperature relationships. *Geochem. Geophy. Geosys.* 6, Q04D14, doi:10.1029/2004GC000872.

Fryer, B.J, Jackson, S.E. and Longerich, H.P. (1995). Design, operation and role of the laser-ablation microprobe coupled with an inductively-coupled plasma - mass-spectrometer (LAM-ICP-MS) in the earth-sciences. *Canadian Mineralogist* 33: 303-312.

Fuge, R., Palmer, T.J., Pearce, N.J.G., Perkins, W.T. (1993). Minor and trace element chemistry of modern shells: a laser ablation inductively coupled plasma spectrometry study. *Appl. Geochem. suppl*. 2, 111-116.

Gagan, M.K., Ayliffe, L.K., Beck, J.W., Cole, J.E., Druffel, E.R.M., Dunbar, R.B. and Schrag, D.P. (2000). New views of tropical paleoclimates from corals. *Quaternary Science Reviews* 19 (1-5):45-64.

George, S.G. and Coombs, T.L. (1977). The Effect of chelating agents on the uptake and accumulation of cadmium by *Mytilus edulis*. *Mar. Biol*. 39, 261-268.

Gerringa, L.J.A., Hummel H. and Moerdijk-Poortvliet, T.C.W. (1998). Relations between free copper and salinity, dissolved and particulate organic carbon in the Oosterschelde and Westerschelde, Netherlands. *J. Sea Res.* 40, 193-203.

Gillikin, D. P., De Ridder F., Ulens H., Elskens M., Keppens E., Baeyens W. and Dehairs, F. (*in press*-a). Assessing the reproducibility and reliability of estuarine bivalve shells (*Saxidomus giganteus*) for sea surface temperature reconstruction: implications for

paleoclimate studies. *Palaeogeogr. Palaeoclimatol. Palaeoecol.* doi:10.1016/j.palaeo.2005.03.047.

Gillikin, D.P., De Wachter, B. and Tack, J.F. (2004). Physiological responses of two ecologically important Kenyan mangrove crabs exposed to altered salinity regimes. *J. Exp. Mar. Biol. Ecol.* 301, 93-109.

Gillikin, D. P., Dehairs, F., Baeyens, W., Navez, J., Lorrain, A. and André, L. (*in press*-b). Inter- and intra-annual variations of Pb/Ca ratios in clam shells (*Mercenaria mercenaria*): a record of anthropogenic lead pollution? *In press Marine Pollution Bulletin*. doi:10.1016/j.marpolbul.2005.06.020.

Gillikin, D. P., Ulens, H., Dehairs, F., Baeyens, W., Navez, J., Andre, L., Keppens, E. and the CALMARs group. (2004a). Sr and Mg Profiles in Aragonitic Bivalves: Do They Record Temperature? *Eos Trans. AGU* 84(52), *Ocean Sci. Meet. Portland*, OR, *Suppl., Abstract* OS42B-06.

Gillikin, D.P. (2005). Geochemistry of Marine Bivalve Shells: the potential for paleoenvironmental reconstruction. Ph.D. thesis. Vrije Universiteit Brussel, Belgium, 258 p.

Gillikin, D.P., Dehairs, F., Lorrain, A., Steenmans, D., Baeyens, W., André, L. (*in press*-c). Barium uptake into the shells of the common mussel (*Mytilus edulis*) and the potential for estuarine paleo-chemistry reconstruction. *Geochim. Cosmochim. Acta*.

Gillikin, D.P., Lorrain, A., Navez, J., Taylor, J.W., André, L., Keppens, E., Baeyens, W. and Dehairs, F. (2005). Strong biological controls on Sr/Ca ratios in aragonitic marine bivalve shells: *Geochemistry, Geophysics, Geosystems*, v. 6, p. Q05009, doi: 10.1029/2004GC000874.

Goodwin, D.H., Flessa, K.W., Schöne, B.R., Dettman, D.L. (2001). Cross-calibration of daily growth increments, stable isotope variation, and temperature in the Gulf of California bivalve mollusk *Chione cortezi*: implications for paleoenvironmental analysis. *Palaios* 16, 387-398.

Govindaraju, K. (1994). 1994 Compilation of working values and sample description for 383 geostandards. *Geostandards Newsletter XVIII Special issue*: 1-158.

Guillong, M. and Gunther, D. (2002). Effect of particle size distribution on ICP-induced elemental fractionation in laser ablation-inductively coupled plasma-mass spectrometry. *Journal of Analytical Atomic Spectrometry* 17: 831-837.

Günther, D. and Hattendorf, B. (2005). Solid sample analysis using laser ablation inductively coupled plasma mass spectrometry. *TrAC Trends in Analytical Chemistry* 24: 255-265.

Haase-Schramm, A., Böhm, F., Eisenhauer, A., Dullo, W.-C., Joachimsky, M.M., Hansen, B. and Reitner, J. (2003). Sr/Ca ratios and oxygen isotopes from sclerosponges: temperature and history of the Caribbean mixed layer and thermocline during the Little Ice Age. *Palaeoceanography* 18 (3): 1073-1088.

Hamwi, A. and Haskin, H.H. (1969). Oxygen consumption and pumping rates in the Hard Clam *Mercenaria mercenaria*: A direct method. *Science* 163: 823-824.

Hart, S. R., Cohen, A. L. and Ramsay, P. (1997). Microscale analysis of Sr/Ca and Ba/Ca in Porites, *Proceedings of the 8th International Coral Reef Symposium* 2, 1707 - 1712.

Hartman, W.D. and Goreau, T.F. (1972). Ceratoporella (Porifera: Sclerospongiae) and the chaetetid "corals". *Transactions of the Connecticut Academy of Arts and Sciences* 44: 133-148.

Hartman, W.D. and Goreau, T.F. (1976). A New Ceratoporellid Sponge (Porifera: Sclerospongiae) from the Pacific. Pp. 329-347. In: Harrison, F.W. & Cowden, R.R. (Eds), Aspects of Sponge Biology. (Academic Press: New York & London): i-xiii, 1-354.

Havach, S. M., Chandler, T., Wilson-Finelli, A. and Shaw, T. J. (2001). Experimental determination of trace element partition coefficients in cultured benthic foraminifera. *Geochim. Cosmochim. Acta* 65, 1277–1283.

Herman, P.M.J., Middelburg, J.J., Widdows, J., Lucas, C.H. and Heip, C.H.R. (2000). Stable isotopes as trophic tracers: combining ¢eld sampling and manipulative labelling of food resources for macrobenthos. *Marine Ecology Progress Series* 204, 79-92.

IPCC (Intergovernmental Panel on Climate Change) (2001) *IPCC Third Assessment Report: Climate Change 2001*. Watson RT, & the Core Writing Team (eds.) IPCC, Geneva, Switzerland. pp. 184. Available online at http://www.ipcc.ch/

Jacoby, G.C. (1989) Overview of tree-ring analysis in tropical regions. *IAWA Journal* 10(2): 99-108.

Kautsky, N. (1982). Growth and size structure in a Baltic *Mytilus edulis* population. *Mar. Biol.* 68, 117-133.

Keller, N., Del Piero, D. and Longinelli, A. (2002). Isotopic composition, growth rates and biological behaviour of *Chamelea gallina* and *Callista chione* from the Gulf of Trieste (Italy). *Marine Biology* 140: 9-15.

Kinsman, D.J.J. and Holland, H.D. (1969). The co-precipitation of cations with $CaCO_3$ - IV. the co-precipitation of Sr^{2+} with aragonite between 16 degrees and 96 degrees C. *Geochim. Cosmochim. Acta* 33, 1-17.

Klein, R.T., Lohmann, K.C. and Thayer, C.W. (1996a). Bivalve skeletons record sea-surface temperature and $\delta^{18}O$ via Mg/Ca and $^{18}O/^{16}O$ ratios. *Geology* 24, 415-418.

Klein, R.T., Lohmann, K.C. and Thayer, C.W. (1996b). Sr/Ca and $^{13}C/^{12}C$ ratios in skeletal calcite of *Mytilus trossulus*: Covariation with metabolic rate, salinity, and carbon isotopic composition of seawater. *Geochimica et Cosmochimica Acta* 60: 4207-4221.

Lazareth, C.E., Vander Putten, E., André, L. and Dehairs, F. (2003). High-resolution trace element profiles in shells of the mangrove bivalve *Isognomon ephippium*: a record of environmental spatio-temporal variations? *Est. Coast. Shelf Sci.* 57, 1103-1114.

Lazareth, C.E., Willenz, Ph., Navez, J., Keppens, E., Dehairs, F. and Andre, L. (2000). Sclerosponges as a new potential recorder of environmental changes: Lead in *Ceratoporella nicholsoni*. *Geology* 28, 515-518.

Lea, D.W. and Spero, H.J. (1992). Experimental determination of barium uptake in shells of the planktonic foraminifera *Orbulina universa* at 22°C. *Geochim. Cosmochim. Acta* 56, 2673–2680.

Lea, D.W. and Spero, H.J. (1994). Assessing the reliability of paleochemical tracers: Barium uptake in the shells of planktonic foraminifera. *Paleoceanography* 9, 445-452.

Lea, D.W. and Boyle, E. (1989). Barium content of benthic foraminifera controlled by bottom-water composition. *Nature* 338, 751-753.

Lea, D.W. and Boyle, E. (1991). Barium in planktonic foraminifera. *Geochim. Cosmochim. Acta* 55, 3321-3331.

Lea, D.W. and Boyle E. (1993). Determination of carbonate-bound barium in foraminifera and corals by isotope dilution plasma-mass spectrometry. *Chem. Geol.* 103, 73 - 84.

Lea, D.W., Shen, G.T. and Boyle, E.A. (1989). Coralline barium records temporal variability in equatorial Pacific upwelling. *Nature* 340: 373–376.

Lea, D.W. (2003). Elemental and Isotopic Proxies of Marine Temperatures, pp. 365-390. In *The Oceans and Marine Geochemistry* (ed. H. Elderfield, ed.) Vol. 6 Treatise on Geochemistry (eds H.D. Holland and K.K. Tuerekian), Elsevier-Pergamon, Oxford.

Lea, D.W. Mashiotta, T.A. and Spero, H.J. (1999). Controls on magnesium and strontium uptake in planktonic foraminifera determined by live culturing. *Geochimica et Cosmochimica Acta* 63 (16): 2369-2379.

Lear, C.H., Rosenthal, Y. and Slowey, N. (2002). Benthic foraminiferal Mg/Ca-paleothermometry: A revised core-top calibration. *Geochimica et Cosmochimica Acta* 66 (19): 3375-3387.

Linsley, B.K., Messier, R.G. and Dunbar, R.B. (1999). Assessing between-colony oxygen isotope variability in the coral *Porites lobata* at Clipperton Atoll. *Coral Reefs* 18: 13-27.

Lobel, P.B., Longerich, H.P., Jackson, S.E. and Belkhode, S.P. (1991). A major factor contributing to the high degree of unexplained variability of some elements concentrations in biological tissue - 27 elements in 5 organs of the mussel *Mytilus* as a model. *Arch. Environ. Con. Tox.* 21, 118-125.

Longerich, H.P., Gunther, D., Jackson, S.E. (1996). Elemental fractionation in laser ablation inductively coupled plasma mass spectrometry. *Fresenius Journal of Analytical Chemistry* 355: 538-542.

Lorens, R.B. (1978). A study of biological and physiological controls on the trace metal content of calcite and aragonite. *Ph.D. thesis*, University of Rhode Island.

Lorens, R.B. (1981). Sr, Cd, Mn and Co distribution coefficients in calcite as a function of calcite precipitation rate. *Geochim. Cosmochim. Acta* 45, 553-561.

Lorens, R.B. and Bender, M.L. (1980). The impact of solution chemistry on *Mytilus edulis* calcite and aragonite. *Geochim. Cosmochim. Acta* 44, 1265-1278.

Lorrain, A., Gillikin, D.P., Paulet, Y.M., Chauvaud, L., Le Mercier, A., Navez, J. and André, L. (*in press*). Strong kinetic effects on Sr/Ca ratios in the calcitic bivalve *Pecten maximus*. *Geology*, 1 December 2005 issue.

Lorrain, A. (2002). Utilisation de la coquille Saint-Jacques comme traceur environnemental: approches biologique et biogéochimique. PhD thesis, Université de Bretagne occidentale, Brest, France.

Lorrain, A., Paulet Y.-M., Chauvaud, L., Dunbar, R., Mucciarone, D. and Fontugne, M. (2004). $\delta^{13}C$ variations in scallop shells: Increasing metabolic carbon contribution with body size? *Geochim. Cosmochim. Acta* 68, 3509-3519.

Lorrain, A., Paulet, Y.-M., Chauvaud, L., Savoye, N., Nézan, E. and Guérin, L. (2000). Growth anomalies in *Pecten maximus* from coastal waters (Bay of Brest, France): Relationship with diatom blooms: Journal of the Marine Biological Association of the United Kingdom, v. 80, p. 667–673.

Lorrain, A., Paulet, Y.M., Chauvaud, L., Savoye, N., Donval, A. and Saout, C. Differential delta C-13 and delta N-15 signatures among scallop tissues: implications for ecology and physiology. *Journal of Experimental Marine Biology and Ecology* 275 (1):47-61, 2002.

Marin, F. and Luquet, G. (2004). Molluscan shell proteins. *C. R. Palevol* 3, 469–492.

McConnaughey, T.A., Burdett, J., Whelan J.F. and Paull C.K. (1997). Carbon isotopes in biological carbonates: Respiration and photosynthesis. *Geochim. Cosmochim. Acta* 61, 611–622.

McConnaughey, T.A. (1989). ^{13}C and ^{18}O isotopic disequilibrium in biological carbonates: 2. in vitro simulation of kinetic isotope effects. *Geochimica et Cosmochimica Acta* 53, 163-171.

McCorkle, D.C., Emerson, S.R. and Quay, P.D. (1985). Stable carbon isotopes in marine porewaters. *Earth and Planetary Science Letters* 74: 13-26.

McDonald, K. (1999). High-pressure freezing for preservation of high resolution fine structure and antigenicity for immunolabelling. In: M.A. Nasser Hajibagheri, ed. *Methods in Molecular Biology, vol. 117: Electron Microscopy Methods and Protocols*. Humana Press Inc., New Jersey. (1999) pp. 77-98.

Meibom, A., Cuif, J.P., Hillion, F.O., Constantz, B.R., Juillet-Leclerc, A., Dauphin, Y., Watanabe, T., Dunbar, R.B. (2004). Distribution of magnesium in coral skeleton. *Geophys. Res. Lett.* 31, L23306, doi: 10.1029/2004GL021313.

Middelburg, J.J., Barranguet, C., Boschker, H.T.S., Herman, P.M.J., Moens, T. and Heip, C.H.R. The fate of intertidal microphytobenthos carbon: An in situ ^{13}C-labeling study. *Limnology and Oceanography* 45 (6):1224-1234, 2000.

Middleton, W.E.K. (1966). *A History of the Thermometer and Its Use in Meteorology*. Johns Hopkins University Press, Maryland USA. 268 pp.

Mitsuguchi, T., Matsumoto, E., Abe, O., Uchida, T., Isdale, P.J. (1996). Mg/Ca thermometry in coral-skeletons. *Science* 274, 961-963.

Miyajima,T., Yamada, Y., Hanba, Y.T., Yoshii, K., Koitabashi, T. and Wada, E. (1995). Determining the stable-isotope ratio of total dissolved inorganic carbon in lake water by GC/C/IRMS. *Limnology and Oceanography* 40: 994-1000.

Morse, J.W. and Bender, M.L. (1990). Partition-coefficients in calcite - examination of factors influencing the validity of experimental results and their application to natural systems. *Chem. Geol.* 82, 265-277.

Mubiana, V.K. and Blust, R. (*in press*). Uptake kinetics of heavy metals (Ag, Ca, Cd, Co, Cu, Hg & Pb) in isolated gills of the marine mussel, Mytilus edulis and the involvement of different uptake pathways. Aquatic Toxicology.

Mubiana, V.K., Qadah, D., Meys, J. and Blust, R. (2005). Temporal and spatial trends in heavy metal concentrations in the marine mussel *Mytilus edulis* from the Western Scheldt Estuary (The Netherlands). *Hydrobiologia*. 540, 169 – 180.

Mucci, A., Morse, J.W. (1983). The incorporation of Mg^{2+} and Sr^{2+} into calcite overgrowths - influences of growth-rate and solution composition. *Geochim. Cosmochim. Acta* 47, 217-233.

Munksgaard, N.C., Antwertinger, Y. and Parry, D.L. (2004). Laser ablation ICP-MS analysis of Faviidae corals for environmental monitoring of a tropical estuary. *Environmental Chemistry* 1: 188-196.

Murozumi, M., Chow, T.J. and Patterson, C. (1969). Chemical concentrations of pollutant lead aerosols, terrestrial dusts and sea salts in Greenland and Antarctic snow strata: *Geochimica et Cosmochimica Acta*, 33: 1247 1294.

NCSCO (2004) North Carolina State Climate Office. http://www.nc-climate.ncsu.edu/climate/hurricanes.html (accessed May 2004).

Nriagu, J.O. (1989). A global assessment of natural sources of atmospheric trace metals. *Nature* 338: 47 49.

Nürnberg, D., Bijma, J. and Hemleben, C. (1996). Assessing the reliability of magnesium in foraminiferal calcite as a proxy for water mass temperatures. *Geochim. Cosmochim*. *Acta* 60, 803-814.

O'Donnell, T.H., Macko, S.A., Chou, J., Davis-Hartten, K.L. and Wehmiller, J.F. Analysis of delta C-13, delta N-15, and delta S-34 in organic matter from the biominerals of modern and fossil *Mercenaria* spp. *Organic Geochemistry* 34 (2):165-183, 2003.

Paquette, J. and Reeder, R.J. (1995). Relationship between surface-structure, growth-mechanism, and trace-element incorporation in calcite: *Geochimica et Cosmochimica Acta*, v. 59, p. 735–749.

Paulson, A.J. and Feely, R.A. (1985). Dissolved trace-metals in the surface waters of Puget Sound. *Mar. Poll. Bull.* 16, 285-291.

Peterson, C.H. and Fegley, S.R. Seasonal allocation of resources to growth of shell, soma, and gonads in *Mercenaria mercenaria*, *Biol. Bull*., 171,597-610, 1986.

Pingitore, N.E. and Eastman, M.P. (1984). The experimental partitioning of Ba^{2+} into calcite. *Chem. Geol.* 45, 113-120.

Pitts, L.C. and Wallace, G.T. (1994). Lead deposition in the shell of the bivalve, *Mya arenaria* - an indicator of dissolved lead in seawater. *Est. Coast. Shelf Sci*. 39, 93-104.

Planchon, F.A.M., van de Velde, K., Rosman, K., Wolff, E.W., Ferrari, C.P. Boutron, C.F. (2003). One hundred fifty-year record of lead isotopes in Antarctic snow from Coats Land. *Geochim. Cosmochim. Acta* 67: 693-708.

Prosser, S.J., Brookes, S.T., Linton A. and Preston, T. (1991). Rapid, automated-analysis of ^{13}C and ^{18}O of CO_2 in gas samples by continuous-flow, isotope ratio mass-spectrometry. *Biological Mass Spectrometry* 20: 724-730.

Qiu, J.W., Tremblay, R. and Bourget, E. (2002). Ontogenetic changes in hyposaline tolerance in the mussels *Mytilus edulis* and *M. trossulus*: implications for distribution. *Mar. Ecol. Prog. Ser.* 228, 143-152.

Rainbow, P.S. (2002). Trace metal concentrations in aquatic invertebrates: why and so what? *Environ. Pollut*. 120, 497-507.

Reitner, J. (1989). Struktur, Bildung und Diagenese der Basalskelette bei rezenten Pharetroniden unter besonderer Berücksichtigung von {I*Petrobioma massiliana*} Vacelet & Lévi 1958 (Minchinellida, Porifera). *Berliner Geowissenschaftliche Abhandlungen* 106: 343-383

Ren, L., Linsley, B.K., Wellington, G.M., Schrag, D.P. and Hoegh-Guldberg, O. (2003). Deconvolving the delta O-18 seawater component from subseasonal coral delta O-18 and Sr/Ca at Rarotonga in the southwestern subtropical Pacific for the period 1726 to 1997. *Geochimica et Cosmochimica Acta* 67: 1609-1621.

Renaud, C.B., Nriagu, J.O. and Wong, H.K.T. (1995). Trace metals in fluid-preserved museum fish specimens. *Science of The Total Environment* 159 (1): 1-7.

Reuer, M.K., Boyle, E. and Cole, J.E. (2003). A mid-twentieth century reduction in tropical upwelling inferred from coralline trace element proxies. *Earth and Planetary Science Letters* 210: 437-452.

Richardson, C.A., Chenery, S.R.N. and Cook, J.M. (2001). Assessing the history of trace metal (Cu, Zn,Pb) contamination in the North Sea through laser ablation ICP-MS of horse mussel *Modiolus modiolus* shells. *Marine Ecology-Progress Series* 211, 157-167.

Richardson, C.A., Peharda, M., Kennedy, H., Kennedy, P. and Onofri, V. (2004). Age, growth rate and season of recruitment of *Pinna nobilis* (L) in the Croatian Adriatic determined from Mg:Ca and Sr:Ca shell profiles. *J. Exp. Mar. Biol. Ecol*. 299, 1-16.

Riu, J., Rius, F.X. (1996). Assessing the accuracy of analytical methods using linear regression with errors in both axes. *Ana. Chem*. 68, 1851-1857.

Roberts, D., Rittschof, D., Gerhart, D.J., Schmidt, A.R. and Hill, L.G. (1989). Vertical migration of the clam *Mercenaria mercenaria* (L) (Mollusca, Bivalvia) - environmental correlates and ecological significance. *Journal of Experimental Marine Biology and Ecology* 126: 271-280.

Roesijadi, G. and Unger, M.E. (1993). Cadmium uptake in gills of the mollusc *Crassostrea virginica* and inhibition by calcium channel blockers. *Aquat. Toxicol*. 24, 195-206.

Romanek, C.S., Grossman, E.L., and Morse, J.W. (1992). Carbon isotopic fractionation in synthetic aragonite and calcite - effects of temperature and precipitation rate. *Geochimica et Cosmochimica Acta* 56: 419-430.

Rosenheim, B.E., Swart, P.K., Thorrold, S.R., Willenz, Ph., Berry, L., Latkoczy, C. (2004). High-resolution Sr/Ca records in sclerosponges calibrated to temperature in situ. *Geology* 32, 145-148.

Rosenthal, Y. and Katz, A. (1989). The applicability of trace elements in freshwater shells for paleogeochemical studies. *Chem. Geol.* 78, 65-76.

Rowley, R.J. and Mackinnon, D.I. (1995). Use of the flourescent marker calcein in biomineralisation studies of brachiopods and other marine organisms. *Bulletin de l'Institut Oceanographique, Monaco* 14, 111-120.

Ryan, K.P., Purse, D.H., Robinson, S.G. and Wood, J.W. (1987) The relative efficiency of cryogens used for plunge-cooling biological specimens. *Journal of Microscopy*, 145 (1): 89-96.

Salata, G.G., Roelke, L.A. and Cifuentes, L.A. (2000). A rapid and precise method for measuring stable carbon isotope ratios of dissolved inorganic carbon. *Marine Chemistry* 69: 153-161.

Schöne, B.R., Oschmann, W., Rossler, J., Castro, A.D.F., Houk, S.D., Kroncke, I., Dreyer, W., Janssen, R., Rumohr, H. and Dunca, E. (2003a). North Atlantic Oscillation dynamics recorded in shells of a long-lived bivalve mollusk. *Geology* 31: 1037-1040.

Scott, P.J.B. (1990). Chronic pollution recorded in coral skeletons in Hong Kong. *J. Exp*. *Mar. Biol. Ecol*. 139, 51-64.

Schaule, B.K. and Patterson, C. (1983). Perturbations of the natural lead depth profile in the Sargasso Sea by Industrial lead. In: Trace elements in Seawater. Wong C.S., Boyle E.A., Bruland K., Burton D. and Goldberg E.D., eds: 487 503. Plenum, New York.

Shen, C.C., Lee, T., Chen, C.Y., Wang, C.H., Dai, C.F. and Li, L.A. (1996). The calibration of D[Sr/Ca] versus sea surface temperature relationship for Porites corals. *Geochimica et Cosmochimica Acta* 60 (20):3849-3858.

Shen, G.T. and Boyle, E.A. (1988). Determination of lead, cadmium and other trace-metals in annually-banded corals. *Chemical Geology* 67 (1-2):47-62.

Shen, G.T. and Boyle, E.A. (1987). Lead in corals - reconstruction of historical industrial fluxes to the surface ocean. *Earth Planet. Sci. Lett*. 82, 289-304.

Sherrell, R.M. and Boyle, E.A. (1992). The trace metal composition of suspended particles in the oceanic water column near Bermuda. *Earth and Planetary Science Letters* 111: 155 174.

Simkiss, K. and Taylor, M.G. (1989). Metal fluxes across the membrane of aquatic organisms. *CRC Critical Rev. Aquat. Sci*. 1, 173-188.

Simkiss, K. and Taylor, M.G. (2001). Trace element speciation at cell membranes: aqueous, solid and lipid phase effects. *J. Environ. Monitor*. 3, 15-21.

Sinclair, D.J. (2005). Non river-flood barium signals in the skeletons of corals from coastal Queensland , Australia. *Earth Planet. Sci. Lett.* 237, 354-369.

Spero, H.J., Bijma, J., Lea, D.W., Bemis, B.E. (1997). Effect of seawater carbonate concentration on foraminiferal carbon and oxygen isotopes. *Nature* 390 (6659), 497-500.

Spurr, A.R. (1969). A low-viscosity epoxy resin embedding medium for electron microscopy. *Journal of Ultrastructural Research* 26: 31-43.

Stecher, H.A. and Kogut, M.B. (1999). Rapid barium removal in the Delaware estuary. *Geochim. Cosmochim. Acta* 63, 1003-1012.

Stecher, H.A. III, Krantz, D.E., Lord, C.J., Luther, G.W., Bock, K.W. (1996). Profiles of strontium and barium in *Mercenaria mercenaria* and *Spisula solidissima* shells. *Geochim. Cosmochim. Acta* 60, 3445-3456.

Steenmans, D. (2004). Do marine bivalve shells record paleo-productivity? *M.Sc. thesis*. Vrije Universiteit Brussel, Belgium.

Stoll, H.M., Encinar, J.R., Alonso, J.I.G., Rosenthal, Y., Probert, I. and Klaas, C. (2001). A first look at paleotemperature prospects from Mg in coccolith carbonate: Cleaning techniques and culture measurements: *Geochemistry, Geophysics, Geosystems*, v. 2, doi: 10.1029/2000GC000144.

Stoll, H.M., Klaas, C.M., Probert, I., Ruiz Encinar, J. and Garcia Alonso, J.I. (2002). Calcification rate and temperature effects on Sr partitioning in coccoliths of multiple species of coccolithophorids in culture: *Global and Planetary Change*, v. 34, p. 153–171.

Sukhotin, A.A. and Pörtner, H.-O. (2001.) Age-dependence of metabolism in mussels *Mytilus edulis* (L.) from the White Sea. *Journal of Experimental Marine Biology and Ecology* 257: 53-72.

Swaileh, K.M. (1996). Seasonal variations in the concentrations of Cu, Cd, Pb and Zn in *Arctica islandica* L (Mollusca: Bivalvia) from Kiel Bay, western Baltic Sea. *Mar. Poll. Bull*. 32, 631-635.

Swart, P., Moore, M., Charles, C. and Böhm, F. (1998). Sclerosponges may hold new keys to marine paleoclimate. *EOS, Transactions, American Geophysical Union* 79 (52): 633-636.

Swart, P.K., Healy, G.F., Dodge, R.E., Kramer, P., Hudson, J.H., Halley, R.B. and Robblee, M.B. (1996). The stable oxygen and carbon isotopic record from a coral growing in

Florida Bay: A 160 year record of climatic and anthropogenic influence. *Palaeogeography Palaeoclimatology Palaeoecology* 123: 219-237.

Swart, P.K., Thorrold, S., Rosenheim, B., Eisenhauer, A., Harrison, C.G.A., Grammer, M., Latkoczy, C. (2002). Intra-annual variation in the stable oxygen and carbon and trace element composition of sclerosponges. *Paleoceanography* 17, 1045, doi: 10.1029/2000PA000622.

Takesue, R.K., van Geen, A. (2004). Mg/Ca, Sr/Ca, and stable isotopes in modern and Holocene *Protothaca staminea* shells from a northern California coastal upwelling region. *Geochim. Cosmochim. Acta* 68, 3845-3861.

Tesoriero, A.J. and Pankow, J.F. (1996). Solid solution partitioning of Sr^{2+}, Ba^{2+}, and Cd^{2+} to calcite. *Geochim. Cosmochim. Acta* 60, 1053-1063.

Toland, H., Perkins, B., Pearce, N., Keenan, F., Leng, M.J. (2000). A study of sclerochronology by laser ablation ICP-MS. *J. Ana. Atom. Spectro*. 15, 1143-1148.

Torres, M. E., Barry J. P., Hubbard, D.A. and Suess, E. (2001). Reconstructing the history of fluid flow at cold seep sites from Ba/Ca ratios in vesicomyid clam shells. *Limnol. Oceanogr.* 46, 1701-1708.

Toyofuku, T., Kitazato, H., Kawahata, H., Tsuchiya, M. and Nohara, M. (2000). Evaluation of Mg/Ca thermometry in foraminifera: Comparison of experimental results and measurements in nature. *Paleoceanography* 15 (4): 456-464

USEPA, 1997. The incidence and severity of sediment contamination in surface waters of the United States. EPA 823-R-97-006. US Environmental Protection Agency, Washington, DC.

Vacelet, J. (1991). Recent Calcarea with a reinforced skeleton ("Pharetronids"). pp. 252-265. In: Reitner, J. & Keupp, H. (eds) 'Fossil and Recent Sponges'. (Springer-Verlag: Berlin).

Vacelet, J. (2002) Family Astroscleridae Lister, 1900. *In*: Systema Porifera: A guide to the Classification of Sponges. Hooper J.N.A. and Van Soest R.W.M. Kluwer Academic/Penum Publishers, New York (2002). Volume 1, pp 824 – 830.

van der Wal, P., de Bruijn, W.C. and Westbroek, P. (1985). Cytochemical and X-ray microanalysis studies of intracellular calcium pools in scale baring cell of the coccolithophorid *Emiliania huxleyi*. *Protoplasma* 124 (1-2): 1-9.

Vander Putten, E., Dehairs, F., Keppens, E. and Baeyens, W. (2000), High resolution distribution of trace elements in the calcite shell layer of modern Mytilus edulis: Environmental and biological controls. *Geochimica et Cosmochimica Acta*, v. 64, p. 997–1011.

Vercauteren, K. and Blust, R. (1999). Uptake of Cd and Zn by the mussel *Mytilus edulis* and inhibition by calcium channel and metabolic blockers. *Mar. Biol.*, 135, 615-626.

Verheyden, A. (2004). *Rhizophora mucronata* as a proxy for changes in the environmental conditions, a study on the wood anatomy, stable isotope chemistry and inorganic composition of a Kenyan mangrove species. *PhD thesis* Vrije Universiteit Brussel, Brussels, Belgium, 228 pp.

Verheyden, A., Roggeman, M., Bouillon, S., Elskens, M., Beeckman, H. and Koedam, N. (2005). Comparison between δ13C of α-cellulose and bulk wood in the mangrove tree Rhizophora mucronata: implications for dendrochemistry. *Chemical Geology* 219: 275-282.

Verheyden, A., Helle, G., Schleser, G.H., Dehairs, F., Beeckman, H. and Koedam, N. (2004). Annual cyclicity in high-resolution stable carbon and oxygen isotope ratios in the wood of the mangrove tree Rhizophora mucronata. *Plant, Cell and Environment* 27, 1525–1536.

Veron, A.J., Church, T.M., Flegal, A.R., Patterson, C.C. and Erel, Y. (1993). Response of lead cycling in the surface Sargasso Sea to changes in tropospheric input. *Journal of Geophysical Research* 98 (C10): 18,269 18,276.

Wada, K. and Fujinuki, T. (1976). Biomineralization in bivalve molluscs with emphasis on the chemical composition of the extrapallial fluid, In *The Mechanisms of Mineralization in the Invertebratesand Plants* (eds.N. Watabe and K. M. Wilbur) University of South Carolina Press, Columbia, pp. 175–190.

Wang, S., Hong, H. and Wang, X. Bioenergetic responses in green lipped mussels (*Perna viridis*) as indicators of pollution stress in Xiamen coastal waters, China. *Marine Pollution Bulletin In press*.

Wang, W.-X. and Rainbow, P.S. (2005). Influence of metal exposure history on trace metal uptake and accumulation by marine invertebrates. *Ecotox. Environ. Saf*. 61, 145-159.

Wang, W.-X. and Fisher, N.S. (1999). Effect of calcium and metabolic inhibitors on trace elements uptake in two marine bivalves. *J. Exp. Mar. Biol. Ecol*. 236, 149-164.

Weber, J.N. and Woodhead, P.M.J. (1970). Carbon and oxygen isotope fractionation in the skeletal carbonate of reef-building corals. *Chemical Geology* 6: 93-117.

Weber, J.N. (1973). Incorporation of strontium into reef coral skeletal carbonate. *Geochimica et Cosmochimica Acta* 37: 2173-2190.

Weber, J.N. and Raup, D.M. (1966). Fractionation of stable isotopes of carbon and oxygen in marine calcareous organisms – the Echinoidea. Part II. Environmental and genetic factors. *Geochiica et Cosmochimica Acta*. 30: 705-736.

Weber, J.N. and Raup, D.M. (1968). Comparison of C13/C12 and O18/O16 in the skeletal calcite of recent and fossil echinoids. *Journal of Paleontology*. 42 (1): 37-50.

Weinbauer, M.G., Brandstätter, F. and Velimirov, B. (2000). On the potential use of magnesium and strontium concentrations as ecological indicators in the calcite skeleton of the red coral (*Corralium rubrum*). *Marine Biology* 137:801-809

Wheeler, A.P. (1992). Mechanisms of molluscan shell formation. In *Calcification in Biological Systems* (ed. E. Bonucci). CRC press. pp. 179-216.

Wilbur, K.M. and Saleuddin, A.S.M. (1983). Shell formation. In *The Mollusca* (eds. A. S. M. Saleuddin and K. M. Wilbur). Academic Press, Inc. pp. 235-287.

Willenz, Ph. and Hartman, W.D. (1985). Calcification rate of *Ceratoporella nicholsoni* (Porifera: Sclerospngiae): an in situ study with calcein. *Proceedings of the Fifth International Coral Reef Congress, Tahiti,* 5: 113-118

Willenz, Ph. and Hartman, W.D. (1999). Growth and regeneration rates of the calcareous skeleton of the Caribbean coralline sponge *Ceratoporella nicholsoni*: a long term survey. *Memoirs of the Queensland Museum* 44: 675-685.

Willenz, Ph. and Hartman, W.D. (1989). Micromorphology and ultraastructure of Caribbean scerosponges. 1. *Ceratoporella nicholsoni* and *Stromatospongia norae* (Ceratoporellidae, Porifera). *Marine Biology*, 103 (3): 387-401

Wright, D.A. (1995). Trace metal and major ion interactions in aquatic animals. *Mar. Poll. Bull.* 31, 8-18.

Wu, J. and Boyle, E.A. (1997). Lead in the western North Atlantic Ocean: Completed response to leaded gasoline phaseout. *Geochimica et Cosmochimica Acta* 61(15): 3279 3283.

Yap, C.K., Ismail, A., Tan, S.G., Rahim, I.A. (2003). Can the shell of the green-lipped mussel *Perna viridis* from the west coast of Peninsular Malaysia be a potential biomonitoring material for Cd, Pb and Zn? *Est. Coast. Shelf Sci*. 57, 623-630.

Zacherl, D.C., Paradis, G., Lea, D.W. (2003). Barium and strontium uptake into larval protoconchs and statoliths of the marine neogastropod *Kelletia kelledi*. *Geochim. Cosmochim. Acta* 67, 4091-4099.

Zwolsman, J.J.G. and Van Eck, B.T.M. (1999). Geochemistry of major elements and trace metals in suspended matter of the Scheldt estuary, southwest Netherlands, *Mar.Chem*. 66, 91-111.

ANNEX 1

Table A1: List of museum samples (1: Museum d'Histoire Naturelle de Paris; 2: Institut Royal de Sciences Naturelles de Belgique; 3: Laboratoire de Biologie Marine, Université Libre de Bruxelles).

Species	N° Museum	Location	Year	Latitude	Longitude
Asterias rubens **(syn. *Asterias vulgaris*)**	Ec2679As[1]	France, Arcachon	1961	44.66N	1.16W
	Ec1951As[1]	USA, Bar Harbor	1894	44.40N	68.23W
	Ec2493As[1]	France, Roscoff	1961	48.72N	3.98W
	I.G. 8188/102 IRSNB	Belgium, Port d'Ostende	1906	51.24N	2.92E
	I.G. 8188/142 IRSNB	Belgian Coast, Ostende	1905	51.36N	2.62E
	BIOMAR	The Netherlands, Scharendijke	1988	51.73N	3.85E
	BIOMAR	The Netherlands, Scharendijke	1986	51.73N	3.85E
	Ec714As[1]	Feroe Islands, Rituvik	1898	62.10N	6.69W
	I.G. 11.626 N°4	Icelandic Sea	1938	63.74N	21.33W
	I.G. 11548	Icelandic Sea	1938	63.92N	22.97W
	Ec709As[1]	Iceland, Rekjavik	1892	64.11N	21.85W
	Ec708As[1]	Iceland, Patreksfjördur	1892	65.58N	24.00W
	I.G. 11.626 N°17	Icelandic Sea	1938	65.76N	22.0W
	Ec711As[1]	Iceland, Isafjördur	1892	66.08N	23.15W
Sphaerechinus granularis	Ec8098Es[1]	Azores, Topo	1867	38.54N	27.79W
	Ec8480Es[1]	Azores, Topo	1971	38.54N	27.79W
	Ec5182Es	France, Brest	1867	48.40N	4.48W
	BIOMAR	France, Brest	1986	48.40N	4.48W
	I.G.3152	France, Cannes	1898	43.55N	7.02E
Strongylocentrotus droebachiensis	Ec7902Es[1]	USA, Boston	1867	42.36N	71.06W
	Ec5710Es[1]	St.Pierre et Miquelon, St.Pierre	1934	46.79N	56.20W
	Ec8150Es[1]	New Foundland, Saint John's	1927	47.58N	52.74W
	Ec7607Es[1]	Sweden, Malmö	1862	55.58N	13.00E
	Ec6090Es[1]	Labrador, Makkovik	1894	55.11N	59.19W
	I.G. 4394	Norway, Bergen	1897	60.39N	5.32E
	Ec7913Es[1]	Greenland, Godhaat	1856	64.20N	53.52W
	Ec7910Es[1]	Norway, Jan Mayen	1935	70.98N	8.0W
Lytechinus variegatus	Ec7615Es[1]	Guadeloupe, Pointe d'Antigues	1870	16.44 N	61.54W
	Ec5792Es[1]	Brasil, Rio de Janeiro	1960	22.90S	43.20W
	Ec7609Es[1]	Bermuda, Somerset Village	1894	32.31N	64.87W
Paracentrotus lividus	Ec6455Es[1]	Morocco, Ile de Mogador	1922	31.50N	9.77W
	Ec8645Es[1]	Turkey, Antalya	1984	36.89N	30.70E
	Ec6817Es[1]	Açores, Topo	1969	38.54N	27.79W
	Ec5842Es[1]	France, Etang de Sijean	1960	43.08N	3.00W
	Ec7728Es[1]	France, Bretagne, Port Etienne	1929	48.11N	4.37W
Tripneustes ventricosus	Ec7930Es[1]	Martinique, Fort de France	1842	14.62N	61.07W
	Ec5949Es[1]	Puerto Rico, San Juan	1969	18.48N	66.07W

Table A2 Field collected starfish

Starfish

species	location	latitude	longitude
Asterias rubens	France, Atlantic, Aber	48.22N	4.3W
Asterias rubens	France, Atlantic, Morgat	48.23N	4.5W
Asterias rubens	Belgium, North Sea, Knokke	51.35N	3.27E
Asterias rubens	The Netherlands, North Sea, Scharendijke	51.73N	3.85E
Asterias rubens	Netherlands, North Sea, Texel	52.87N	4.72E
Asterias rubens	Germany, North Sea, Sylt	54.91N	8.28E
Asterias rubens	Norway, North Sea,Sørfjørd	60.41N	6.53E
Asterias rubens	Russia, White Sea, Cape Kartesh	66.33N	33.66E
Asterias rubens	Russia, Barents Sea, Warsino	68.34N	39.14E

ANNEX 2

CALMARS 2001-2005 Publications

Peer Reviewed Journals

Chauvaud L, **Lorrain A**, Dunbar RB, Paulet Y-M., Thouzeau G, Jean F, Guarini J-M, & Mucciarone D (*In press*) The shell of the Great Scallop *Pecten maximus* as a high frequency archive of paleoenvironmental change. *Geochemistry, Geophysics, Geosystems* 6, XXXXXX, doi:10.1029/2004GC000890.

De Ridder, F., R. Pintelon, J. Schoukens and **D. P. Gillikin** (2005). Modified AIC and MDL model selection criteria for short data records. *IEEE Transactions on Instrumentation and Measurement* 54: 144-150.

De Ridder, F., R. Pintelon, J. Schoukens and A. Verheyden (2005). Reduction of the Gibbs phenomenon applied on Non-harmonic Time Base Distortions. *IEEE Transactions on Instrumentation and Measurement* 54: 1118-1125.

De Ridder, F., R. Pintelon, J. Schoukens, **D. P. Gillikin**, **L. André**, **W. Baeyens**, A. de Brauwere and **F. Dehairs** (2004). Decoding Non-linear Growth Rates in Biogenic Environmental Archives. *Geochemistry, Geophysics, Geosystems* 5, Q12015, doi:10.1029/2004GC000771.

De Ridder, **F.,** R. Pintelon, J. Schoukens, **J. Navez**, **L. André** and **F. Dehairs** (2002). An Improved Multiple Internal Standard Normalisation for drift in LA-ICP-MS Measurements. *Journal of Analytical Atomic Spectrometry* 17(11): 1461-1470.

Gillikin, D. P., F. De Ridder, **H. Ulens,** M. Elskens, **E. Keppens, W. Baeyens** and **F. Dehairs** (2005a). Assessing the reproducibility and reliability of estuarine bivalve shells (*Saxidomus giganteus*) for sea surface temperature reconstruction: implications for paleoclimate studies. *Palaeogeography Palaeoclimatology Palaeoecology* doi:10.1016/j.palaeo.2005.03.047

Gillikin, D. P., **A. Lorrain**, **J. Navez,** J. W. Taylor, **L. André, E. Keppens**, **W. Baeyens** and **F. Dehairs** (2005b). Strong biological controls on Sr/Ca ratios in aragonitic marine bivalve shells. *Geochemistry, Geophysics, Geosystems* 6, Q05009, doi:10.1029/2004GC000874

Gillikin, D. P., F. Dehairs, A. Lorrain, D. Steenmans, **L. André, J. Navez and W. Baeyens** (*Under revision*). Barium uptake into the shells of the common mussel (*Mytilus edulis*) and the potential for estuarine paleo-chemistry reconstruction. Geochemica et Cosmochimica Acta.

Gillikin, D. P., F. Dehairs, W. Baeyens, J. Navez, A. Lorrain and L. André (*In press***)**. Inter- and intra-annual variations of Pb/Ca ratios in clam shells (*Mercenaria mercenaria*): a record of anthropogenic lead pollution? *Marine Pollution Bulletin.*

Janssen, S., Van Leeuwen, H.P and **Blust, R.** 2002. Metal speciation dynamics and bioavailability: Case studies for metal uptake by bivalves and fish. Environmental Science and Technology, 36: 2164-2170.

Lazareth C.E., E. Vander Putten, **L. André** and **F. Dehairs** (2003). High-resolution trace element profiles in shells of a mangrove bivalve (*Isognomon ephippium*): A record of environmental spatio-temporal variations? *Estuarine, Coastal and Shelf Science*, 57: 1103-1114.

Lorrain A., D. P. Gillikin, Y.-M. Paulet, L. Chauvaud, **J. Navez**, A. Le Mercier, **L. André** (*Under revision*). Strong kinetic effects on Sr/Ca ratios in the calcitic bivalve *Pecten maximus*. Geology.

Lorrain, A., Y.-M. Paulet, L. Chauvaud, R. Dunbar, D. Mucciarone and M. Fontugne (2004). $\delta^{13}C$ variations in scallop shells: Increasing metabolic carbon contribution with body size? *Geochimica et Cosmochimica Acta* 68(17): 3509-3519.

Ranner H, de Jonghe C, Monin L, Navez J, André L, Gilikin D, Keppens E, Dubois Ph. (2004). Recording of environmental parameters in the skeleton of *Asterias rubens* and

Sphaerechinus granularis. *In*: *Echinoderms München*, Heinzeller Th, Nebelsick JH (eds), pp. 249-251. Taylor & Francis, Balkema.

Rosenheim, B.E., P. K. Swart, S. R. Thorrold, A. Eisenhauer, and **Ph. Willenz** (2005). Salinity change in the subtropical Atlantic: Secular increase and teleconnections to the North Atlantic Oscillation. *Geophyical Research Letters* 32 (2), L02603 doi: 10.1029/2004GL021499.

Rosenheim, B.E., P.K. Swart, S.R. Thorrold, **Ph. Willenz**, **L. Berry** and C. Latkoczy (2004). High-resolution Sr/Ca records in sclerosponges calibrated to temperature *in situ*. *Geology* 32(2): 145-148.

Verheyden, A., **F. De Ridder**, N. Schmitz, H. Beeckman and N. Koedam (2005). High-resolution time series of vessel density in Kenyan mangrove trees reveal link with climate. *New Phytologist.* 167: 425-435.

Verheyden, S., B. Rosenheim, S. Thorrold, D. Langlet, P. Swart, **Ph. Willenz, D.P. Gillikin, J. Navez and L. André** (*Submitted*)**.** Regional and water depth lead trends in sclerosponges. Earth and Planetary Science Letters.

Willenz, Ph. and Hartman, W.D. (2004). Storage Cells and Spermatic Cysts in the Caribbean Coralline Sponge *Goreauiella auriculata* (Astroscleridae, Agelasida, Demospongiae): a Relationship ? *Bollettino dei Musei e degli Istituti Biologici della (R.) Università di Genova,* 68: 673-681.

Book

Hooper, J.N.A. & Van Soest, R.W.M. (Eds), **Willenz, Ph**. (Bibliographic Ed.) (2002). Systema Porifera. A Guide to the Classification of Sponges. Kluwer Academic / Plenum Publishers, 1708 pp.

Book Reviews

Berry, L (2003). Soaking up the limelight. *Nature*, **421** (6925) p791.

Congresses

Bashar B., F. De Ridder, E. Keppens, C. Lazareth, Ph. Willenz, F. Dehairs, L. André and **the CALMARS group** (2005). Stable Isotopes and Mg/Ca, Sr/Ca Ratios in a Sclerosponge Archive. EGU General Assembly 2005, Vienna, Austria. Geophysical Research Abstracts, Vol. 7, 08881.

Berry L., V. Sivel, H. Zandbergen, **Ph. Willenz** and **the CALMARS group** (2005). The Use of Hypercalcified Sponges as Proxy Indicators of Climate Change: Biological Investigations. EGU General Assembly 2005, Vienna, Austria. Geophysical Research Abstracts, Vol. 7, 04881.

Berry L., V. Sivel, H. Zandbergen, **Ph. Willenz** and the CALMARS group (2005). Insights into the Skeletal Growth Pattern of the Hypercalcified Sponge *Petrobiona massiliana*. EGU General Assembly 2005, Vienna, Austria. Geophysical Research Abstracts, Vol. 7, 04874.

Berry L., Verheyden S., André L., Willenz Ph, and the CALMARS group (2002). Variation in Coralline Sponge Aragonitic Skeleton Pb Profiles: Physiological and/or Environmental Influences ? *Bollettino Dei Musei e Degli Istituti Biologici. Univ. Genoa.* 66-67: 28.

Berry, L., Sivel, V , Zandberen, H., **Willenz, Ph.** & **the CALMARS Group** (2004). Uptake of trace elements in sponges with a hypercalcified skeleton. (Poster), 13th European Microscopy Congress. Antwerp, Belgium, August 22-27, 2004.

Berry, L.S. , Willenz, Ph. & **the CALMARS group** (2004). Biological validation of calcified sponges as recorders of climate change: following uptake of trace elements using X-ray microanalysis. Proceedings of the 13th European Microscopy Congress. Schryvers, D. & Timmermans, J.-P. (Eds), Vol. 3 (Life Sciences): 155.

Blust, R. (2002). A comparison of static and dynamic models of metal accumulation and toxicity in aquatic organisms. International Seminar on Exposure and Effects Modelling in Environmental Toxicology. Joint Setac UIR seminar, 4-7 February 2002, University of Antwerp, Belgium.

Blust, R. (2002). Models for the bioaccumulation of metals in aquatic organisms. Metal and radionuclides bioaccumulation in marine organisms CIESM Workshop, 27-30 October 2002, Ancona, Italy.

Blust, R. (2003). Models for the bioaccumulation of metals in aquatic organisms. In Metal and Eadionuclides Bioaccumulation in Aquatic Organisms. CIESM Workshop Monographs n°19, pp 71-74.

Blust, R., Lorenzo, J., **Mubiana, V.K.**, Beiras, R., Bervoets, L. (2002). Role of free metal ions and complexes in metal uptake by aquatic invertebrates and fish. 12th Annual Meeting of SETAC-Europe: Challenges in Environmental Risk Assessment and Modelling. 12-16 May 2002, Vienna, Austria.

Blust, R., Steen-Redeker, E., Van Campenhout, K., Bervoets, L. (2002). Dynamic models for metal accumulation under ecologically realistic exposure scenarios. 12th Annual Meeting of SETAC-Europe: Challenges in Environmental Risk Assessment and Modelling. 12-16 May 2002, Vienna, Austria.

De Ridder F, R. Pintelon, J. Schoukens, **L. André, F. Dehairs** (2004). An Improved Multiple Internal Standard Normalisation for Drift in LA-ICP-MS Measurements. Eos Trans. AGU, 84(52), Ocean Sci. Meet. Suppl., Abstract OS22D-12.

De Ridder F. (2002). The variation in LA-ICP-MS measurements at 6th european Laser ablation ICP-MS workshop, 24-25 June, 2002, Utrecht.

De Ridder F., A. Verheyden, **Ph. Willenz, F. Dehairs**, J. Schoukens, R. Pintelon (2002). Internal normalisation in LA-ICP-MS & Non-linear growth rates in biota. IAP V/22 study day, November 26, 2002, Louvain-La-Neuve.

De Ridder F., J. Schoukens, R. Pintelon, **W. Baeyens, L. André and F. Dehairs** (2003). Non-Linear Growth Rates of marine calcareous organisms and the problem of decoding the recorded environmental change signal, VLIZ Jongerencontactdag 2003.

De Ridder F., R. Pintelon, J. Schoukens, **J. Navez, L. André and F. Dehairs** (2002). An improved multiple internal standard normalisation for the drift in LA-ICP-MS measurements. 6th European Laser ablation ICP-MS workshop, 24-25 June, 2002, Utrecht.

De Ridder F., R. Pintelon, J. Schoukens, **J. Navez, L. André and F. Dehairs** (2002). Reduction of the disturbing noise in the calibration of LA-ICP-MS measurements. 3rd internaltional chemometrics research meeting.

De Ridder F., R. Pintelon, J. Schoukens, **J. Navez, L. André and F. Dehairs** (2001). An improved multiple internal standard calibration for LA-ICP-MS measurements. 2nd international conference on high-resolution sector field ICP-MS 12-15/9/2001, Vienna.

De Ridder, F. , A. De Brauwere, R. Pintelon, J. Schoukens, **F. Dehairs** (2004). Identification of the Time Base in Environmental Archives. *Eos Trans. AGU*, 85(46), Fall Meet. San Francisco, CA, Suppl., Abstract NG41A-0424.

De Ridder, F., R. Pintelon , J. Schoukens, **D.P.Gillikin, L. André, W. Baeyens,** A. de Brauwere, **F. Dehairs** and **the CALMARS group** (2005). Decoding Nonlinear Growth Rates in Annually Resolved Archives. EGU General Assembly 2005, Vienna, Austria. Geophysical Research Abstracts, Vol. 7, 07540.

Gillikin D. P., F. Dehairs, W. Baeyens, J. Navez, L. André, and the CALMARS Group (2003). The potentials of high resolution trace element profiles in bivalve shells as a record of paleoenvironment: exploring *Mercenaria mercenaria*.. *Geophysical Research Abstracts*, Vol. 5, 11503.

Gillikin D. P., J. Navez, F. Dehairs, W. Baeyens and **L. André** (2003). Validation of LA-ICP-MS results with SN-HR-ICP-MS. Fourth International Conference on High Resolution Sector Field ICPMS, 15th-17th October 2003, Venice, Italy.

Gillikin, D. P. , **F. Dehairs,** D. Steenmans, L. Meng, T. Haifeng, J. Navez, **L. André, W. Baeyens, E. Keppens,** and **the CALMARS group** (2004). Trace element proxies (Sr/Ca, Ba/Ca and Pb/Ca) in Bivalve shells: environmental signals or not? *Eos Trans. AGU*, 85(46), Fall Meet. San Francisco, CA, Suppl., Abstract B13E-08.

Gillikin, D. P., D. Steenmans, F. Dehairs, W. Baeyens, J. Navez, L. André, E. Keppens, and the CALMARS Group (2004). Calibration and validation of the mussel Mytilus edulis

as an environmental archive. 1st EGU General Assembly, Nice, France, 26 - 30 April 2004. Abstract EGU04-A-04054.

Gillikin, D. P., F. Dehairs, W. Baeyens, J. Navez, L. André, E. Keppens, and **the CALMARS Group** (2004). The potentials of aragonitic bivalves as paleoclimate proxies: d18O, Sr/Ca and Mg/Ca. International Paleo-environments Symposium (QRA2004), Brussels, Belgium, 15-17 September.

Gillikin, D. P., J. Navez, F. Dehairs, W. Baeyens and L. André (2004). Validation of Laser Ablation-ICP-MS results with Solution Nebulization-HR-ICP-MS. European Science Foundation workshop: Isotopic microsampling in Earth, Environmental and Archaeological Sciences, September 9-11, 2004, Durham, UK.

Gillikin, D. P., Ulens, H., **Dehairs, F., Baeyens, W., Navez, J., Andre, L., Keppens, E.,** and **the CALMARs group** (2004). Sr and Mg Profiles in Aragonitic Bivalves: Do They Record Temperature? Eos Trans. AGU, 84(52), Ocean Sci. Meet. Portland, OR, Suppl., Abstract OS42B-06.

Gillikin, D. P., Ulens, H., **Dehairs**, F., **Baeyens**, W., **Navez**, J., **André**, L., **Keppens**, E., and **the CALMARS Group** (2003). Wetland bivalves as environmental archives. Eighth Symposium on Biogeochemistry of Wetlands, Gent, Belgium, September 14-17, 2003.

Gillikin, D.P., Steenmans, D., Meng, L., Haifeng, T., Ulens, H., **Dehairs, F., Baeyens, W., Navez, J., André, L., Keppens, E. and the CALMARS Group** (2004). Bivalves as environmental archives, *In*: Mees, J.; Seys, J. (Eds.) (2004). VLIZ Young Scientists' Day, Brugge, Belgium 5 March 2004: book of abstracts. VLIZ Special Publication, 17: pp. 51.

Gillikin, D.P., A. Lorrain, Li Meng, **F. Dehairs, W. Baeyens, E. Keppens** and **the CALMARS Group** (2005). Toward a mechanistic understanding of $\delta^{13}C$ in the aragonitic bivalve shells of *Mercenaria mercenaria*. EGU General Assembly 2005, Vienna, Austria. Geophysical Research Abstracts, Vol. 7, 00072.

Gillikin, D.P., F. Dehairs, D. Steenmans, **A. Lorrain, L. André, J. Navez, W. Baeyens** and **the CALMARS Group** (2005). Barium uptake into the shells of the common mussel (*Mytilus edulis*): results from a field and laboratory experiment. EGU General Assembly 2005, Vienna, Austria. Geophysical Research Abstracts, Vol. 7, 00073.

Langlet D., L. Alleman, **L. André** and P.-D. Plisnier (2005) Upwelling events in Lake Tanganyika traced by Mn content in bivalve shells. EGU General Assembly 2005, Vienna, Austria. Geophysical Research Abstracts, Vol. 7, 05731.

Lorenzo J.I., Beiras R., **Mubiana V.K.**, **Blust R.** (2002). Indications of Regulation on Copper Accumulation in the blue Mussel Mytilus edulis. 4th Interanational Conference on Molluscan Shellfish Safety, Santiago de Compostela, Spain.

Lorrain A, Y Paulet, L Chauvaud, R Dunbar, D Mucciarone, M Fontugne (2004). $\delta^{13}C$ Variations in Scallop Shells: Increasing Metabolic Carbon Contribution With Body Size? Eos Trans. AGU, 84(52), Ocean Sci. Meet. Suppl., Abstract OS42B-09.

Lorrain A., D.P. Gillikin, Y.-M. Paulet, L. Chauvaud, **J. Navez, A.** Lemercier, **L. André** and **the CALMARS Group** (2005). Strong kinetics effects on Sr/Ca ratios in the calcitic bivalve *Pecten maximus*. EGU General Assembly 2005, Vienna, Austria. Geophysical Research Abstracts, Vol. 7, 01470.

Lorrain A., Paulet, Y.M., Chauvaud, L., Dunbar, R., Mucciarone, D., Pécheyran, C., Amouroux, D., Fontugne, M. (2003). Scallops skeletons as tools for accurate proxy calibration. AGU.EGU.EGS. Nice. 6-11 Avril 2003.

Lorrain A., Pécheyran, C., Paulet, Y.M., Chauvaud, L., Amouroux, D., Krupp, E., Donard, O.F.X. (2003). Trace element study in scallop shells by laser ablation ICP-MS: the example of Ba/Ca ratios. AGU.EGU.EGS. Nice. 6-11 Avril 2003.

Lorrain, A., D. P. Gillikin, Y.M. Paulet, C. Paillard, **J. Navez, L. André, F. Dehairs, W. Baeyens** and **the CALMARS Group** (2004). Toward a mechanistic understanding of trace element proxy incorporation in bivalve shells. International Paleo-environments Symposium (QRA2004), Brussels, Belgium, 15-17 September.

Lorrain, A., D. P. Gillikin, Y.-M. Paulet, L. Chauvaud, **J. Navez**, A. Le Mercier, **L. André**, (2005). Strong kinetics effects on Sr/Ca ratios in the calcitic bivalve *Pecten maximus*. ASLO 2005 Summer Meeting, June 19 – 24, Santiago de Compostela, Spain.

Lorrain, A., Barats, A., Paulet, Y-M., Chauvaud, L., Amouroux, A., Pécheyran, C., **André, L**. (2005). High resolution Ba/Ca profiles in the shells of the calcitic bivalve *Pecten maximus*. ASLO 2005 Summer Meeting, June 19 – 24, Santiago de Compostela, Spain.

Meert I., **D. P. Gillikin, F. Dehairs,** A. Ervynck, B. Hillewaert**, E. Keppens** and the CALMARS Group. (2005). Environmental conditions of the Belgian coastal area over the past millennium from *Mytilus edulis* shells: preliminary results. EGU General Assembly 2005, Vienna, Austria. Geophysical Research Abstracts, Vol. 7, 04693.

Meert, I., D. P. Gillikin, A. Ervnyk, B. Hillewaert, **E. Keppens, F. Dehairs** (2005). Reconstructing the environmental conditions in the coastal area of the Southern Bight over the past millennium using *Mytilus edulis* shells, *In*: Mees, J.; Seys, J. (Eds.) (2005). VLIZ Young Scientists' Day, 25 February 2005: book of abstracts. VLIZ Special Publication, 20: pp. 45.

Mubiana V.K., R. Blust and **the CALMARS Group** (2005). Exploring the uptake pathways of calcium and some trace elements in the marine bivalve, *Mytilus edulis* using isolated gill tissues. EGU General Assembly 2005, Vienna, Austria. Geophysical Research Abstracts, Vol. 7, 07816.

Mubiana, V.K., Qadah, D., **Blust, R.** (2002). Evolution of spatial variability of heavy metals in mussels (*Mytilus edulis* L.) in the Scheldt estuary (1996-2002). Ecological Structures and Functions in the Scheldt Estuary: from past to future. 7-10 October, Antwerp, Belgium.

Mubiana, V.K., Vercauteren, K., **Blust, R.** (2003). Modelling the effects of salinity, temperature and complexation on the uptake and accumulation of heavy metals in the marine bivalve Mytilus edulis. 13th Annual Meeting of The Society of Environmental Toxicology and Chemistry (SETAC Europe), Hamburg, Germany.

Navez, J., A. Lorrain and **L. André** (2003). Trace element profiles in carbonate skeletons - Comparison between two analytical techniques. Colloquium Spectroscopicum International XXXIII (CSI XXXIII), Granada, Spain, 7-12 September 2003.

Ranner H., O. Ladriére, J. Navez, L. André, D. Gillikin, E. Keppens, P. Dubois and **the CALMARS group** (2005). Do echinoderms store temperature changes in their skeleton? EGU General Assembly 2005, Vienna, Austria. Geophysical Research Abstracts, Vol. 7, 01098.

Ranner, H., **de Jonghe, C., Monin, L., Navez, J.**, **André, L., Gillikin, D., Keppens, E., Dubois Ph.** and **the CALMARS Group** (2003). Recording of environmental parameters in the skeleton of *Asterias rubens* and *Sphaerechinus granularis*, 11th International Echinoderm Conference, Munich 2003 .

Ranner, H., **Ladrière, O., Navez, J.**, **André, L., Gillikin, D., Keppens, E., Dubois, Ph.** and **the CALMARS Group** (2004). Effects of temperature on the chemistry of the echinoderm skeleton. International Paleo-environments Symposium (QRA2004), Brussels, Belgium, 15-17 September.

Ranner, H., **Ladrière, O.**, **Navez, J.**, **André, L., Gillikin, D., Keppens, E., Dubois Ph.** and **the CALMARS Group** (2004). Effects of temperature on the chemistry of the echinoderm skeleton. Gordon Research Conference on Biomineralization, Colby-Sawyer College, New London, NH, USA

Ranner H, Ladrière O, de Jonghe C, Monin L, Navez J, André L, Dubois Ph. (In prep). Temperature control on Mg and trace metal incorporation into the echinoderm skeleton.

Ranner H, Ladrière O, Gilikin D, Keppens E, Dubois Ph. (In prep) Temperature control on d18O and d13C incorporation into the echinoderm skeleton.

Ranner H, Navez J, André L, Dubois Ph. (In prep). Tracing of bauxite residues in the tropical sea urchin *Tripneustes ventricosus* and sediments from Discovery Bay, Jamaica.

Ridder, F., Pintelon, R., Schoukens, J., **Gillikin, D. P., Andre, L., Baeyens, W., Dehairs, F.** (2004). Decoding Non-linear Growth Rates in Biogenic Archives. Eos Trans. AGU, 84(52), Ocean Sci. Meet. Portland, OR, Suppl., Abstr. OS42B-01.

Rosenheim, B.E., Swart, P.K., **Willenz, Ph.**, Thorrold, S. & Eisenhauer, A. (2002). Calibration of Caribbean Sclerosponges to their Ambient Environment: Indirect and Direct Methods. Eos Transactions of the American Geophysical Union 83(47): Abstract PP52B-06.

Steenmans, D., **D.P. Gillikin, F. Dehairs, W. Baeyens, J. Navez, L. André, E. Keppens,** and **the CALMARS Group** (2004). Barium in mussel shells: a proxy of environmental conditions? International Paleo-environments Symposium (QRA2004), Brussels, Belgium, 15-17 September.

Verheyden A., **F. De Ridder**, H. Beeckman and N. Koedam (2002). Can wood anatomy and carbon isotope ratio reveal stress factors in the mangrove Rhizophora mucronata Lamk.? The 13th FESPP (Federation of European Societies of Plant Physiology) congress, September, 1-6 2002, Heraclion, Greece.

Verheyden S., D. Gillikin, V. Vandeginste, F. De Ridder, J. Navez, L. André, F. Dehairs and E. Keppens (2002). Geochemistry of Sclerosponges and Bivalves. *Geologica Belgica International Meeting*.

Verheyden S., D. Langlet, L. André, Ph. Willenz, J. Navez, P. Swart and **The Calmars Group** (2002). The Oceanic Lead Trends Recorded by Sclerosponges. *AGU Fall meeting- December 2002.*

Verheyden, A., H. Beeckman, **F. De Ridder** and N. Koedam (2002). Vessel frequency reveals growth zones in the mangrove Rhizophora mucronata Lamk. 6th International Conference on dendrochronology, August 22-27, Québec City, Canada.

Wepener, V., Bervoets, L., **Mubiana, V.K.**, **Blust, R.** (2002). Relationship between Biomarker Responses and Metal Bioaccumulation in *Mytilus edulis*. 37th Annual Conference of the Southern African Society of Aquatic Scientists (SASAqS), July 2002, Bloemfontein, S. Africa.

Theses

de Jonghe, C. (2002). Recording of environmental conditions in the skeleton of *Asterias rubens* (L.) (Asteroidea, Echinodermata), Lic. Thesis Université Libre de Bruxelles, Belgium Promotor: **Ph. Dubois**, Mentor: **H. Ranner.**

De Ridder, F. (2004). Identification of the time base in environmental archives. Ph.D. Thesis, Vrije Universiteit Brussel, Belgium, 244 p.

Gillikin, D.P. (2005). Geochemistry of Marine Bivalve Shells: the potential for paleoenvironmental reconstruction. Ph.D. thesis. Vrije Universiteit Brussel, Belgium, 258 p.

Ladrière, O. (2004). Effects of temperature on the skeletal composition of the starfish *Asterias rubens* (L.) (Asteroidea, Echinodermata), Lic. Thesis Université Libre de Bruxelles, Belgium Promotor: **Ph. Dubois**, Mentor: **H. Ranner** .

Meng, L. (2004). Can bivalves be used as archives of anthropogenic carbon input to the marine environment? M.Sc. thesis Vrije Universiteit Brussel, Belgium. Promoter: **F. Dehairs**; Co-promoter: **D.P. Gillikin.**

Ranner, H., Effects of temperature on the chemsitry of the echinoderm skeleton. PhD thesis. Université Libre de Bruxelles: due December 2005.

Steenmans, D. (2004). Do Marine Bivalve Shells Record Paleo-Productivity? M.Sc./ lic. thesis. Vrije Universiteit Brussel, Belgium. Promoter: **F. Dehairs**; Co-promoter: **D.P. Gillikin.**

Ulens, H. (2003). The potentials of *Saxidomus giganteus* as a paleoclimate proxy. MareLac M.Sc. thesis. Gent University, Belgium. Promoter: **F. Dehairs**; Mentor: **D.P. Gillikin.**

Website

The CALMARS website has been running for 4 years and has received more than 1400 hits in the past year alone. http://www.vub.ac.be/calmar/ Peer-reviewed publications and abstracts presented at various meeting can be found are directly accessible on: http://www.vub.ac.be/calmar/calmarpubs.htm.

General public articles

Willenz, Ph., **L. André, F. Dehairs Ph. Dubois**, **R. Blust,** and **the CALMARS Group** (2005). Les squelettes calcaires, archives d'un passé proche des océans. Science Connection, Le magazine de la Politique scientifique fédérale. II.05, 6-10.

Willenz, Ph., **L. André, F. Dehairs Ph. Dubois**, **R. Blust,** and **the CALMARS Group** (2005).

Idem NL

Website CALMAR

http://www.vub.ac.be/calmar/